2 mil

CR 114709
Available to the Public

CONCEPTS FOR A THEORETICAL AND EXPERIMENTAL STUDY OF LIFTING ROTOR RANDOM LOADS AND VIBRATIONS

(The Effects of Some Rotor Feedback Systems on Rotor-Body Dynamics)

Phase VII-A Report under Contract NAS2-4151

by

Kurt H. Hohenemser

and

S. K. Yin

Department of Mechanical and Aerospace Engineering

Washington University
School of Engineering and Applied Science
St. Louis, Missouri

June, 1973

CONCEPTS FOR A THEORETICAL AND EXPERIMENTAL STUDY OF LIFTING ROTOR RANDOM LOADS AND VIBRATIONS

(The Effects of Some Rotor Feedback Systems on Rotor-Body Dynamics)

Phase VII-A Report under Contract NAS2-4151

Prepared for the Ames Directorate, AMRDL, at Ames Research Center, Moffett Field, California

by Kurt H. Hohenemser

Kurt H. Hohenemser

and Sheng K. Yin

S. K. Yin

Washington University
School of Engineering and Applied Science
St. Louis, Missouri

June, 1973

I

Reports and Publications Under Contract NAS2-4151

The following reports under subject research contract have been submitted:

1. Phase I Report of September 1967, Analytical Concepts for a Random Loads and Vibration Analysis of Lifting Rotors.

2. Phase II Report of August 1968, Perturbation Solution Method for Random Blade Flapping.

3. Phase III Report of June 1969, Random Blade Flapping Response to Atmospheric Turbulence at High Advance Ratio.

4. Phase IV Report of June 1970, Threshold Crossing Statistics for Rotor Blade Random Flapping.

5. Phase V-A Report of June 1971, Effects of Torsional Blade Flexibility on Single Blade Random Gust Response Statistics.

6. Phase V-B Report of June 1971, Analysis of Gust Alleviation Methods on Rotor Dynamic Stability.

7. Phase V-C Report of June 1971, Development of Experimental Methods in Support of the Analysis.

8. Phase VI-A Report of June 1972, Part I, Random Gust Response Statistics for Coupled Torsion-Flapping Rotor Blade Vibrations.

   Part II, Flap Bending Corrections to the Rigid Blade Analysis of Lifting Rotors.

   Part III, Effects of Rotor Support Flexibility.

9. Phase VI-B Report of June 1972, Experiments with Progressing/Regressing Forced Rotor Flapping Modes.

10. Phase VII-A Report of June 1973, The Effects of Some Rotor Feedback Systems on Rotor-Body Dynamics.

11. Phase VII-B Report of June 1973, Identification of Lifting Rotor System Parameters from Transient Response Data.

12. Phase VII-C Report of June 1973, Further Experiments with Progressing/Regressing Rotor Flapping Modes.

The following papers and articles sponsored under subject research contract have been published to date:

1. Gaonkar, G. H. and Hohenemser, K. H., "Flapping Response of Lifting Rotor Blades to Atmospheric Turbulence", Journal of Aircraft, Vol. 6, Nov.-Dec. 1969, pp. 496-503. First presented as AIAA Paper 69-206 at the AIAA/AHS VTOL Meeting, Atlanta, Georgia, February 1969.

2. Gaonkar, G. H. and Hohenemser, K. H., "Stochastic Properties of Turbulence Excited Rotor Blade Vibrations", AIAA Journal, Vol. 9, No. 3, March 1971, pp. 419-424. First presented as AIAA Paper 70-548 at the AIAA Atmospheric Flight Mechanics Conference, Tullahoma, Tennessee, May 1970.

3. Gaonkar, G. H. and Hohenemser, K. H., "Comparison of Two Stochastic Models for Threshold Crossing Studies of Rotor Blade Flapping Vibrations", presented as AIAA Paper 71-389 at the AIAA/ASME 12th Structures Conference, Anaheim California, April 1971.

4. Yin, S. K. and Hohenemser, K. H., "The Method of Multiblade Coordinates in the Linear Analysis of Lifting Rotor Dynamic Stability and Gust Response", presented as AHS Preprint No. 512 at the 27th Annual National Forum of the AHS, Washington, D.C., May 1971.

5. Hohenemser, K. H. and Yin, S. K., "Some Applications of the Method of Multiblade Coordinates", Journal of the American Helicopter Society, Vol. 17, No. 3, July 1972.

6. Gaonkar, G. H. and Hohenemser, K. H., "An Advanced Stochastic Model for Threshold Crossing Studies of Rotor Blade Vibrations", AIAA Journal, Vol. 10 No. 8, pp. 1100-1101, August 1972.

7. Prelewicz, D. A., "Response of Linear Periodically Time Varying Systems to Random Excitation", AIAA Journal, Vol. 10 No. 8, pp. 1124-1125, August 1972.

8. Hohenemser, K. H. and Crews, S. T., "Unsteady Wake Effects on Progressing/Regressing Forced Rotor Flapping Modes", AIAA 2nd Atmospheric Flight Mechanics Conference, Palo Alto, California. AIAA Paper No. 72-957, September 1972.

9. Gaonkar, G. H., Hohenemser, K. H, and Yin, S. K., "Random Gust Response Statistics for Coupled Torsion-Flapping Rotor Blade Vibrations", Journal of Aircraft, Vol. 9 No. 10, pp. 726-729, October 1972.

10. Hohenemser, K. H. and Crews, S. T., "Model Tests on Unsteady Rotor Wake Effects", Journal of Aircraft, Vol. 10 No. 1, pp. 58-60, January 1973.

11. Hohenemser, K. H. and Yin, S. K., "On the Question of Adequate Hingeless Rotor Modeling in Flight Dynamics", 29th Annual National Forum of the American Helicopter Society, Washington, D.C., Preprint No. 732, May 1973.

CONCEPTS FOR A THEORETICAL AND EXPERIMENTAL STUDY OF LIFTING ROTOR RANDOM LOADS AND VIBRATIONS

Phase VII-A

(The Effects of Some Rotor Feedback Systems on Rotor-Body Dynamics)

by

Kurt H. Hohenemser

and

S. K. Yin

Washington University
St. Louis, Missouri

Abstract

The effects of three gyroless rotor feedback systems - coning feedback, proportional tilting feedback and a combination of these - on the rotor-body dynamics of hingeless rotorcraft are studied with a simplified analytical model in the advance ratio range from 0 to .8. Combinations of feedback phase angles and control phase angles are selected to minimize control cross coupling and control sensitivity changes between low and high speed flight. For the feedback systems thus selected the effects of feedback gain and control actuator time lag on the stability both with fixed hub and in free flight is studied, whereby the rotorcraft is free in pitch, roll and vertical motion but otherwise restrained. For the free flight conditions the effects of a horizontal tail are also determined in itself and in combination with the rotor

feedback systems. Finally random responses to atmospheric turbulence are determined for the various configurations within the range of stable behavior. The survey was made with two hingeless rotors: a three bladed rotor with uniform mass and stiffness blades having a first flap-bending frequency of 1.21, and a three bladed rotor with tapered in thickness blades having a first flap bending frequency of 1.47. In both cases gyroless rotor feedback systems could be determined which in combination with a small horizontal tail removed control cross-coupling, control oversensitivity, pitch divergence and gust oversensitivity up to .8 rotor advance ratio. Because of the various simplifications in the analytical model the results represent mainly a trend study. Reliable absolute characteristics would require more sophistication in the analytical model.

CONCEPTS FOR A THEORETICAL AND EXPERIMENTAL STUDY OF LIFTING ROTOR RANDOM LOADS AND VIBRATIONS

Phase VII-A

(The Effects of Some Rotor Feedback Systems on Rotor-Body Dynamics)

Table of Contents

Nomenclature

a	Lift slope
b	Number of blades per rotor
c	Blade chord
C_{ij} or C	Aerodynamic blade damping coefficient
D	Drag force
g	Acceleration of gravity
h	Distance hub-aircraft c.g.
I	Moment of inertia
K_{ij} or K	Aerodynamic blade stiffness coefficient
K_p , K_o	Proportional and coning feedback gains
L	Rolling moment, or lift force
M	Pitching moment
m	Aircraft mass, or blade mass per unit length, or aerodynamic blade moment
m_r	Total blade mass
P	First natural blade frequency
p	Rolling velocity, positive right
q	Pitching velocity, positive up
R	Rotor radius
r	Yawing velocity, positive right
S	Mass moment
t	Time
U or u	Forward velocity
U_T	Tangential velocity

U_p	Normal velocity
V or v	Velocity to right
W or w	Downward velocity
x	Non-dimensional radial distance
X	Force in forward direction
Y	Force to right
Z	Force in downward direction
α_I	Pitching angular deflection, positive down
α_{II}	Rolling angular deflection, positive left
β	Blade flapping angle for flexible blade defined by straight line through tip
β_I	Forward rotor tilting angle
β_{II}	Left rotor tilting angle
ϕ	Control phase angle, or roll attitude earth fixed
ϕ_b	Blade inflow angle
ψ	Azimuth angle, or yaw angle earth fixed
$\gamma = \rho acR^2/\int x^2 dm$	Rigid blade Lock number
$\gamma_1 = \rho acR^2/\int \eta^2 dm$	Model Lock number, first mode
δ_I	Forward control input
δ_{II}	Left control input
δ_o	Collective control input
λ	Inflow ratio, positive up
μ	Advance ratio
Ω	Rotor angular speed

ω	Non-dimensional frequency
ρ	Air density
σ	Standard deviation, or blade solidity
τ	Control actuator time constant
θ	Blade pitch angle, or aircraft attitude angle, earth fixed
θ_l	Blade linear twist
$\theta_I = -\theta_s$	Forward cyclic pitch
$\theta_{II} = \theta_c$	Left cyclic pitch
η	First blade flap-bending mode with unit tip deflection
$\S$	Real part of characteristic value

Superscripts

$\cdot$	$d\cdot\cdot/dt$
$-$	Space-fixed reference system
$'$	$d\cdot\cdot/dx$

Subscripts

b	Blade
h	Hub or rotor
k	kth blade
xyz	Referring to x,y,z body axes (forward, right, down)
$u,v,w,p,q,r,\theta_I,\theta_{II},\alpha_I,\alpha_{II}$	Derivatives
o	Mean value for all blades

Integration

$\int^*$	Indicates that integration limits depend on flow region

Note: The same symbols are used also for non-dimensional quantities for which unit length = R, unit velocity = ΩR, unit force = $mR\Omega^2$, unit moments about x,y,z axes: $\Omega^2 I_x, \Omega^2 I_y, \Omega^2 I_z$

Introduction

Reference 1 dealt with flap bending corrections to the rigid blade analysis of lifting rotors and came to the conclusion that except for very high advance ratios hub moments and stability characteristics of hingeless rotors can be computed with reasonable approximation if only the first rotating flap bending mode is considered. This result is in essential agreement with Reference 2 which, however, indicates that at low blade flap frequencies increasing effects of the second flap bending modes beyond rotor advance ratios of .5 occur. Reference 2 uses an expansion of the blade deflection in terms of non-rotating natural modes. When using rotating modes as in Reference 1 the effects of second and higher modes are less important. The conclusions of References 1 and 2 are in contradiction to those of Reference 3, where rotating natural modes were used. Reference 3 shows even at the advance ratio of .5 very large second mode effects on the blade response to cyclic pitch as expressed by the trim values, particularly for 6° twisted blades. The work reported in the following section was directed toward finding an explanation for this discrepancy. This effort was successful and confirmed the findings of References 1 and 2 that at .5 advance ratio hingeless rotor hub moments can be approximately determined with a single elastic flap bending mode analysis. The result pertains to a linear analysis including reversed flow effects and moderate blade twist. The result may not be valid for non-linear high lift stall conditions and for highly twisted

blades. Also the second flap-bending mode becomes increasingly important for rotor advance ratios beyond 1.0. For conventional advance ratios up to .4 References 2 and 4 show that even the rigid blade analysis with an equivalent hinge off-set gives approximate hub moments and can therefore be used in the flight dynamics of hingeless rotorcraft. In the rotor-body dynamics studied in this report the .4 rotor advance ratio cases have been computed with the rigid blade model, while the .8 rotor advance ratio cases used elastic flap-bending of the blades using the first mode only.

The purpose of the rotor-body dynamics study is to shed some light on the question of how to best overcome the disadvantages of hingeless rotor craft with respect to control and stability characteristics at high rotor advance ratio. Hingeless rotorcraft, on which much interest has been recently focused because of their expected better maintainability, have good handling qualities at low advance ratio. As compared to articulated rotorcraft the response to cyclic pitch input occurs with a much shorter time delay, the pitch and roll damping values are much higher, so is the control power which allows a larger center of gravity travel of the aircraft. However, the handling qualities of hingeless rotorcraft deteriorate with increasing advance ratio. The longitudinal control sensitivity increases substantially, control cross coupling effects occur, pitch-up divergence develops which increases with advance ratio and the rotorcraft becomes increasingly gust sensitive. All of these trends take place also

in articulated rotorcraft with off-set hinges, only to a lesser degree. Because of its high control power and unfavorable handling qualities at high advance ratio the hingeless rotorcraft is a good candidate for a fly-by-wire control system with full authority feedback controls. Theoretically one need not measure rotor states but only some of the body state variables like rates of pitch, roll and yaw. The remaining state variables can be estimated with the help of an on board computer and then used as inputs to a feedback system optimized with respect to a certain quadratic performance index which could include dynamic loads and handling qualities. Quite apart from the fact that such a system proposed for example in Reference 5, will remain beyond the state of the art for some time, it has a basic defect since it assumes that the parameters of the rotor-body dynamic system are known. For a rotorcraft these parameters are not only time varying but they also depend on the state, since the system is non-linear, and they are only incompletely known. Pending the solution of these difficulties and the acceptance of full authority real time computer controlled fly-by-wire systems, there are two ways of solving the problem. The first way is to use an inner loop multiple channel electronic (or fluidic) feedback system, possibly with inputs from rotor states, but otherwise similar to present ASE systems. In case of failure of one channel the pilot would reduce speed to a level where he could safely revert to the mechanical back up controls in case of a complete failure of the electronic system. Such a system is

described in Reference 6. The second way is to use an integrated mechanical rotor feedback system with the safety features of the primary controls. This approach was taken for the various Lockheed helicopter prototypes. The original Lockheed feedback control system suffered from spurious feedbacks from blade torsion and blade edgewise motions and has been replaced by one with pure blade flapping feedback described and analysed in Reference 7. The system is rather complex since it uses a freely floating spring restrained and damped gyroscope. The system, though quite effective in alleviating a step gust, is not very effective in reducing dynamic rotor loads from atmospheric turbulance.

In the following a number of gyroless rotor feedback systems are studied with respect to their effects on control sensitivity, control cross-coupling, stability with fixed hub, stability of the rotor-body system and atmospheric turbulence response. It is assumed that the feedback makes use of the blade root flap bending deflections as direct inputs to the hydraulic control actuators which respond with a first order time lag. If the control system above the actuators is sufficiently flexible, a purely structural feedback of flap-bending and lag-bending deflections into blade pitch is possible and has been studied in References 4 and 8. These structural feedbacks are limited in their potential effects by the usual requirement of a stiff control system. They nevertheless can considerably improve the handling characteristics of hingeless rotorcraft at moderate rotor advance ratios. For higher advance ratios feedbacks to the input side of the control actuators are needed.

Since equations for the rotor-body dynamics have not been published to date - though most of the helicopter manufacturers have developed such analytical models - the equations are first presented for the general non-linear case and subsequently linearized. The equations include reversed flow effects but they do not include dynamic inflow, stall or large angle effects. The equations also do not include edgewise or torsional blade flexibility, though some of the rotor feedback systems studied could be approximated by elastic and inertial couplings between flap-bending and blade pitch to which a steady edgewise blade deflection can contribute. From studies like Reference 6 it appears that rotor feedback systems using blade flapping as inputs are not substantially affected by the edgewise blade dynamics, unless edgewise moments couple with the rotor controls as was the case for the original Lockheed gyro control system.

The rotor feedback systems are first screened with respect to minimizing control cross coupling and longitudinal control sensitivity changes. Those which result in low cross coupling and low control sensitivity changes over the flight range from 0 to .8 advance ratio are then further studied with respect to fixed hub stability limits and free body stability limits, at .4 and .8 advance ratio whereby linear longitudinal and lateral and angular yaw motions were restrained to concentrate on the problem of pitch-roll divergence. The numerical examples refer to a winged helicopter with two types of blades: a relatively soft constant thickness blade with first flap-bending frequency of 1.21,

and a stiff tapered thickness blade with a flap-bending frequency of 1.47. The effects of varying gain factors and actuator time constants are studied for three feedback systems. For some of the configurations responses to atmospheric turbulence are determined for an advance ratio of .8.

It should be noted that even the softer of the two hingeless rotor configurations studied herein with a flap-bending frequency of 1.21 is relatively stiff as compared to current hingeless rotors which vary in blade flap bending frequency from 1.06 to 1.12. The designs with stiffer blades are structurally easier to handle and alleviate the large edgewise blade bending moments from inertial forces inherent in hingeless rotor types. However, the detrimental flying qualities at high advance ratio are getting worse with increasing flap-bending stiffness and the need for rotor feedback systems becomes more urgent. Since we are here interested in the rotor-body dynamics as affected by rotor feedback systems, a higher blade flap bending stiffness than currently used has been assumed for the constant thickness blade.

Effects of Coupling Between Blade Flap-Bending Modes

The problem of explaining the discrepancies between References 1 and 2 on the one side and Reference 3 on the other side has been briefly treated in Reference 9. Here a somewhat more detailed discussion will be given.

The equations of blade flap bending as derived in Reference 1 are

$$(1/\gamma_i)\ddot{\beta}_i + (1/2)\sum_j C_{ij}\dot{\beta}_j + (1/\gamma_i)\omega_i^2\beta_i + (1/2)\sum_j K_{ij}\beta_j = (1/2)(\lambda\psi_{\lambda_i} + \theta\psi_{\theta_i} + \theta_1\psi_{\theta_{1i}}) \qquad (1)$$

In the rotor analysis of Reference 3 the coupling terms between the modes, C_{ij}, K_{ij} for $i \neq j$ were neglected. During the discussion following the presentation of Reference 9 some surprise was expressed that normal mode equations could be coupled. In fact, the normal modes used refer to an operating condition of the rotor in vacuum without any airloads. One could establish the normal modes including linear aerodynamics. In this case modes and eigenvalues would be complex valued, but the generalized coordinate equations would be uncoupled. Instead, we followed the usual practice of using generalized coordinates for real normal modes and eigenvalues only realized in vacuum, but then the equations for the normal coordinates β_i become coupled by aerodynamic terms C_{ij} and K_{ij}, $i \neq j$.

Fig. 1, which is reproduced from Fig. 3 of Reference 3, shows the longitudinal pitch required to trim a constant pitching moment vs. advance ratio μ for an unloaded rotor with blade

Lock number $\gamma = 12$ and blade first flapwise frequency of $\omega_1 = 1.21$. Without blade twist Fig. 1 shows a small change in trim when the second mode is added. With a linear blade twist of $\theta_1 = -.1$ radius, there is a substantial second mode effect and increased aft stick deflection is required to trim the rotor. In order to examine the effect of the coupling between the modes on moment derivatives and trim conditions, a four bladed unloaded rotor with Lock number $\gamma = 12$, $\omega_1 = 1.21$, $\omega_2 = 4.33$ is selected. Blade mass and stiffness distributions are uniform. The characteristics of the selected rotor are quite similar to those used for Fig. 1. Since in Reference 3 the modified Lock number γ^* is used to account for the effect of first harmonic induced velocity variations we have

$$\gamma^* = \gamma/(1 + a\sigma/8\mu) = 10.26 \qquad (2)$$

for $\mu = .5$ and $a\sigma = .68$.

The methods ABC refer to:

A	single mode analysis
B	two mode analysis including intermode coupling
C	two mode analysis for $K_{21}=K_{12}=C_{12}= 0$

Table 1 shows the hub moment responses to inputs of unit cyclic pitch, collective pitch, inflow and blade linear twist. There is not much difference between the results of methods A and B, however there are substantial differences between the results of methods B and C, particularly for the rolling response to θ_c which changes from -.0169 to -.0184 when omitting the intermodal coupling terms.

Table 2 shows the cyclic and collective pitch required to balance a 10,000 ft-lb nose down hub pitching moment at $\mu = .5$, which is the case assumed in Reference 3 shown in Fig. 1. With untwisted blades, the values of θ_s, θ_o, θ_c required for trim are nearly the same for all three methods. When blades are linearly twisted with $\theta_1 = -.1$, the variation between the results of methods A and B remains small, however the neglect of the coupling terms for method C now has a substantial effect. The longitudinal cyclic pitch for trim changes from $\theta_s = .0306$ to .0460 which is a 50% increase. By looking into the computational details, one finds that this large difference in trim is mainly caused by the above mentioned rolling moment derivative with lateral control which changes from -.0169 to -.0184. This error is greatly amplified in the trim analysis due to taking small differences of large numbers. Tables 1 and 2 indicate that the large second blade flapping mode effect found in Reference 3 for the case of Fig. 1 is caused by omitting the intermode coupling terms. The omission of these coupling terms can cause larger errors than the omission of the entire second mode.

In order to show that indeed the omission of the second blade flap-bending mode has almost no effect on the stability margins, the same rotor assumed for Tables 1 and 2, except for $\gamma = 5$ and three blades was studied with respect to its characteristic values at advance ratio .8 when the gain of a lagged hub moment feedback control K_i was varied. Fig. 2 shows the results of the stability analysis except for the high frequency

Table 1

Control Derivatives

$\mu = .5$, $\gamma = 12 (\gamma^* = 10.26)$, $\omega_1 = 1.21$, $\omega_2 = 4.33$

Input	Response	A	B	C
$\theta_s = 1$	$C_m/a\sigma$	.0328	.0321	.0322
	$C_\ell/a\sigma$	-.0034	-.0043	-.0029
$\theta_o = 1$	$C_m/a\sigma$	.0364	.0356	.0355
	$C_\ell/a\sigma$	.0021	.0009	.0025
$\theta_c = 1$	$C_m/a\sigma$	-.0089	-.0086	-.0085
	$C_\ell/a\sigma$	-.0172	-.0169	-.0184
$\lambda = 1$	$C_m/a\sigma$	.0284	.0274	.0247
	$C_\ell/a\sigma$	.0054	.0035	.0057
$\theta_1 = 1$	$C_m/a\sigma$	.0275	.0270	.0285
	$C_\ell/a\sigma$	.0041	.0036	.0041

Table 2

Trim Values

$\mu = .5$, $\gamma = 12 (\gamma^* = 10.26)$, $\omega_1 = 1.21$, $\omega_2 = 4.33$,
$C_T = 0$, $\lambda = 0$, (M = -10,000 Ft-lb)

Blade Twist	Pitch Control	A	B	C
$\theta_1 = 0$	θ_s	.0229	.0230	.0235
	θ_o	-.0140	-.0140	-.0143
	θ_c	-.0062	-.0066	-.0056
$\theta_1 = -.1$	θ_s	.0314	.0306	.0460
	θ_o	.0496	.0504	.0410
	θ_c	-.0238	-.0266	-.0243

characteristic values due to the second flap-bending mode which remains quite stable over the selected range of feedback gains. The single mode moment balance method is explained in Reference 1, also the mode shape factor κ. It is seen that all three methods agree very well with each other so that the single mode analysis, even in its simplified form, is very adequate for the rotor configuration indicated in Fig. 2. Examples of stability characteristics with the same rotor feedback system and comparing the same 3 methods for a much stiffer blade with tapered thickness are given in Reference 9 with the result that the single mode analysis is very good for $\mu = .8$ but leads to small errors for $\mu = 1.6$.

Non-Linear Rotor-Body Dynamics

As a first approximation to Rotorcraft flight dynamics one can use an approach which has been widely applied for rotorcraft. In this approach the effect of the rotor on the body is described by a 6 x 6 derivative matrix. If the rotorcraft is symmetrical with respect to the plane through longitudinal and vertical axis and if the origin of the body fixed reference system x,y,z is in the center of gravity of the aircraft, the equations of motion are:

$$
\begin{aligned}
&\dot{u} - vr + wq = -g \sin\theta + X/m \\
&\dot{v} - wp + ur = g \sin\phi \cos\theta + Y/m \\
&\dot{w} - uq + vp = g \cos\phi \cos\theta + Z/m \\
&\dot{p} + rq(I_z - I_y)/I_x - (pq + \dot{r})I_{xz}/I_x = L/I_x \\
&\dot{q} + pr(I_x - I_z)/I_y - (r^2 - p^2)I_{xz}/I_y = M/I_y \\
&\dot{r} + pq(I_y - I_x)/I_z - (\dot{p} - rq)I_{xz}/I_z = N/I_z \\
&\dot{\phi} = p + (r \cos\phi + q \sin\phi)\tan\theta \\
&\dot{\theta} = q \cos\phi - r \sin\phi \\
&\dot{\psi} = (r \cos\phi + q \sin\phi)/\cos\theta
\end{aligned}
\qquad (3)
$$

Here the positive body axes x,y,z are forward, right, down respectively. Positive linear velocities u,v,w are in the directions of the positive body axes x,y,z. Positive angular velocities p,q,r are clockwise seen in the positive x,y,z directions. The only off-diagonal non-zero term of the inertial tensor is I_{xz}. The attitude angles ϕ,θ,ψ are taken with respect to earth fixed axes. If the location of the hub center with respect to

the aircraft c.g. is defined by h_x, h_z, the rotor contributions to X,Y,Z,L,M,N are, according to the derivative concept, given by

$$X_h = X_{ho} + X_{hu}u_h + X_{hv}v_h + X_{hw}w_h + X_{hp}p + X_{hq}q + X_{hr}r \tag{4}$$

and corresponding equations for Y_h and Z_h.

$$\begin{aligned} L_h = {} & L_{ho} + h_z Y_{ho} + (L_{hu} + h_z Y_{hu})u_h + (L_{hv} + h_z Y_{hv})V_h \\ & + (L_{hw} + h_z Y_{hw})W_h + (L_{hp} + h_z Y_{hp})p \\ & + (L_{hq} + h_z Y_{hq})q + (L_{hr} + h_z Y_{hr})r \end{aligned} \tag{5}$$

and corresponding equations of M_h and N_h.

Thus the rotor behavior is described by the 36 derivatives of the hub forces and moments with respect to the linear and angular velocities. In addition control derivatives and feedback effects must be included. For articulated rotors with small hinge off-set the hub moments are small as compared to the moments of the hub forces about the c.g. For hingeless rotors the opposite is true, the more so the stiffer the blades.

The derivative approach to rotorcraft flight mechanics assumes that the rotor instantaneously adjusts to changes in linear or angular velocities or to changes in control positions. While the slow flight dynamics modes like the phugoid or dutch roll modes are described well by the derivative approach, the short period modes may be in error. Very little has been published from which the magnitude of this error could be obtained as a function of the basic rotor design parameters. Reference 10 shows that the inclusion of 3 rotor degrees of

freedom produces a pronounced short period response of the rotorcraft which is absent in the conventional 6 x 6 derivative analytical model. This result refers to an articulated rotor with off-set hinges. Whether or not for hingeless rotors the effect of the rotor degrees of freedom will be smaller or larger is not known. It may be also possible, to substantially improve the derivative approach by using a first order filter for the rotor response to angular pitching or rolling velocities or to cyclic control inputs. Pending the accumulation of more experience with the effects of rotor modes, it is prudent to include at least the first cyclic and collective flap-bending modes in a flight dynamics analysis, particularly if high gain rotor feedback systems are to be studied, which is the approach taken in this report.

When formulating rotor-body dynamics in a body-fixed reference system which is necessary for flight dynamics purposes, numerous additional terms occur. There are also inflow terms involved which are by no means fully known at present. In a first approximation, following Reference 3, the dynamic inflow effects can be treated by reducing the blade inertia number. The following results refer to a rotor analytical model with straight blades flexibly hinged at the rotor center. The hub is assumed to perform linear velocities and accelerations in all three directions and pitching and rolling velocities and accelerations. Gravitational effects are omitted. The first of the following equations is for a blade in a rotating reference system

attached to a moving and accelerated hub. The following equations are for the rotor moments and forces. The inflow λ may be varying with radius and with azimuth.

Flapping Equation

$$\left\{(\ddot{\beta} + p^2\beta) - \beta(p\cos\psi - q\sin\psi)^2 + 2\Omega(q\sin\psi - p\cos\psi) - (\dot{q}\cos\psi + \dot{p}\sin\psi)\right\} R^3\int_o^1 m\chi^2 d\chi + \left\{\left[(\dot{u}_h + qw_h)\cos\psi - (\dot{v}_h - pw_h)\sin\psi\right]\beta - (\dot{w}_h + pv_h - qu_h)\right\} R^2\int_o^1 m\chi d\chi$$

$$= (1/2)\rho acR^2\int^{*}\left\{(U_h\sin\psi + V_h\cos\psi)^2 + 2\chi R(U_h\sin\psi + V_h\cos\psi)\left[\Omega - (q\sin\psi - p\cos\psi)\beta\right] + \chi^2R^2\left[\Omega - (q\sin\psi - p\cos\psi)\beta\right]^2\right\}\theta\chi d\chi + (1/2)\rho acR^2\int^{*}\left\{\left[W_h + \lambda\Omega R - (U_h\cos\psi - V_h\sin\psi)\beta\right](U_h\sin\psi + V_h\cos\psi) + \chi R(p\sin\psi + q\cos\psi - \dot{\beta})(U_h\sin\psi + V_h\cos\psi) + \chi R\left[\Omega - (q\sin\psi - p\cos\psi)\beta\right]\left[W_h + \lambda\Omega R - (U_h\cos\psi - V_h\sin\psi)\beta\right] + \chi^2R^2\left[\Omega - (q\sin\psi - p\cos\psi)\beta\right](p\sin\psi + q\cos\psi - \dot{\beta})\right\}\chi d\chi \qquad (6)$$

Pitching Moment From Rotor

$$M_h = -\sum_{\kappa=1}^{b}(p^2 - \Omega^2)\beta_\kappa\cos\psi_\kappa R^3\int_o^1 m\chi^2 d\chi + h_x Z_h - h_z X_h \qquad (7)$$

Rolling Moment From Rotor

$$L_h = -\sum_{\kappa=1}^{b}(p^2 - \Omega^2)\beta_\kappa\sin\psi_\kappa R^3\int_o^1 m\chi^2 d\chi + h_z Y_h \qquad (8)$$

Z Force From Rotor

$$Z_h = \sum_{\kappa=1}^{b}\int^{*} dZ(\psi_\kappa) - m_r(\dot{w}_h + pv_h - qu_h) + \sum_{\kappa=1}^{b}\ddot{\beta}_\kappa R^2\int m\chi d\chi \qquad (9)$$

where

$$X_h = \sum_{\kappa=1}^{b} \int^{*} dX(\psi_\kappa) - m_r(\dot{U}_h + q\ W_h) \tag{10}$$

$$Y_h = \sum_{\kappa=1}^{b} \int^{*} dY(\psi_\kappa) - m_r(\dot{V}_h - p\ W_h) \tag{11}$$

$$dX(\psi) = (dL\phi_b - dD)\sin\psi + dL\beta\cos\psi \tag{12}$$

$$dY(\psi) = (dL\phi_b - dD)\cos\psi - dL\beta\sin\psi \tag{13}$$

$$dZ(\psi) = -\ dL \tag{14}$$

$$\begin{aligned} dL = {} & (1/2)\rho acR\Big\{(U_h\sin\psi+V_h\cos\psi)^2+2\chi R(U_h\sin\psi+V_h\cos\psi) \\ & \Big[\Omega-(q\sin\psi-p\cos\psi)\beta\Big]+\chi^2R^2\Big[\Omega-(q\sin\psi-p\cos\psi)\beta\Big]^2\Big\}\ominus d\chi \\ & + (1/2)\rho acR\Big\{\Big[W_h+\lambda\Omega R-(U_h\cos\psi-V_h\sin\psi\beta\Big](U_h\sin\psi+V_h\cos\psi) \\ & +\chi R(p\sin\psi+q\cos\psi-\dot{\beta})(U_h\sin\psi+V_h\cos\psi)+\chi R\Big[\Omega \\ & -(q\sin\psi-p\cos\psi)\beta\Big]\Big[W_h+\lambda\Omega R-(U_h\cos\psi-V_h\sin\psi)\beta\Big] \\ & +\chi^2R^2\Big[\Omega-(q\sin\psi-p\cos\psi)\beta\Big](p\sin\psi+q\cos\psi-\dot{\beta})\Big\}d\chi \end{aligned} \tag{15}$$

$$\begin{aligned} dD = {} & (1/2)\rho ac\delta R\Big\{(U_h\sin\psi+V_h\cos\psi)^2+2\chi R(U_h\sin\psi+V_h\cos\psi) \\ & \Big[\Omega-(q\sin\psi-p\cos\psi)\beta\Big]+\chi^2R^2\Big[\Omega-(q\sin\psi-p\cos\psi)\beta\Big]^2\Big\}d\chi \end{aligned} \tag{16}$$

$$\begin{aligned} dL\,\phi_b = {} & (1/2)\rho acR\Big\{\Big[W_h+\lambda\Omega R-(U_h\cos\psi-V_h\sin\psi)\beta\Big](U_h\sin\psi+V_h\cos\psi) \\ & +\chi R(p\sin\psi+q\cos\psi-\dot{\beta})(U_h\sin\psi+V_h\cos\psi)+\chi R \\ & \Big[\Omega-(q\sin\psi-p\cos\psi)\beta\Big]\Big[W_h+\lambda\Omega R-(U_h\cos\psi-V_h\sin\psi)\beta\Big] \\ & +\chi^2R^2\Big[\Omega-(q\sin\psi-p\cos\psi)\beta\Big](p\sin\psi+q\cos\psi-\dot{\beta})\Big\}\ominus d\chi \\ & + (1/2)\rho acR\Big\{\Big[W_h+\lambda\Omega R-(U_h\cos\psi-V_h\sin\psi)\beta\Big]^2+2\chi R \\ & \Big[W_h+\lambda\Omega R-(U_h\cos\psi-V_h\sin\psi)\beta\Big](p\sin\psi+q\cos\psi-\dot{\beta}) \\ & +\chi^2R^2(p\sin\psi+q\cos\psi-\dot{\beta})^2\Big\}d\chi \end{aligned} \tag{17}$$

The preceding equations are all dimensional. For the applications they must be non-dimensionalized. Depending on the flight condition - curved flight or straight flight - different linearizations of these equations must be made. In the following section the straight flight condition is treated.

Linearized Rotor-Body Dynamics

We will assume that the aircraft performs a uniform forward motion and is restrained in yaw and side motion. The aircraft is, however, free to pitch and roll and to move vertically. Thus we have added the roll motion to the usual longitudinal flight dynamics since for hingeless rotors pitch and roll are strongly coupled. Phugoid and dutch roll cannot occur with the assumed restraint. The main purpose of the analysis is to obtain information on pitch divergence which is one of the flight dynamic problems of hingeless rotors. The inclusion of roll should considerably improve the data on pitch divergence as compared to a purely longitudinal type of motion, since the rotor is represented by advancing, regressing and coning modes. Rotor wake effects are not included and can be assumed to be covered by an "equivalent Lock number" for the asymmetric wake and by an "equivalent coning feedback" for the symmetrical wake. The fuselage is assumed to carry a fixed wing and a horizontal tail surface. The wing contributes to vertical and roll damping. Comparisons with configurations without wing - not shown in this report - have consistently resulted in slightly less stable conditions than with the wing. Wing AC and aircraft CG are assumed to coincide so that the wing does not contribute to the pitching moment. Pitch damping of the wing is neglected. The effect of downwash lag on the tail is neglected, in other words the equations do not include a rate of angle of attack term. The downwash itself on the tail is considered by a 50% reduction in tail lift slope.

Rather than formulating the problem first for the non-linear case on the basis of the equations in the preceding section, and then performing the linearization, we will proceed here by first writing the linear equations in a space-fixed reference system and then transforming to a body fixed system. The equations are first written for straight blades and have been used in this form for the numerical examples at .4 rotor advance ratio. First mode blade flexibility and reversed flow have been used for the numerical examples at .8 advance ratio. Three blades have been assumed throughout. The moment of the rotor horizontal forces with respect to the aircraft c.g. have been neglected as compared to the blade root moments. In contrast to the equations of the preceding section, non-dimensional quantities are used from now on without changing the symbols.

Flapping Equation

$$\ddot{\bar{\beta}}_k + (\gamma/2)C(\psi_k)\dot{\bar{\beta}}_k + [(\gamma/2)K(\psi_k) + 1]\bar{\beta}_k + (P^2-1)(\bar{\beta}_k - \alpha_k) - \bar{w}\, S_b/I_b = \alpha_I\, m_{\theta_I}(\psi_k) + \alpha_{II}\, m_{\theta_{II}}(\psi_k) + \bar{w} m_{\bar{w}}(\psi_k) \tag{18}$$

Body Equations

$$\ddot{\alpha}_I - \dot{\alpha}_I M_{\dot{\alpha}_I} - \alpha_I M_{\alpha_I} = (P^2-1)(b/2)(I_b/I_y)(\bar{\beta}_I - \alpha_I) \tag{19}$$

$$\ddot{\alpha}_{II} - \dot{\alpha}_{II} L_{\alpha_{II}} = (P^2-1)(b/2)(I_b/I_x)(\bar{\beta}_{II} - \alpha_{II}) \tag{20}$$

$$\dot{\bar{w}} - \alpha_I Z_{\alpha_I} - \bar{w} Z_{\bar{w}} - \alpha_I Z_{\alpha_I} = Z_h \tag{21}$$

This system of equations includes 11 state variables, 6 for the rotor, 5 for the body (α_I, $\dot{\alpha}_I$, α_{II}, $\dot{\alpha}_{II}$, w). Performing a

Floquet type of stability analysis with this system, one finds two of the characteristic values of the state transition matrix to be zero. When transforming to body axes we have only 9 state variables. The transformation to body axes is defined by

$$\bar{\beta}_k = \beta_k + \alpha_I \cos\psi_k + \alpha_{II} \sin\psi_k \tag{22}$$

$$\bar{w} = w + \mu\alpha_I, \quad \dot{\bar{w}} = \dot{w} - \mu q, \quad \dot{\alpha}_I = -q, \quad \dot{\alpha}_{II} = -p$$

The transformed equations read

Flapping Equation

$$\ddot{\beta}_k + P^2\beta_k - \dot{q}\cos\psi_k - \dot{p}\sin\psi_k + 2(q\sin\psi_k - p\cos\psi_k) + (\gamma/2)(C(\psi_k)[\beta_k - q\cos\psi_k - p\sin\psi_k] + (\gamma/2)K(\psi_k)\beta_k - (\dot{w}-\mu q)S_b/I_b = wm_w(\psi_k) \tag{23}$$

Body Equations

$$\dot{q} - qM_q - (w/\mu)M_{w/\mu} = -(P^2-1)(b/2)(I_b/I_y)\beta_I \tag{24}$$

$$\dot{p} - pL_p = -(P^2-1)(b/2)(I_b/I_x)\beta_{II} \tag{25}$$

$$w - q\mu - wZ_w - qZ_q = Z_h \tag{26}$$

The flapping equation can be written in the 3 multiblade coordinates β_I, β_{II}, β_o which results in 3 separate equations. The rotor Z force can also be expressed in these multiblade coordinates. The 9 state variables are then β_I, $\dot{\beta}_I$, β_{II}, $\dot{\beta}_{II}$, β_o, $\dot{\beta}_o$, q, p, w. The corresponding equations including blade flap-bending according to the first mode can be derived with the methods of Reference 1. One obtains

Flapping Equation

$$(\ddot{\beta} + \omega_1^2 \beta) + 2(q \sin\psi - p\cos\psi)\int_o^1 x\eta m dx / \int_o^1 \eta^2 m dx - (\dot{p}\sin\psi + \dot{q}\cos\psi)\int_o^1 x\eta m dx / \int_o^1 \eta^2 m dx + (q\mu - \dot{w})\int_o^1 \eta m dx / \int_o^1 \eta^2 m dx = \frac{\gamma_1}{2}\int^* (U_T^2\theta + U_p U_T)\eta dx \tag{27}$$

where

$$U_T = x + \mu\sin\psi \tag{28}$$

$$U_p = w - \dot{\beta}\eta + x(p\sin\psi + q\cos\psi) - \mu\cos\psi\beta\eta' \tag{29}$$

Body Equations

$$\dot{p} - L_p P = L_h \tag{30}$$

$$\dot{q} - M_q q - M_w w = M_h \tag{31}$$

$$\dot{w} - q\mu - Z_w w - Z_q q = Z_h \tag{32}$$

$$M_h = \frac{R^2 m_b}{I_y}\left[\sum_{k=1}^{b}\left\{(\ddot{\beta}_k + \beta_k)\int_o^1 x\eta m dx / \int_o^1 m dx - \frac{\gamma_1}{2}\frac{\int_o^1 m\eta^2 dx}{\int_o^1 m dx}\int^* (U_T^2\theta + U_p U_T)x dx\right\}\cos\psi_k - b(p + .5\dot{q})\frac{\int_o^1 x^2 m dx}{\int_o^1 m dx}\right] \tag{33}$$

$$Z_h = \frac{m_b}{m}\sum_{k=1}^{b}\left\{\ddot{\beta}_k\int_o^1 \eta m dx / \int_o^1 m dx - \frac{\gamma_1}{2}\frac{\int_o^1 m\eta^2 dx}{\int_o^1 m dx}\int^* (U_T^2\theta + U_p U_T)dx\right\} \tag{34}$$

$$L_h = \frac{R^2 m_b}{I_x}\left[\sum_{k=1}^{b}\left\{(\ddot{\beta}_k + \beta_k)\int_o^1 x\eta m dx \Big/ \int_o^1 m dx - \frac{\gamma_1}{2}\frac{\int_o^1 m\eta^2 dx}{\int_o^1 m dx}\right.\right.$$
$$\left.\left.\int^{*}(U_T^2\,\theta + U_p U_T)\,x dx\right\}\sin\psi_k + b(q - .5\dot{p})\frac{\int_o^1 x^2 m dx}{\int_o^1 m dx}\right] \quad (35)$$

The angle β is here the slope of the line from rotor center to blade tip. Including rotor feedback and control inputs we have for the multiblade pitch

$$\theta_I + \tau\dot{\theta}_I = -K_p(\beta_I \cos\varepsilon - \beta_{II}\sin\varepsilon) + \delta_I \cos\phi - \delta_{II}\sin\phi \quad (36)$$

$$\theta_{II} + \tau\dot{\theta}_{II} = -K_p(\beta_I \sin\varepsilon + \beta_{II}\cos\varepsilon) + \delta_I \sin\phi + \delta_{II}\cos\phi \quad (37)$$

$$\theta_o + \tau\dot{\theta}_o = -K_o\,\beta_o + \delta_o \quad (38)$$

The time lag τ will be assumed the same for all control actuators. The control phase angle ϕ will be selected for minimal control cross coupling. The propontional feedback phase angle ε will be selected for minimal change in longitudinal control sensitivity between advance ratio 0 and .8. Three types of feedback system will be studied in mumerical examples.

$K_o \neq 0, \quad K_p = 0$ Coning Feedback (39)

$K_o = 0, \quad K_p \neq 0$ Proportional Feedback (40)

$K_o = K_p$ Combined Feedback (41)

The systems were selected such that they could be designed in a purely mechanical way, whereby the inputs to the control actuators are assumed to be proportional to β_I, β_{II}, β_o. In

case of electronic sensors shaping filters could be used and a much greater variety of feedback systems would be possible.

The Use of Rotor Feedback to Minimize Control Cross Coupling

There are two types of control cross coupling: First the cross coupling due to a direct control input which is the effect of control applications on the fixed fuselage, second the cross coupling due to fuselage angular rates, which is also called damping cross damping. The stiffer the blades of a hingeless rotor the smaller the time between application of a cyclic control and the asymptotic angular rate response. The pilot will then hardly notice the difference between the two types of cross coupling in flight. A longitudinal control input will result in an angular rate in pitch and roll which is determined both by the direct control cross coupling and by the damping cross coupling.

For an articulated rotor with central hinges the blade flapping natural frequency coincides with the frequency of rotor revolution. If cyclic control is phased such that maximum longitudinal cyclic pitch occurs at 90° azimuth angle, no direct control cross coupling will occur, however, there will be a damping cross coupling, since for example angular pitch up velocity produces not only down tilting from gyroscopic moments but also left tilting from air moments. Since both left and right banked turns involve a pitch up rate, the rotor tilts left in both types of turns leading to the well known differences in lateral control requirements for left and right turns.

As the blade flapping frequency increases by either the use of delta three coupling or of off-set hinges or of increasing flap-bending stiffness of hingeless blades, the azimuth for maximum flapping in response to cyclic control input or to angular rates is rotated opposite to the direction of rotor rotation. The cross damping first disappears and then assumes the opposite sign, whereby a pitch-up rate produces a right tilt. A useful visualization of these relations in the form of complex coordinates has been given in Reference 11. The control phase angle can be adjusted to compensate for the cross-coupled response both from direct control effects and from the angular rate effects, provided the cross coupling remains approximately constant over the flight speed regime and provided the cross-coupling response for pitch-roll is the same as for roll-pitch. Without rotor feedback neither of these two requirements are satisfied and a compromise control phase angle is the more difficult to establish the higher the blade flapping frequency. As will be shown, certain rotor feedback systems go a long way toward satisfying the two requirements, so that small control cross coupling values can be obtained for all μ with the proper control phasing.

We will first consider the direct control responses with fixed hub, then look at rotor responses to pitch and roll rates, and finally present a few examples of dynamic responses with the body free to pitch and roll and heave but restrained

otherwise. The two sample rotors have 3 blades and a Lock number of 5. For the constant thickness blade the flap-bending frequency is 1.21, for the tapered thickness blade it is 1.47, same as in Reference 1. The gains K_o and K_p in the feedback Equs. (36) to (38) have been varied from 0 to 1.5, the feedback phase angle ε from 30° to 90°, and the lag time τ from 0 to 1.0. For a rotor operating with 4 rps a value of $\tau = 1.0$ represents a real time lag of $1/4.2\pi = 1/25$ second, which is a realistic value for a modern hydraulic actuator.

A survey of effects of feedback phase angle not shown here has indicated that from a stability point of view a value of $\varepsilon = 60°$ is close to optimum for $\tau = 0$ to 1.0. This value has been selected for the numerical examples. The stability results to be discussed in a later section show that feedback gains of 1.5 can lead to instability. We have, therefore limited the control cross coupling study to a gain of $K_p = K_o = 1$. The systems will be shown in the sequence: No feedback, coning feedback, proportional feedback, combined feedback.

Figs. 3a to 3d show for the uniform blade the cyclic control power of the 4 systems vs. control phase angle ϕ, whereby $\phi = 0$ applies to the articulated blade. The significance of the control phase angle ϕ can be seen from Eqs. (36) and (37). The 3 curves in each figure correspond to advance ratios $\mu = 0, .4, .8$. The upper and lower graphs represent control power in terms of rotor tilt angles per unit cyclic

pitch, the middle graphs represent control cross coupling power. Fig. 3a without feedback shows large variations of longitudinal control power with μ and large control cross coupling changes with μ. There is no ϕ value where the cross coupling could be compensated for all μ. Fig. 3b with coning feedback indicates a considerable improvement. A value of $\phi = 30°$ would result in reasonably low cross-coupling. Fig. 3c with proportional feedback shows still further improvement with $\phi = 45°$ being now a good choice. Fig. 3d, combined feedback, also gives at $\phi = 45°$ almost no cross coupling and almost no longitudinal sensitivity change between $\mu = 0$ and $\mu = .8$. Figs. 4a to 4d for the tapered blade show the same trend, except that the results are not quite as good. The optimum control phase angle is for all cases about $\phi = 45°$.

Table 3 gives further insights into the cross coupling effects of the 4 systems at $\mu = 0, .4, .8$. The table shows the effects of three inputs: collective control δ_o, roll rate p and pitch rate q on the rotor coning β_o, on forward longitudinal tilt β_I and left lateral tilt β_{II} for the uniform blade and for the tapered blade. Without feedback we have a large increase in collective pitch control sensitivity with μ and a large pitch-up moment with collective pitch increase. Both undesirable characteristics are strongly alleviated with rotor feedback, the combined feedback having the best results. The effects of roll and pitch rate p and q on coning are

Table 3

Cross Coupling Effects

Uniform Blade

K	μ	β_o/δ_o	β_I/δ_o	β_{II}/δ_o	β_o/p	β_I/p	β_{II}/p	β_o/q	β_I/q	β_{II}/q
$K_o = 0$	0	.424	0	0	0	1.254	2.869	0	2.869	-1.254
$K_p = 0$	.4	.528	-.968	.375	.070	1.170	2.623	-.119	3.166	-1.282
	.8	.933	-2.757	.630	.131	.841	2.149	-.393	4.192	-1.239
$K_o = 1$	0	.298	0	0	0	1.254	2.869	0	2.869	-1.254
$K_p = 0$	.4	.345	-.633	.245	.046	1.215	2.606	-.078	3.091	-1.253
	.8	.483	-1.426	.326	.068	1.028	2.106	-.204	3.631	-1.111
$K_o = 0$	0	.424	0	0	0	.940	1.443	0	1.443	-.940
$K_p = 1$	.4	.407	-.406	.269	-.070	.948	1.300	.280	1.321	-.910
$\epsilon = 60°$	.8	.393	-.736	.442	-.086	.886	1.040	.474	1.040	-.813
$K_o = 1$	0	.298	0	0	0	.940	1.443	0	1.443	-.940
$K_p = 1$	.4	.289	-.288	.191	-.050	.928	1.313	.199	1.401	-.963
$\epsilon = 60°$	.8	.282	-.529	.317	-.062	.840	1.067	.340	1.291	-.963

Tapered Blade

K	μ	β_o/δ_o	β_I/δ_o	β_{II}/δ_o	β_o/p	β_I/p	β_{II}/p	β_o/q	β_I/q	β_{II}/q
$K_o = 0$	0	.412	0	0	0	1.029	1.430	0	1.430	-1.029
$K_p = 0$	.4	.516	-.622	.444	.022	1.203	1.449	-.124	1.753	-1.266
	.8	.935	-1.958	.890	.034	1.082	1.202	-.385	2.502	-1.344
$K_o = 1$	0	.292	0	0	0	1.029	1.430	0	1.430	-1.029
$K_p = 0$	.4	.340	-.411	.293	.014	1.211	1.443	-.082	1.702	-1.230
	.8	.483	-1.010	.460	.017	1.116	1.186	-.199	2.113	-1.167
$K_o = 0$	0	.412	0	0	0	.642	.857	0	.857	-.642
$K_p = 1$	.4	.411	-.314	.261	-.025	.760	.859	.170	.883	-.745
$\epsilon = 60°$	.8	.435	-.617	.433	-.018	.692	.700	.295	.747	-.668
$K_o = 1$	0	.292	0	0	0	.642	.857	0	.857	-.642
$K_p = 1$	.4	.292	-.222	.185	-.018	.755	.864	.120	.920	-.777
$\epsilon = 60°$	.8	.303	-.430	.302	-.013	.685	.705	.206	.874	-.757

relatively small and probably not bothersome. The cross damping terms are large in all cases and not much affected by the feedback systems, except that they equalize β_I/p and β_{II}/q over the advance ratio range, so that a single control phase angle would be effective. A control phase angle of $\phi = 45°$ would approximately compensate for the damping cross coupling, at least for the rotor alone without body damping. A confirmation can be seen in Figs. 5 and 6 which show for combined feedback at advance ratio .8 the dynamic response to a longitudinal and lateral step control input using $\phi = 45°$. Lateral stick input produces within a few rotor revolutions steady rate of roll and negligible changes in q and w. Longitudinal stick input produces negligible rate of roll and a rapidly decreasing w. Note that the charts are for a forward step control input, leading to negative w, and for a left lateral stick input leading to negative p.

The coning angle becomes negative for the forward control input and positive for the left control input. The tilt β_I becomes positive (forward) for forward control input, the tilt β_{II} becomes positive (left) for left control input. The lateral tilt is asymptotically zero both for forward and left control inputs, indicating in the first case absence of cross coupling and in the second case on asymptotically constant rate. The type of response is the same for both the rotor with uniform and with tapered blades. It is quite remarkable

that a single very stiff rotor can be made to have very good flying qualities as far as control cross coupling and uniform control sensitivity over a wide advance ratio range are concerned. Both direct control cross coupling and cross damping can be effectively compensated by a 45° control phase angle if the combined gyroless rotor feedback system with gains of unity is used.

The responses were computed with Eqs. (27) to (34). The blade parameters are determined from the blade characteristics defined in Reference 1. The body derivatives were determined for a wing of 6% rotor disk area .5 span over rotor diameter ratio, 4.5 lift slope and for a horizontal tail with 1.2 R moment arm, 1.5% rotor disk area and a 1.8 lift slope including downwash effects. The assumed moment of inertia ratios are

$$I_x/I_b = 5, \quad I_y/I_b = 75, \quad R^2 m_b/I_x = .60$$

while the assumed mass ratio is $m_b/m = .02$. With these values one obtains the body derivatives

Lp = -.0200	from wing
Mq = -.0075	from tail
Mw = -.0063	from tail
Zw = -.0262	from wing
Zw = -.0026	from tail
Zq = -.0031	from tail

The right hand sides of the body Eqs. (30) to (32) depend, according to Eqs. (33) to (35) in a complicated way on flapping

angles and their derivatives, on pitch and roll rates and accelerations, on flap bending mode shape and on inflow and tangential velocities.

The integrals in Eqs. (33) to (35) have for unit blade mass the values

	Uniform Blade	Tapered Blade
$\int_o^1 m dx$	1.000	.455
$\int_o^1 m x^2 dx$	.333	.065
$\int_o^1 m \eta dx$	.415	.067
$\int_o^1 m \eta^2 dx$	.268	.033
$\int_o^1 m x \eta dx$	.296	.043

Note that the dynamic response has not been determined as frequently done by using rotor derivatives, Eqs. (4) and (5), but that instead the complete first flap-bending mode rotor dynamics according to Eqs. (33) to (35) was used. It is planned for a subsequent study to find out, in what respect response data as those shown in Figs. 5 and 6 and stability data to be shown later are affected by the conventional rotor derivative approach as compared to the full rotor dynamics approach used here.

Stability With Fixed Hub

The higher frequency rotor modes are not much affected by body motions. We, therefore, first present stability charts for the fixed hub case involving only rotor modes. In addition to these modes, the rotor-body system has long period or aperiodic modes which will be presented in separate charts with a larger scale.

The analysis derives the Floquet state transition matrix in the multiblade coordinate form and then extracts the characteristic values. The ambivalence in assigning frequency values is overcome in the same way as in the earlier work by the authors by using essentially only the positive frequency region to show all characteristic values. Since we have here 3 bladed rotors, the characteristic values could be moved up or down by a frequency of 3. For advance ratio $\mu = .4$ a straight blade was assumed and Eqs. (23) to (26) used. For advance ratio .8 flexible blades were assumed and Eqs. (27) to (34) used including reverse flow effects. Only the combined feedback case with feedback phase angle $\epsilon = 60°$ is shown which proved to be best from a point of view of minimizing control cross coupling effects. In Figs. 7 to 10 the solid curves refer to the fixed hub conditions, the dash curves refer to the coupled rotor-body modes discussed in the next section. Figs. 7a and 7b give for uniform blade the characteristic values for an actuator lag of $\tau = .5$ at advance ratios .4 and .8 respectively. The gain factor is

increased in steps, using $K_p=K_o$ = 0, .5, 1.0, 1.5. The rotor is almost unstable for a gain of 1.5, whereby the stability margin is slightly less at μ = .8. Figs. 8a and 8b valid for μ = .4 and .8 respectively, give again for the uniform blade the effects of the actuator lag time τ on the characteristic values. $K_o = K_p = 1.0$ is assumed and τ is varied from 0 to 1.0. While for μ = .4, Fig. 8a, the values τ = 0 and 1.0 show higher stability margin than τ = .5, at μ = .8 Fig. 8b shows that τ = 1 gives a lower stability margin. Increasing the actuator lag time further, will most likely lead to instability. Figs. 9 and 10 show the corresponding characteristic values for the tapered blade. The stability margins for the same $K_o = K_p$ values are now somewhat larger. It should be noted again that flapping angles are defined by the slope of the line from the rotor center to the blade tip. For the stiffer blade a given flapping angle corresponds to a larger blade root moment. The feedback gain is here defined as blade pitch angle change per unit flapping angle change, not per unit blade root moment. Figs. 10a and 10b show the effect of the actuator lag time τ. For μ = .4 the increase from τ = .5 to 1.0 has a stabilizing effect, while for μ = .8 the same increase is strongly destabilizing.

Stability Including Body Motions

The stability of the rotor-body system where the body is free to pitch and roll and heave but otherwise restrained has been studied for the two rotors and for the body with the characteristics described before. It was found that at .8 advance ratio stability could not be achieved with any one of the feedback systems alone without a horizontal tail. On the other hand, stability could not be achieved with a horizontal tail alone without a rotor feedback system, even if much larger tail sizes than 1.5% rotor disk were used. In combination with a rotor feedback system the addition of a horizontal tail first brought large improvements in stability, but increasing the tail size beyond 1.5% rotor disk area was found to be ineffective.

Figs. 11 to 14 show the stability charts for the rotor-body system for the uniform blades and for the tapered blades. The combined feedback system in conjunction with the 1.5% horizontal tail is assumed. Only the characteristic values for long period and aperiodic modes are shown in Figs. 11 to 13. The characteristic values for the short period modes are given in Figs. 7 to 10 in dash lines. Where the dash line coincides with a solid line, the characteristic values are the same as for fixed hub.

Figs. 11a and 11b show the case of $\tau = .5$ for uniform blades and varying $K_o = K_p$. The feedback phase angle is again $\varepsilon = 60°$ throughout. For zero feedback we have a divergence

which can be shown to be essentially in pitch. $K_o = K_p = 1.0$ is a stable case both for $\mu = .4$ and $\mu = .8$. Increasing the gain reduces the stability margins at $\mu = .8$ not only for the long period mode of Fig. 11b but also for the short period mode of Fig. 7b.

Figs. 12a and 12b show the effect of the actuator lag time τ on the rotor-body system for $K_o = K_p = 1.0$. There is little effect on the long period or aperiodic modes. Figs. 13 and 14 show the corresponding conditions for the tapered blade. At $\mu = .4$ the stability margin is even for $K_o = K_p = 1$ quite small and becomes larger at $\mu = .8$. The effect of actuator lag time τ is small.

Examples of Turbulence Response

The turbulence response analysis was performed for an advance ratio of $\mu = .8$ using the methos of Reference 12. The ratio of turbulence scale length over rotor radius is 12. The excitation is for a standard deviation of the vertical inflow variable $\sigma_\lambda = 1$. The turbulence analysis even for the simplifying assumption of uniform λ over the rotor disk, becomes quite demanding of computer time for a high order system. In our case of the rotor-body system in body fixed coordinates and with the combined feedback we have 13 state variables: β_o, $\dot{\beta}_o$, β_I, $\dot{\beta}_I$, β_{II}, $\dot{\beta}_{II}$, p, q, w, λ, θ_o, θ_I, θ_{II} resulting in a 13 x 13 covariance matrix, which has been determined for 4 cases: uniform blade with no feedback and with combined feedback; tapered blade with no feedback and with combined feedback. The 6% of rotor disk area wing and the 1.5% horizontal tail were present for all 4 cases. In Figs. 15 and 16 a few of the diagonal terms of the covariance matrix are presented. The random excitation starts at time t = 0. Approximately steady state is reached at t = 26 or after about 4 rotor revolutions. In each Figure curves for zero feedback and for feedback with $K_o = K_p = 1.0$, $\varepsilon = 60°$, $\tau = .5$ are shown.

For uniform blades, Fig. 15, the roll rate standard deviation is little affected by the feedback, while the pitch rate standard deviation is asymptotically much reduced, same as the coning angle standard deviation. The side tilt standard deviation

is little affected by the feedback, however the longitudinal tilt standard deviation is very much reduced. As can be seen from the relative magnitudes, the longitudinal random flapping angles are without feedback much larger than the lateral and coning values, so that blade loads will be mainly determined from longitudinal tilting. With feedback $\sigma_{\beta o}$, $\sigma_{\beta I}$ and $\sigma_{\beta II}$ have about the same value, indicating much reduced random blade loads.

For the tapered blade, Fig. 16, the pitch rate standard deviation is not much affected by the feedback system, while the roll rate standard deviation is much reduced by feedback. All blade variable standard deviations, $\sigma_{\beta o}$, $\sigma_{\beta II}$, $\sigma_{\beta I}$ are very much reduced by the feedback system, so that large reductions in blade loads will occur.

Conclusions

Four flight dynamics problems of hingeless rotors increase in severely with increasing blade flap-bending stiffness and with increasing advance ratio:

1) Longitudinal control sensitivity
2) Control and damping cross coupling
3) Pitch divergence
4) Gust sensitivity

Three gyroless full authority rotor feedback systems with flapping inputs to the control actuators were studied with respect to their effectiveness in alleviating problems 1 and 2. Coning feedback, proportional tilting feedback and a combined feedback were all found effective, the last one giving best results. This best system was further studied with respect to alleviating problems 3 and 4 and was found effective. The following detail conclusions have been obtained assuming two very different blade designs, one with uniform thickness and 1.21 blade flap-bending frequency, the other with tapered thickness and 1.47 blade flap-bending frequency. Both blades have a Lock number of 5. Both rotors have 3 blades.

- For both rotors control and damping cross coupling could be largely removed and control sensitivity made uniform between 0 and .8 advance ratio with a combined rotor feedback system with 60° feedback phase angle and 45° control phase angle.

- Feedback gains should be limited to about one unit of blade pitch angle change per unit of blade flapping angle change (line from rotor center to blade tip) to avoid instability.
- Actuator time lag stabilizes some configurations and destabilizes others and is an important parameter.
- Random rotor loads and body motions are greatly reduced by the combined rotor feedback system.

Further studies should establish in what respect coning feedback alone, or possibly a vertical acceleration feedback into collective pitch, and proportional feedback alone can achieve results which may be still acceptable though not as good as the results shown for the combined feedback system. Other than 3 bladed rotors should be treated.

Though the trends established by the study are believed to be correct, the detail results are affected by a number of simplifications which should be removed in future work, such as the uniform forward velocity, the restraints in lateral motion and yaw, the neglect of horizontal rotor forces and other simplifications. Of interest are also the effects of the rotor feedback systems on curved flight dynamics and on g-loads per unit control deflection.

References

1. Hohenemser, K. H. and Yin, S. K., "Flap Bending Corrections to the Rigid Blade Analysis of Lifting Rotors", Phase VI-A Report under Contract NAS2-4151, Part II, June 1972.

2. Ormiston, R. A. and Peters, D. A., "Hingeless Rotor Response with Non-uniform Inflow and Elastic Balde Bending", Journal of Aircraft, Vol. 9 No. 10, October 1972 pp. 730-736.

3. Curtiss, H. C. Jr. and Shupe, N. K., "A Stability and Control Theory for Hingeless Rotors", Proceedings 27th Annual National Forum, American Helicopter Society, Preprint No. 541, May 1971.

4. Reichert G., and Huber, H., "Influence of Elastic Coupling Effects on the Handling Qualities of a Hingeless Rotor Helicopter", AGARD CP 121, Advanced Rotorcraft Vol. I, September 1971.

5. Hall, W. E. Jr. and Bryson, H. E. Jr., "Inclusion of Rotor Dynamics in Controller Design for Helicopters", Journal of Aircraft Vol. 10 No. 4, April 1973, pp. 200-206.

6. Heimbold, R. L. and Griffith, C. D., "Synthesis of an Electromechanical Control System for a Compound Hingeless Rotor Helicopter", Journal American Helicopter Society Vol. 17 No. 2, April 1972, pp. 55-65.

7. Potthast, A. J. and Blaha, J. T., "Handling Qualities Comparison of Two Hingeless Rotor Control Systems", 29th Annual National Forum Proceedings of the American Helicopter Society Washington D. C. May 1973, Preprint No. 741.

8. Huber, H. B., "Effect of Torsion-Flap-Lag Coupling on Hingeless Rotor Stability" 29th Annual National Forum Proceedings of the American Helocopter Society Washington D. C. May 1973, Preprint No. 731.

9. Hohenemser, K. H. and Yin, S. K., "On the Question of Adequate Hingeless Rotor Modeling in Flight Dynamics" Proceedings 29th Annual National Forum of the American Helicopter Society, Washington D.C. May 1973, Preprint No. 732.

10. Molusis, J. and Briczinski, S., "Helicopter Derivative Identification from Analytic Models and Flight Test Data". NASA Symposium on Parameter Estimation Techniques and Applications in Aircraft Flight Testing, April 1973.

11. Curtiss, H. C. Jr., "Complex Coordinates in Near Hovering Rotor Dynamics", Journal of Aircraft, Vol. 10, No. 5 pp. 289-296, May 1973.

12. Gaonkar, G. H. and Hohenemser, K. H., "An Advanced Stochastic Model for Threshold Crossing Studies of Rotor Blade Vibrations", AIAA Journal Vol. 10, No. 8, August 1972, pp. 1100-1101.

Figure Captions

Fig. 1 — Effect of Second Flap-bending Mode According to Reference 3.

Fig. 2 — Rotor Stability Chart for 3 Analytical Methods.

Fig. 3 — Cyclic Control Power for Uniform Blade
a. No Feedback
b. Coning Feedback, $K_o = 1$
c. Proportional Feedback, $K_p = 1$, $\epsilon = 60°$
d. Combined Feedback, $K_o = K_p = 1$, $\epsilon = 60°$

Fig. 4 — Cyclic Control Power for Tapered Blade
a. No Feedback
b. Coning Feedback, $K_o = 1$
c. Proportional Feedback, $K_p = 1$, $\epsilon = 60°$
d. Combined Feedback, $K_o = K_p = 1$, $\epsilon = 60°$

Fig. 5 — Responses to Step Control Input, $\mu = .8$, $K_o = K_p = 1$, $\epsilon = 60°$, Uniform Blade
a. Longitudinal Step Input
b. Lateral Step Input

Fig. 6 — Responses to Step Control Input, $\mu = .8$, $K_o = K_p = 1$, $\epsilon = 60°$, Tapered Blade
a. Longitudinal Step Input
b. Lateral Step Input

Fig. 7 — Fixed Hub Stability Chart, Uniform Blade $\tau = .5$
a. $\mu = .4$
b. $\mu = .8$

Fig. 8 — Fixed Hub Stability Chart, Uniform Blade, $K_o = K_p = 1.0$
a. $\mu = .4$
$\mu = .8$

Fig. 9 — Fixed Hub Stability Chart, Tapered Blade $\tau = .5$
a. $\mu = .4$
$\mu = .8$

Fig. 10 — Fixed Hub Stability Chart, Tapered Blade $K_o = K_p = 1.0$
a. μ .4
b. $\mu = .8$

Fig. 11 Rotor-Body Stability Chart, Uniform Blade $\tau = .5$

a. $\mu = .4$
b. $\mu = .8$

Fig. 12 Rotor-Body Stability Chart, Uniform Blade $K_o = K_p = 1.0$

a. $\mu = .4$
b. $\mu = .8$

Fig. 13 Rotor-Body Stability Chart, Tapered Blade $\tau = .5$

a. $\mu = .4$
b. $\mu = .8$

Fig. 14 Rotor-Body Stability Chart, Tapered Blade $K_o = K_p = 1.0$

a. $\mu = .4$
b. $\mu = .8$

Fig. 15 Random Response to Vertical Turbulence, Uniform Blade, Zero Feedback and Combined Feedback, $\mu = .8$

Fig. 16 Random Response to Vertical Turbulence, Tapered Blade, Zero Feedback and Combined Feedback, $\mu = .8$

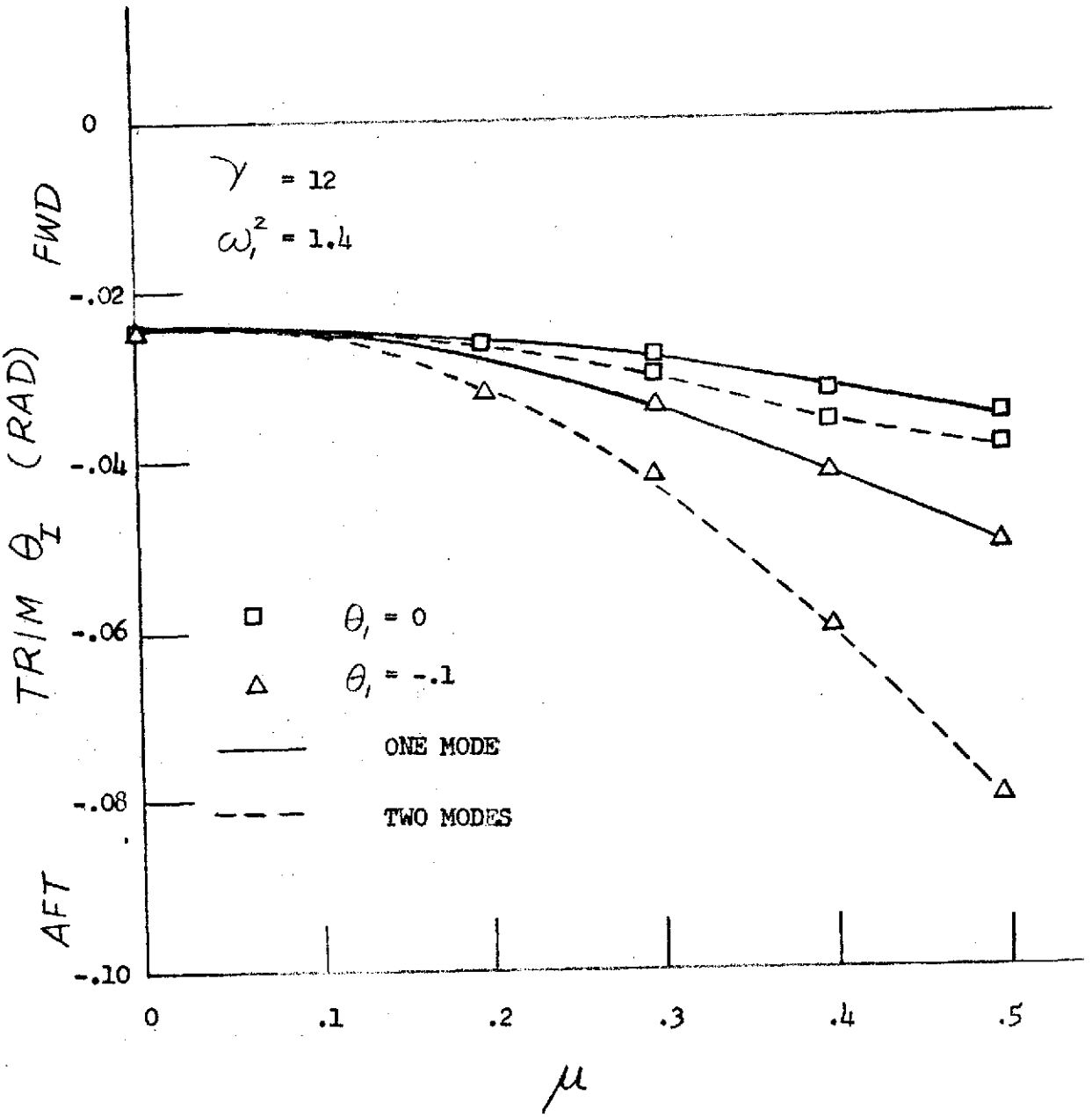
0
-.02
-.04
-.06
-.08
-.10
FWD
AFT
TRIM θ_I (RAD)
γ = 12
ω_1^2 = 1.4
θ_1 = 0
θ_1 = -.1
ONE MODE
TWO MODES
0
.1
.2
.3
.4
.5
μ

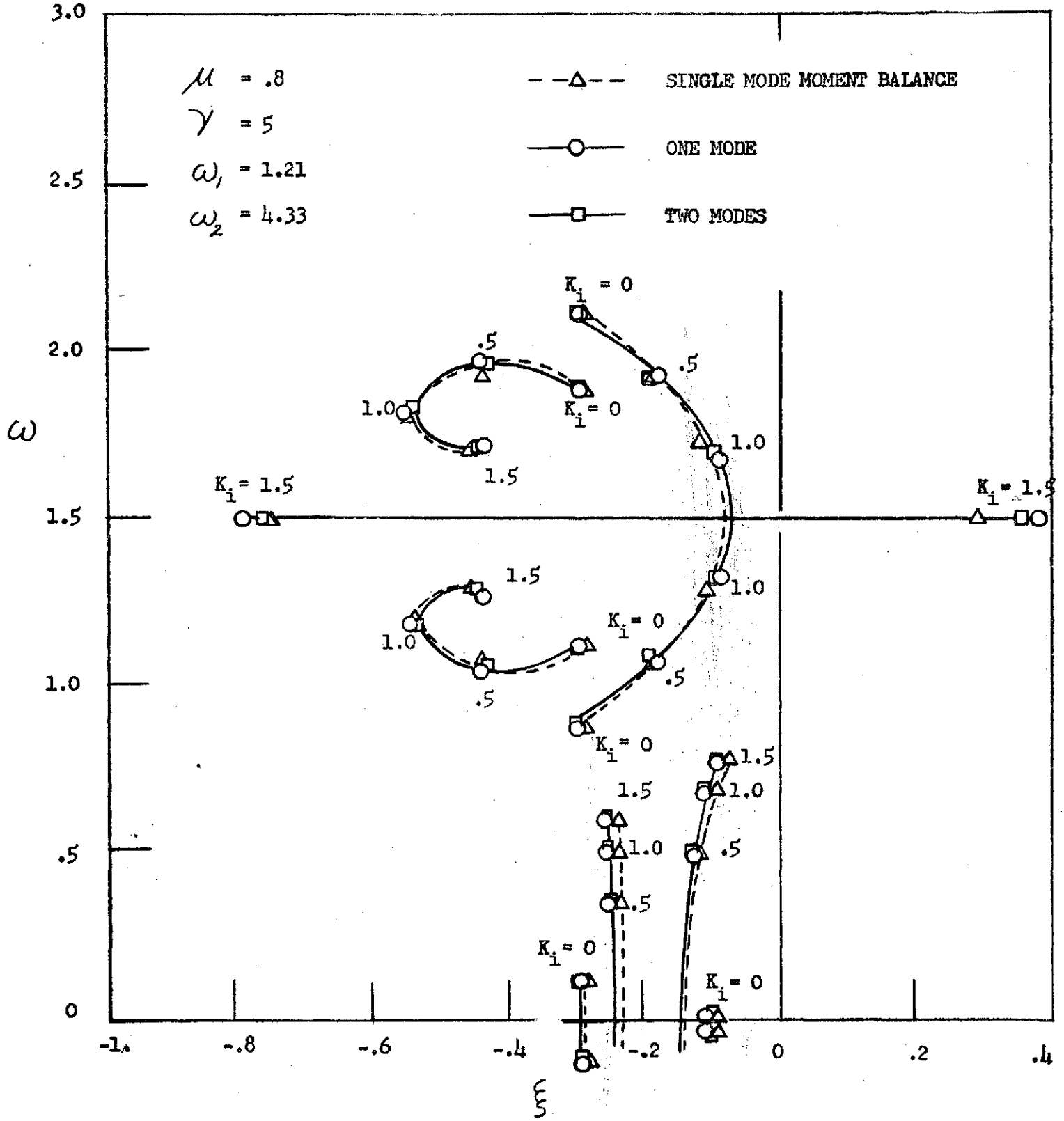
μ = .8
γ = 5
ω1 = 1.21
ω2 = 4.33
SINGLE MODE MOMENT BALANCE
ONE MODE
TWO MODES
ω
ξ
3.0
2.5
2.0
1.5
1.0
.5
0
-1.
-.8
-.6
-.4
-.2
0
.2
.4
Ki = 0
Ki = 1.5
.5
1.0
1.5

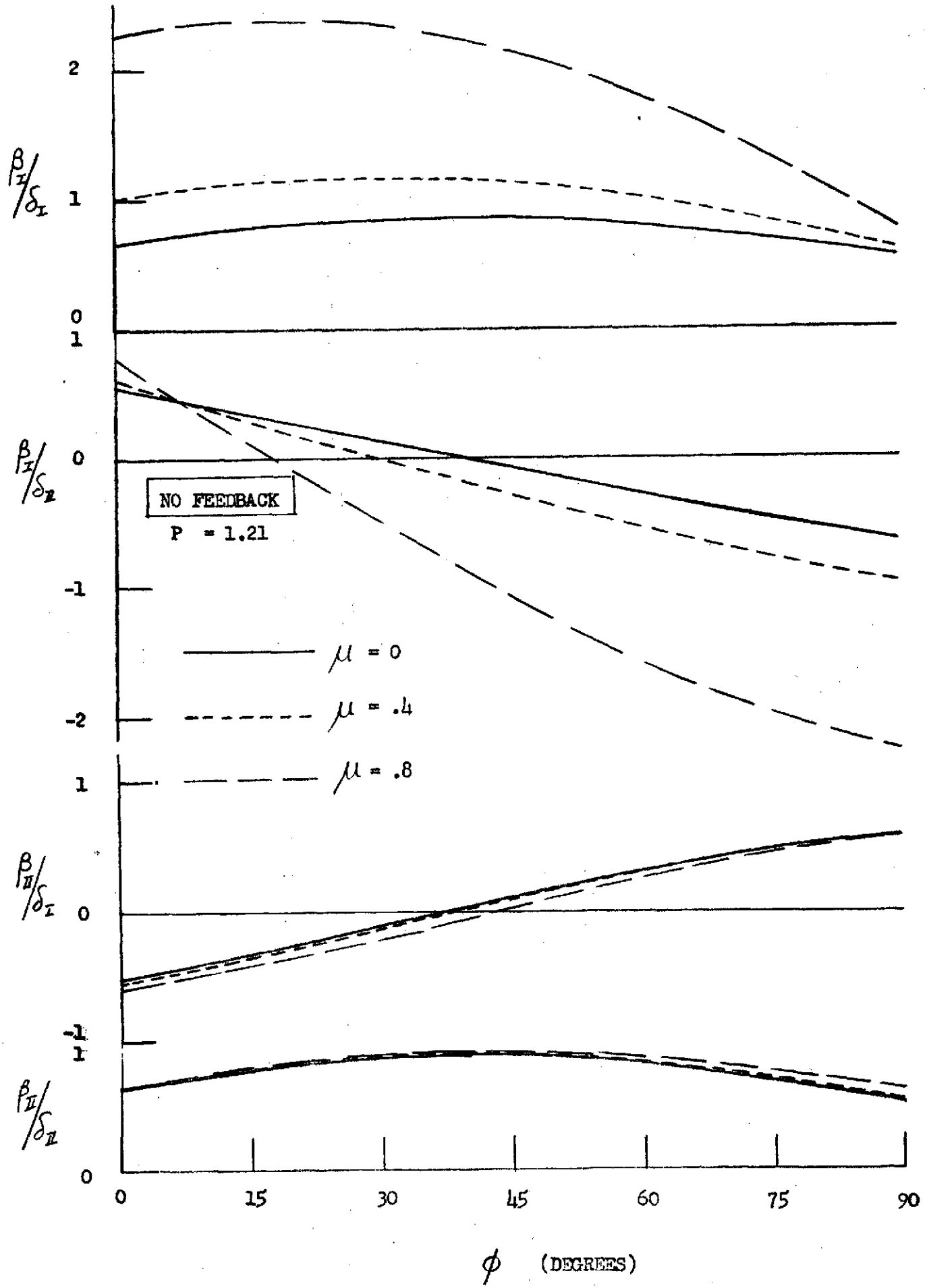
2
1
0
β_I/δ_I
1
0
β_I/δ_{II}
NO FEEDBACK
P = 1.21
-1
-2
μ = 0
μ = .4
μ = .8
1
β_{II}/δ_I
0
-1
1
β_{II}/δ_{II}
0
0
15
30
45
60
75
90
ϕ (DEGREES)

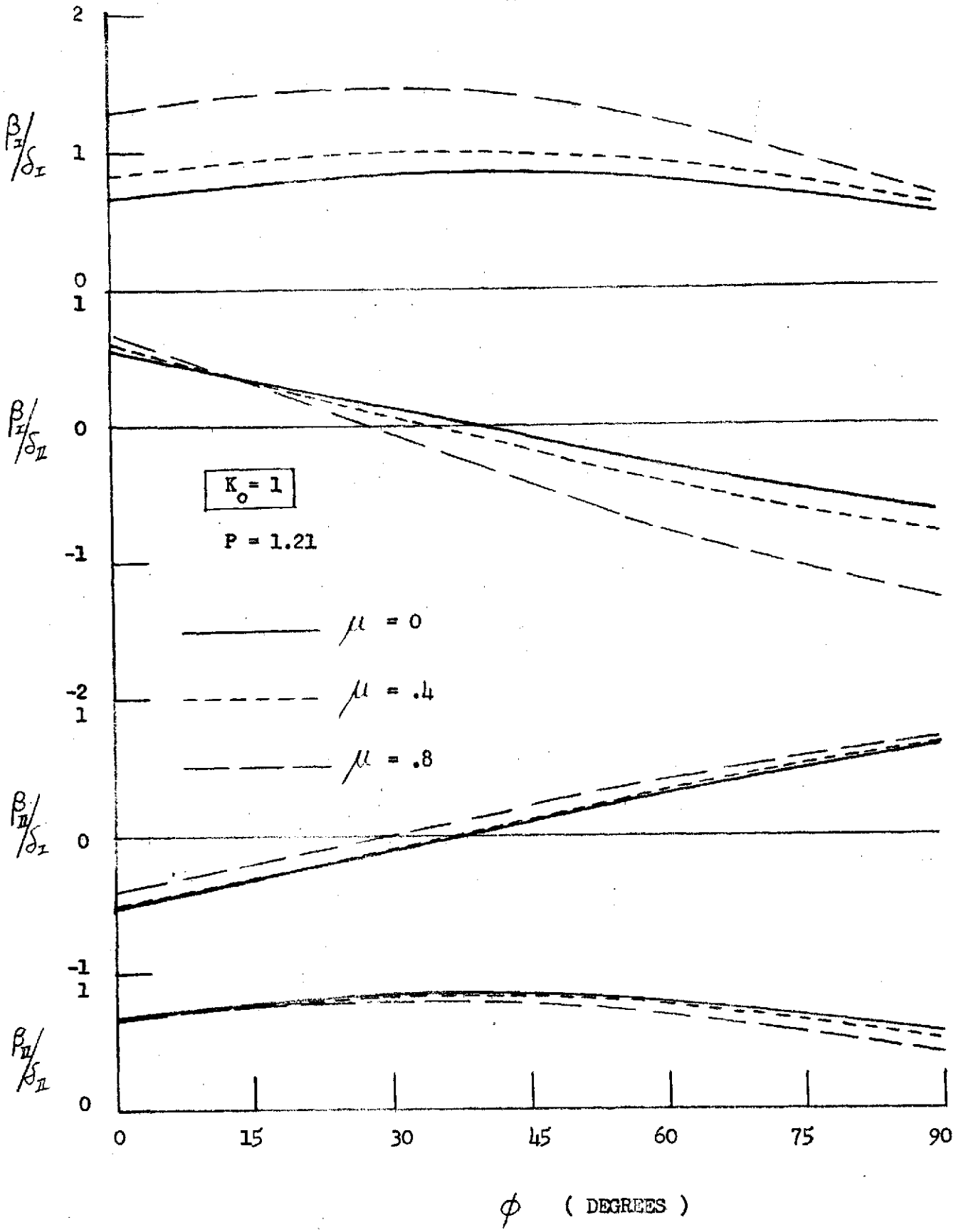
2
1
0
1
0
-1
-2
1
0
-1
1
0
β_I/δ_I
β_I/δ_{II}
β_{II}/δ_I
β_{II}/δ_{II}
$K_o = 1$
P = 1.21
μ = 0
μ = .4
μ = .8
0
15
30
45
60
75
90
ϕ (DEGREES)

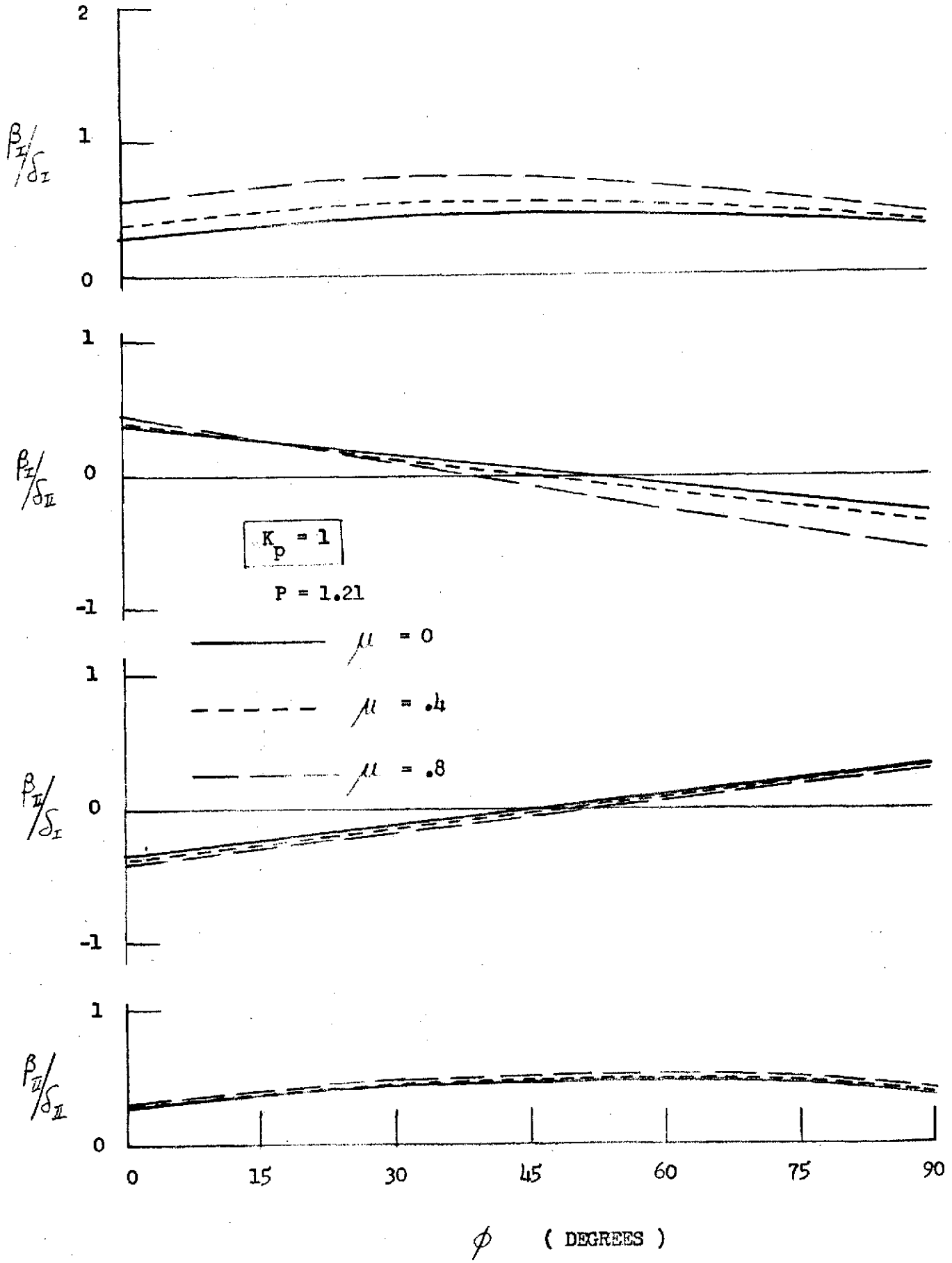
2
1
0
β_I/δ_I
1
0
-1
β_I/δ_{II}
$K_p = 1$
P = 1.21
μ = 0
μ = .4
μ = .8
1
0
-1
β_{II}/δ_I
1
0
β_{II}/δ_{II}
0
15
30
45
60
75
90
ϕ (DEGREES)

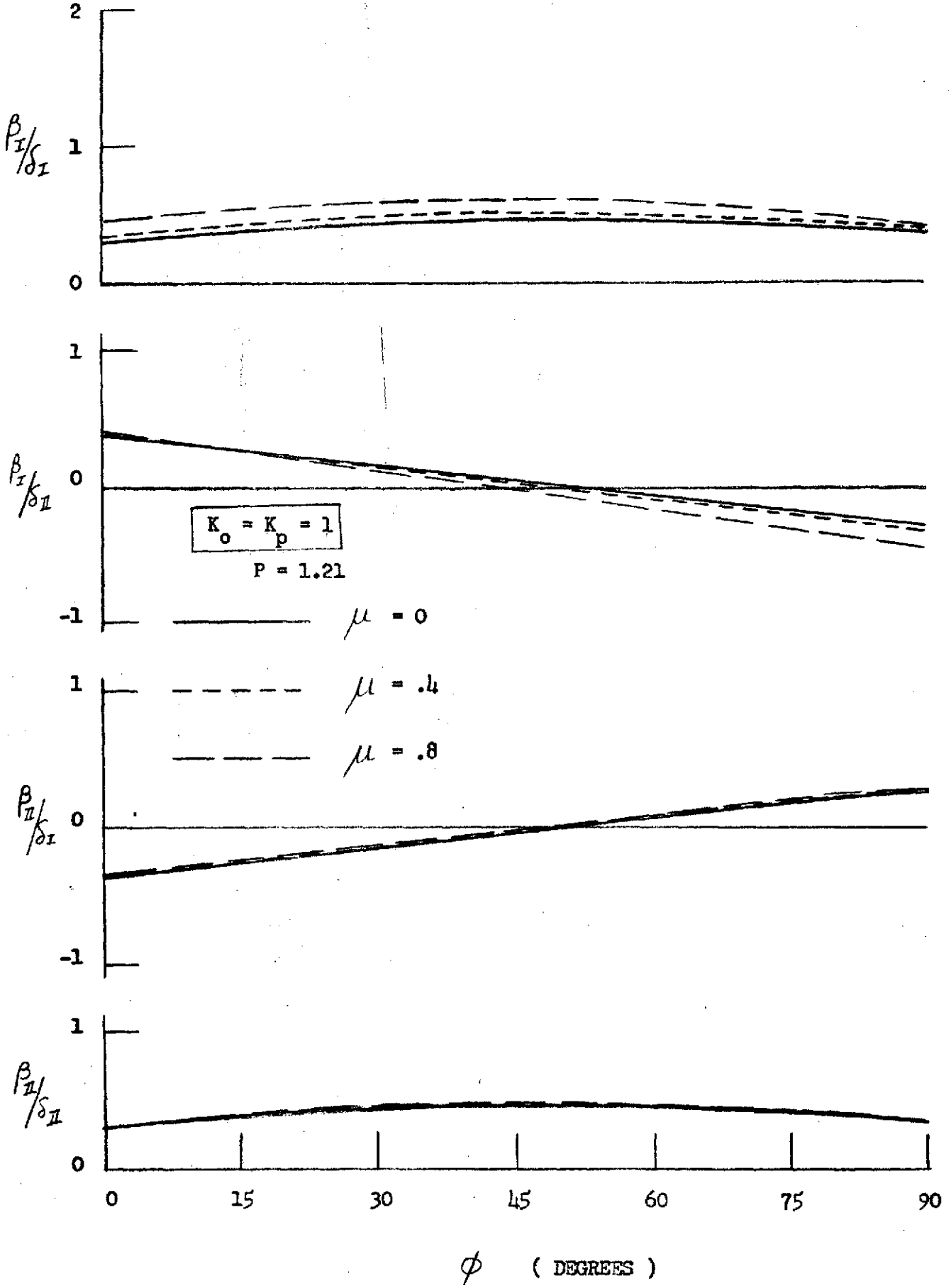
2
1
0
β_I/δ_I
1
0
-1
β_I/δ_{II}
$K_o = K_p = 1$
P = 1.21
μ = 0
μ = .4
μ = .8
1
0
-1
β_{II}/δ_I
1
0
β_{II}/δ_{II}
0
15
30
45
60
75
90
ϕ (DEGREES)

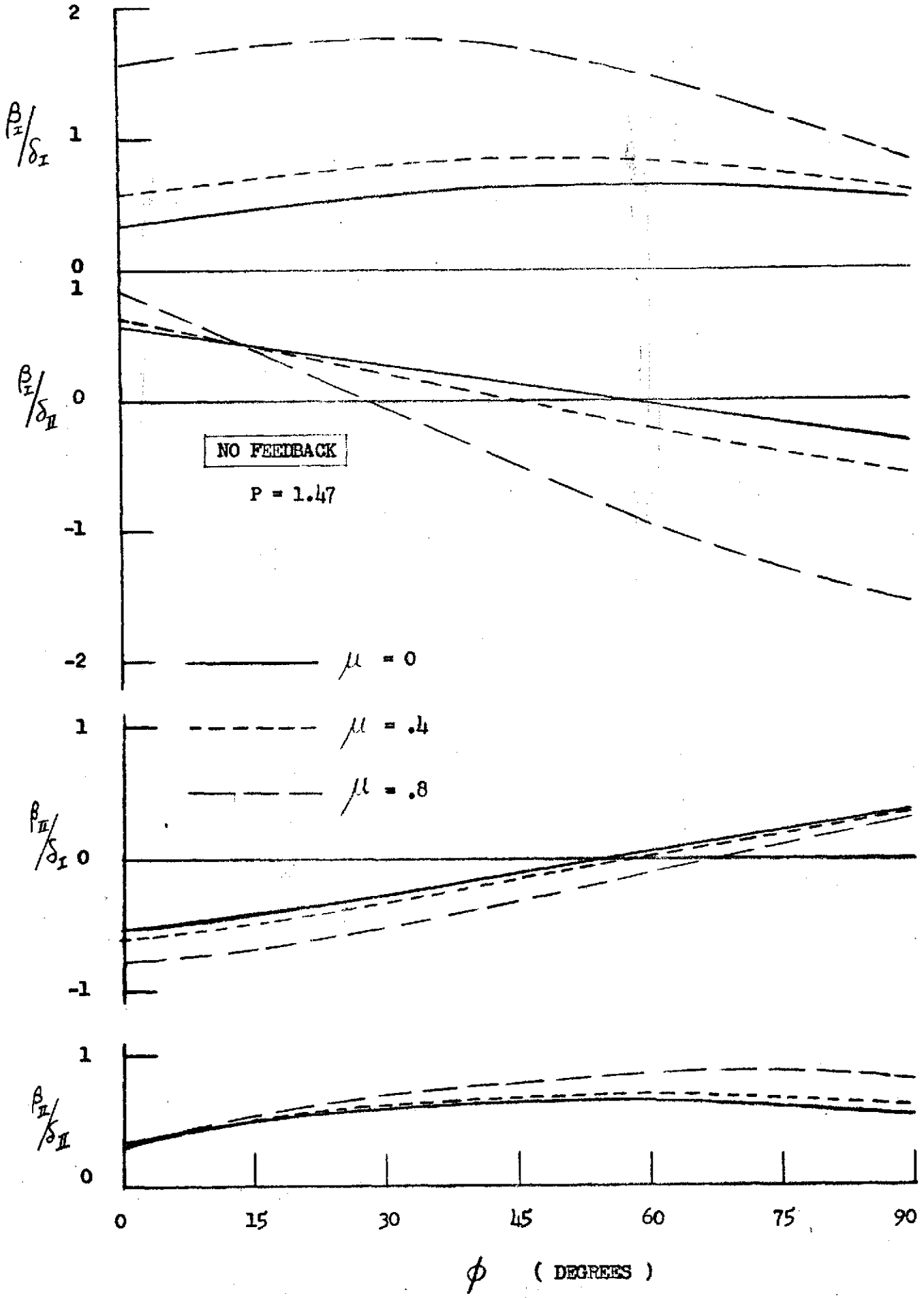
2
1
0
β_I/δ_I
1
0
β_I/δ_{II}
NO FEEDBACK
P = 1.47
-1
-2
μ = 0
μ = .4
μ = .8
1
β_{II}/δ_I 0
-1
1
β_{II}/δ_{II}
0
0
15
30
45
60
75
90
ϕ (DEGREES)

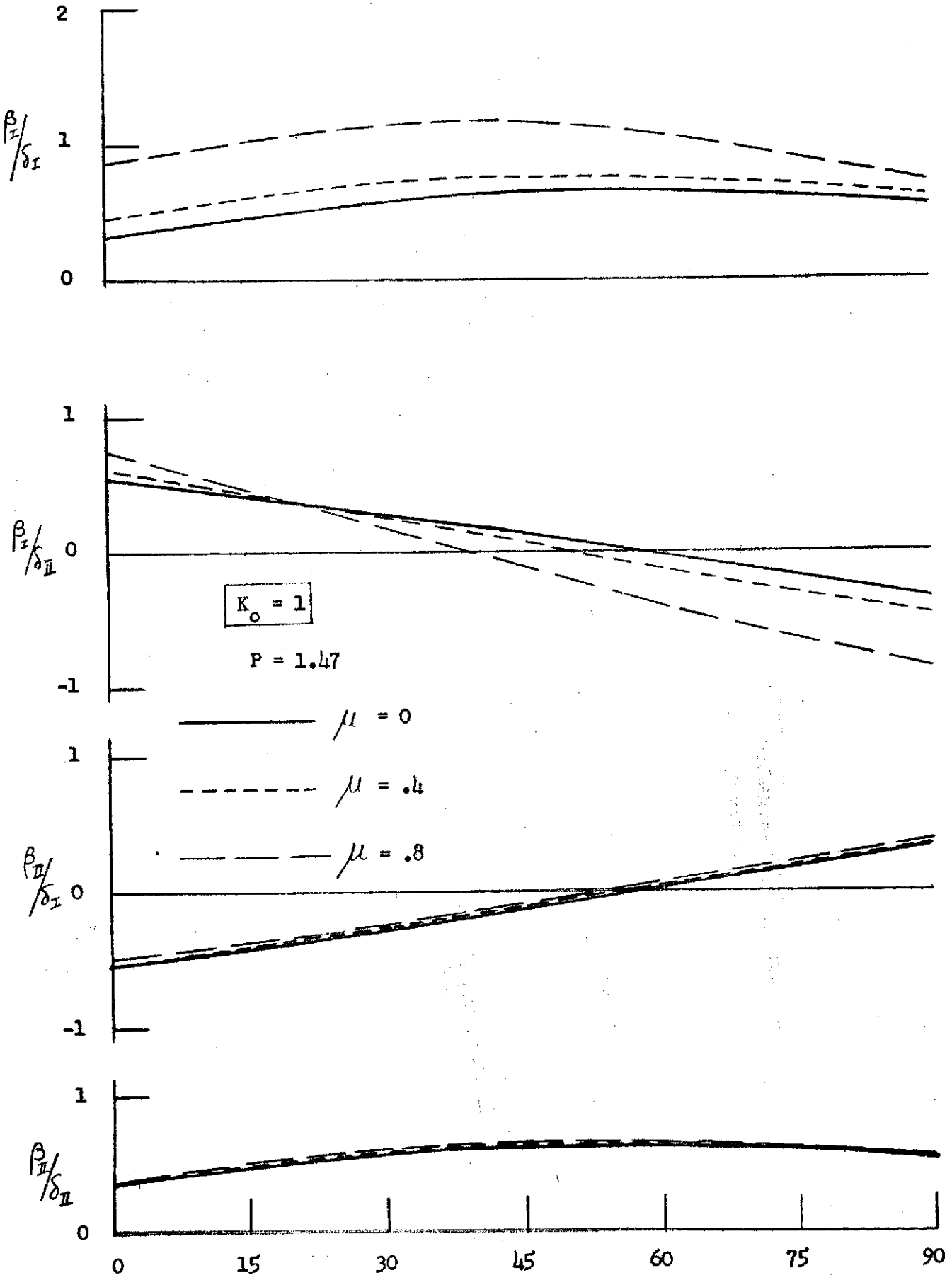
2
1
0
β_I/δ_I
1
0
-1
β_I/δ_{II}
$K_o = 1$
P = 1.47
$\mu = 0$
$\mu = .4$
$\mu = .8$
1
0
-1
β_{II}/δ_I
1
0
β_{II}/δ_{II}
0
15
30
45
60
75
90
ϕ (DEGREES)

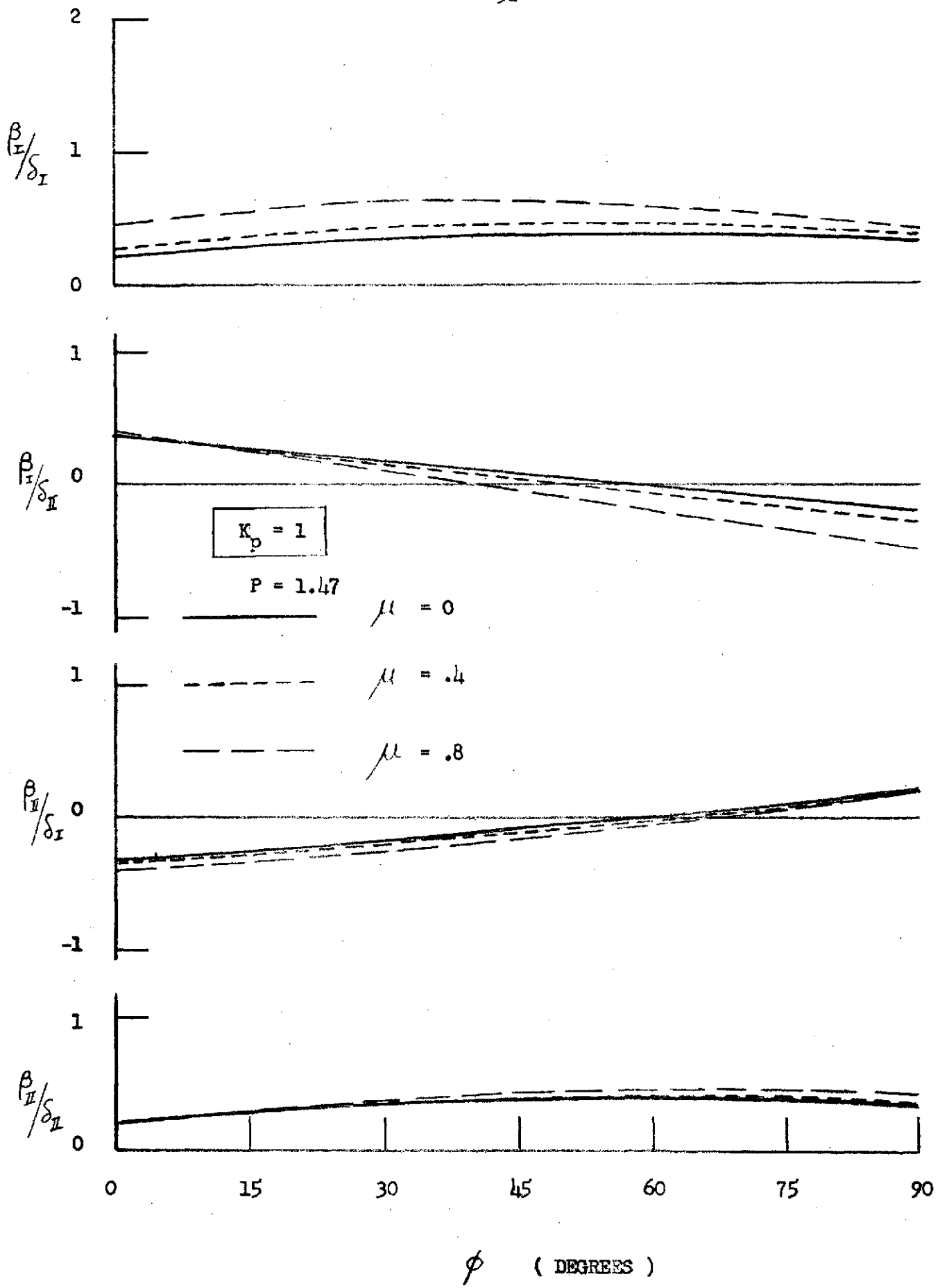
2
1
0
β_I/δ_I
1
0
-1
β_I/δ_{II}
$K_p = 1$
P = 1.47
μ = 0
μ = .4
μ = .8
1
0
-1
β_{II}/δ_I
1
0
β_{II}/δ_{II}
0
15
30
45
60
75
90
ϕ (DEGREES)

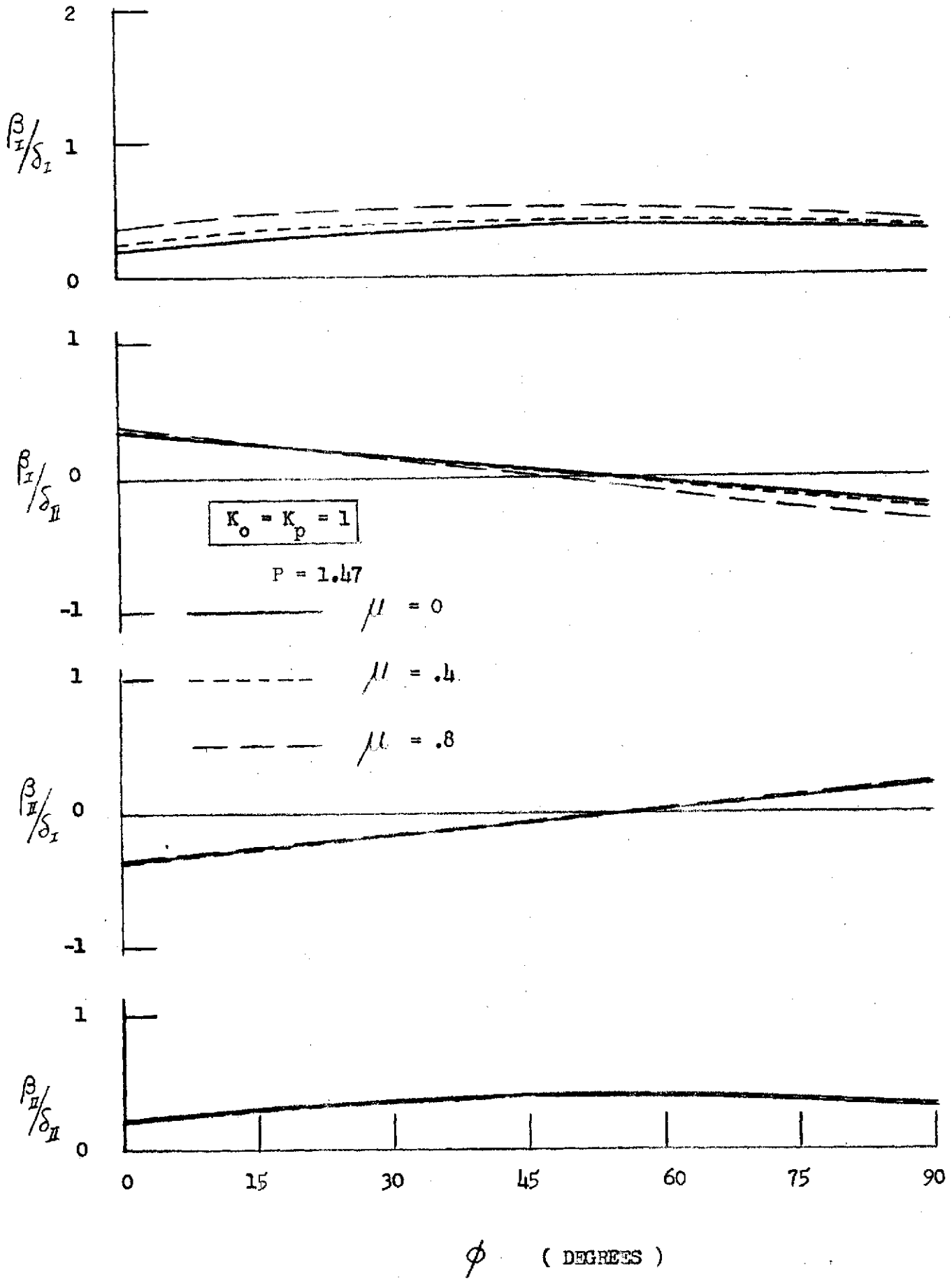
2
β_I/δ_I
1
0
1
β_I/δ_{II}
0
$K_o = K_p = 1$
P = 1.47
-1
μ = 0
1
μ = .4
μ = .8
β_{II}/δ_I
0
-1
1
β_{II}/δ_{II}
0
0
15
30
45
60
75
90
ϕ (DEGREES)

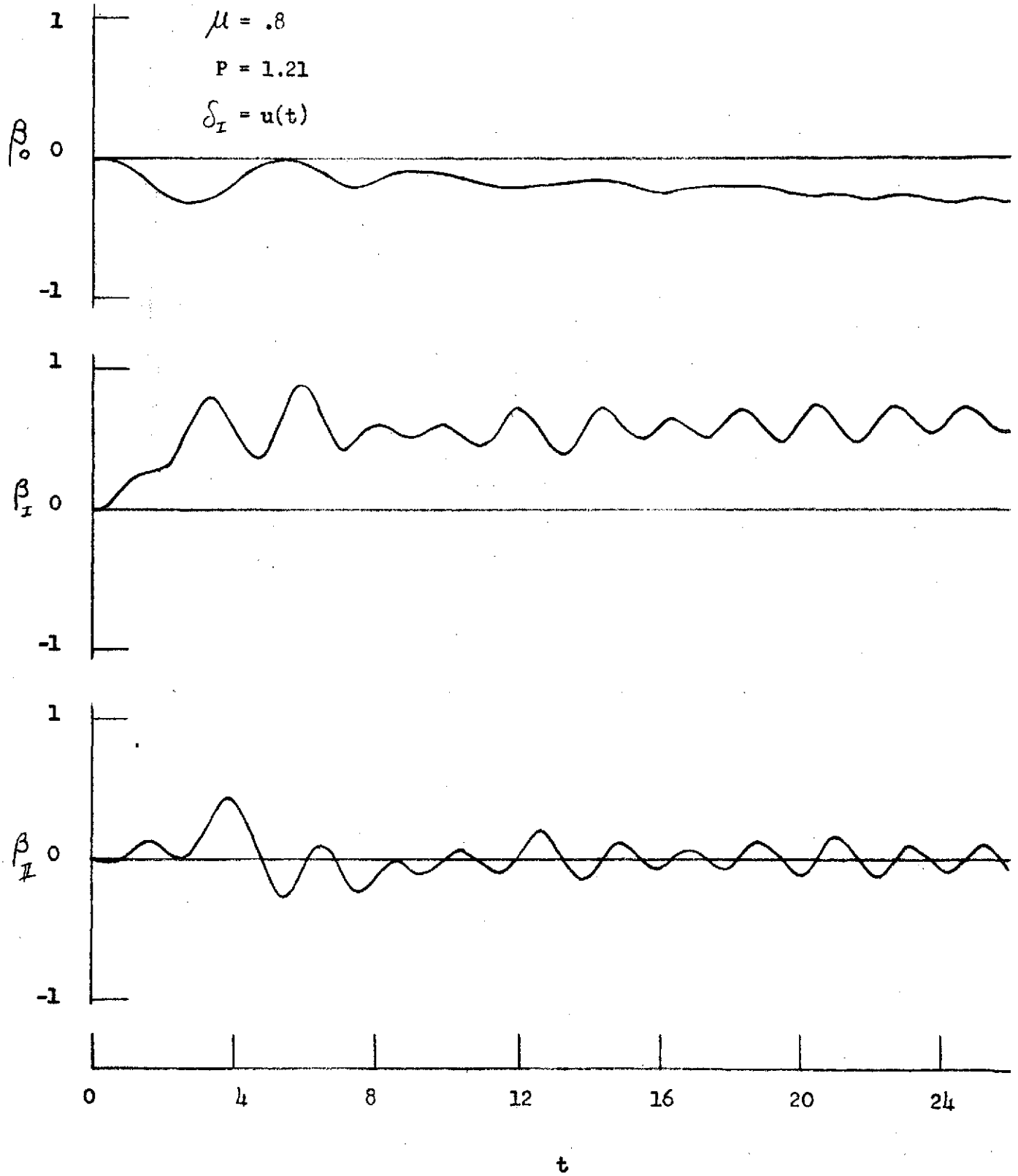
μ = .8
P = 1.21
δ_I = u(t)
1
0
-1
β_o
β_I
β_II
0
4
8
12
16
20
24
t

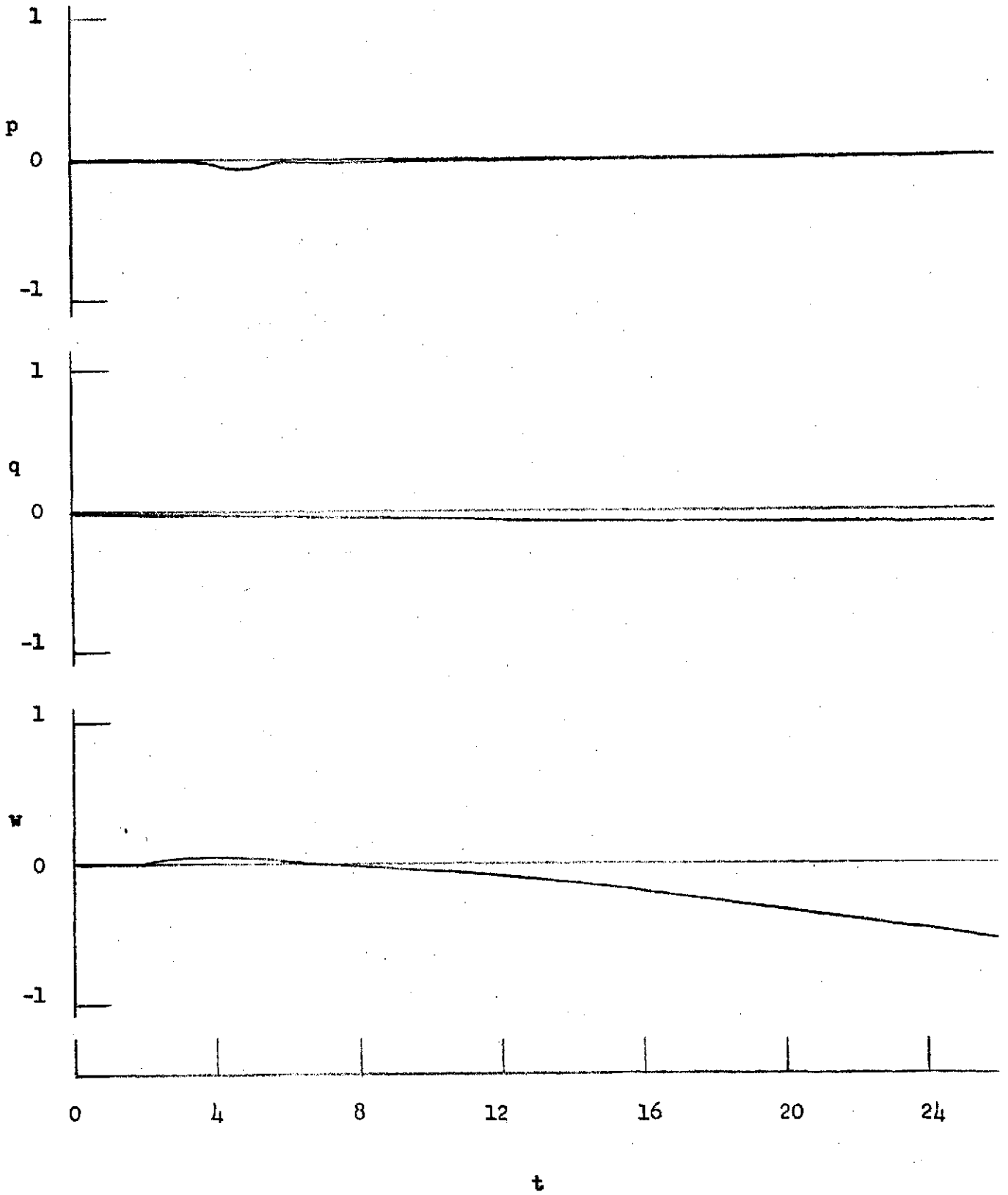
1
p
0
-1
1
q
0
-1
1
w
0
-1
0
4
8
12
16
20
24
t

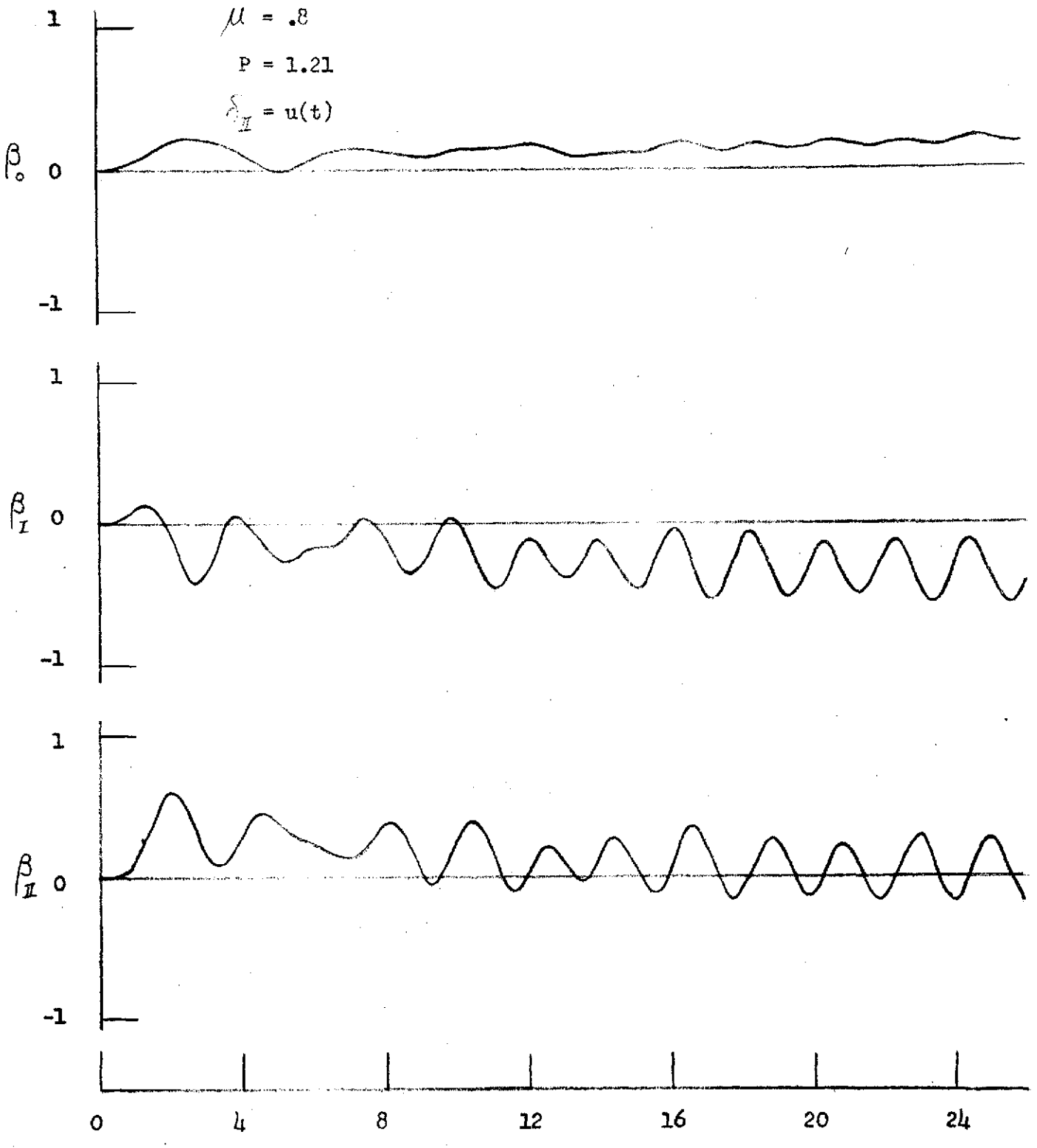
μ = .8
P = 1.21
δ_II = u(t)
1
0
-1
β₀
β_I
β_II
0
4
8
12
16
20
24
t

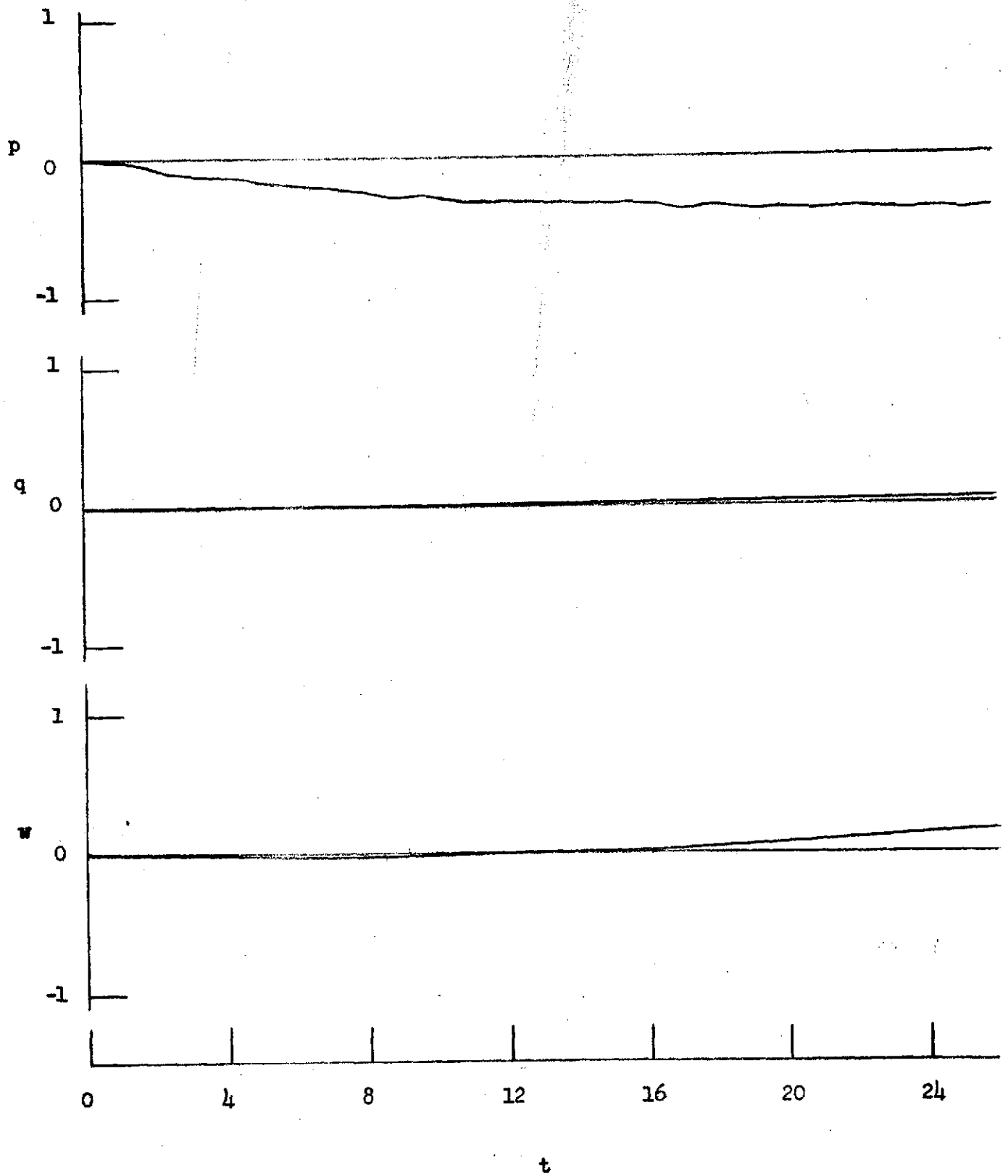
1
p
0
-1
1
q
0
-1
1
w
0
-1
0
4
8
12
16
20
24
t

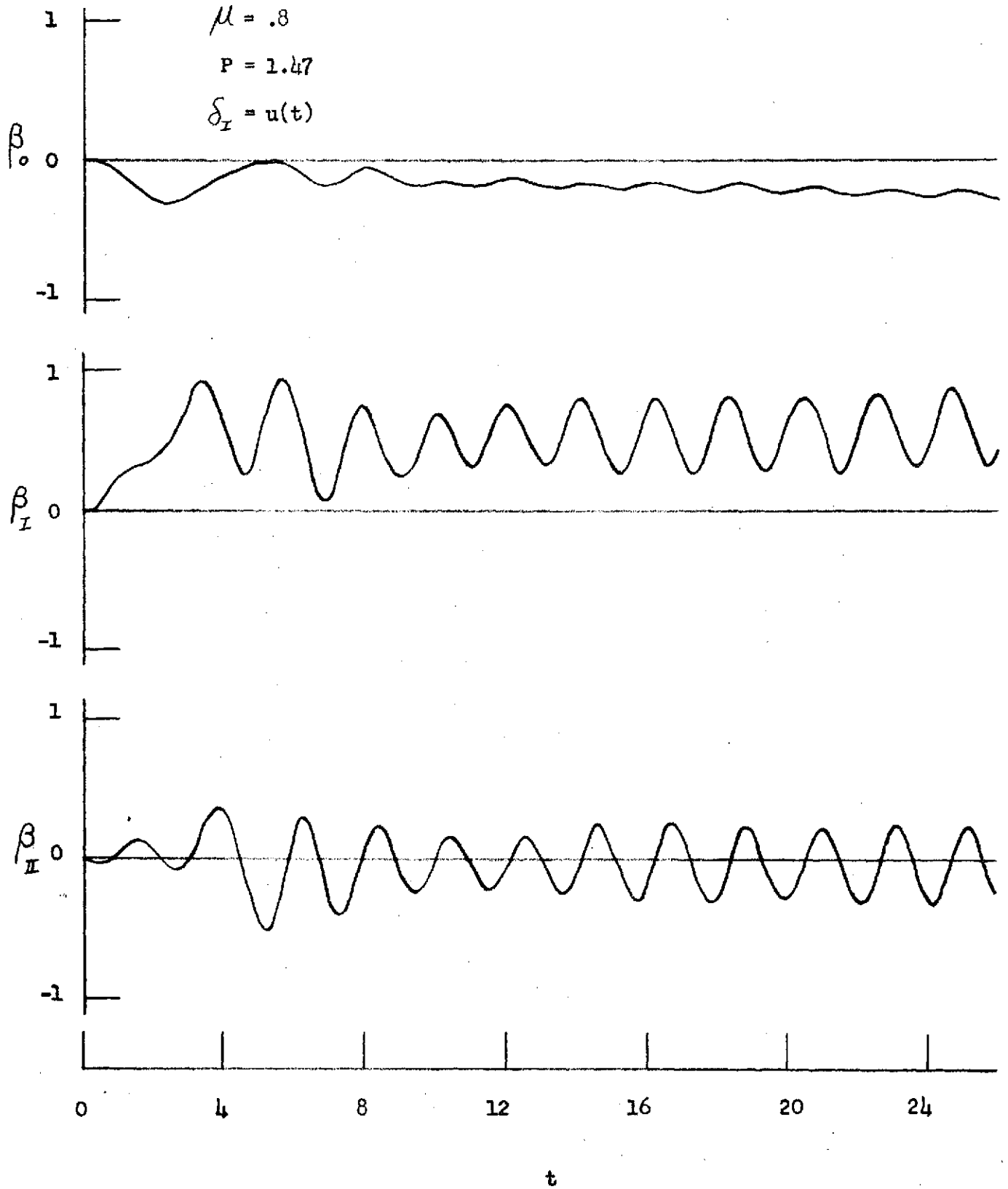
μ = .8
P = 1.47
δ_I = u(t)
β_o
β_I
β_II
1
0
-1
0
4
8
12
16
20
24
t

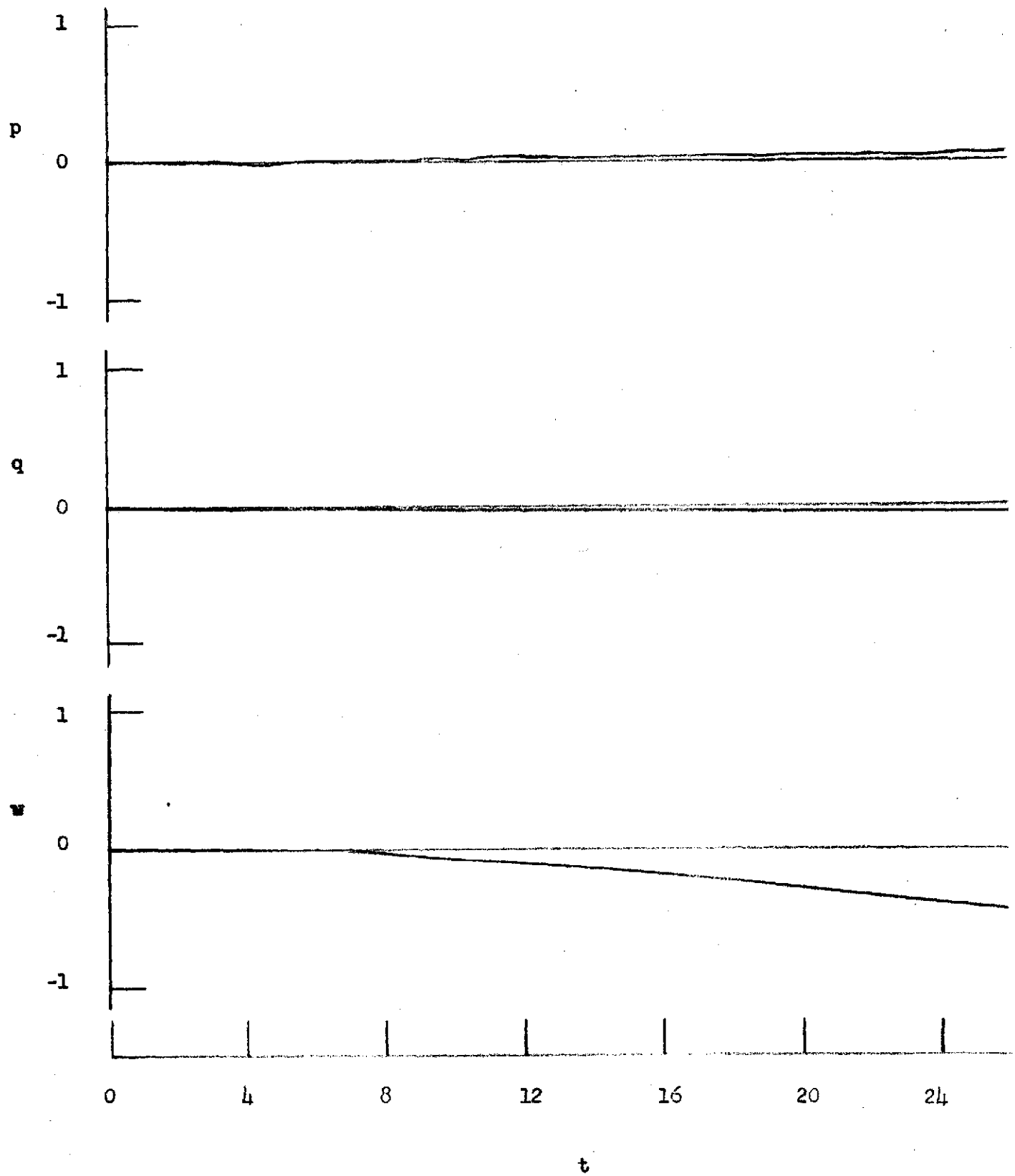
1
p
0
-1
1
q
0
-1
1
w
0
-1
0
4
8
12
16
20
24
t

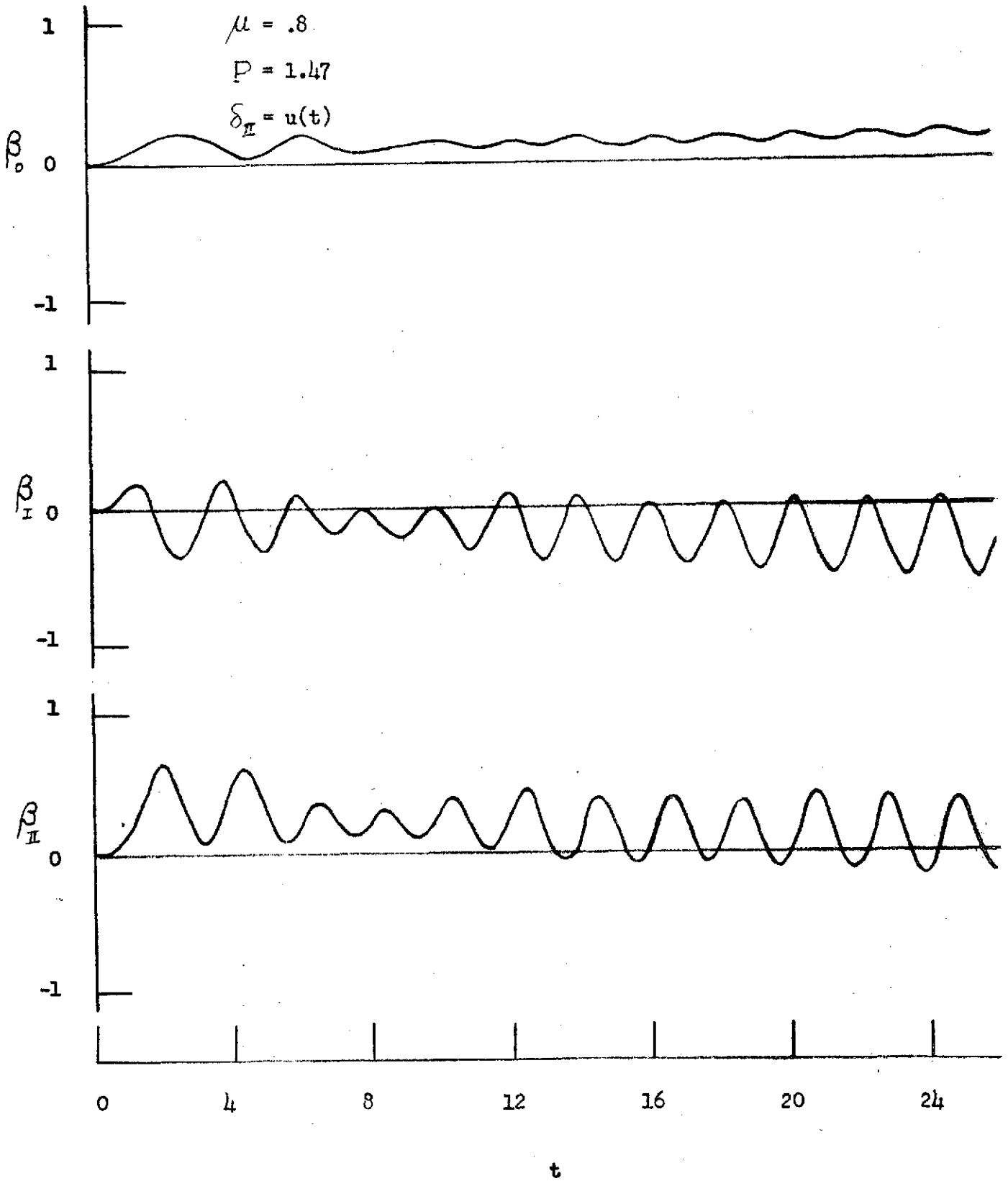
μ = .8
P = 1.47
δ_II = u(t)
1
0
-1
β_o
β_I
β_II
0
4
8
12
16
20
24
t

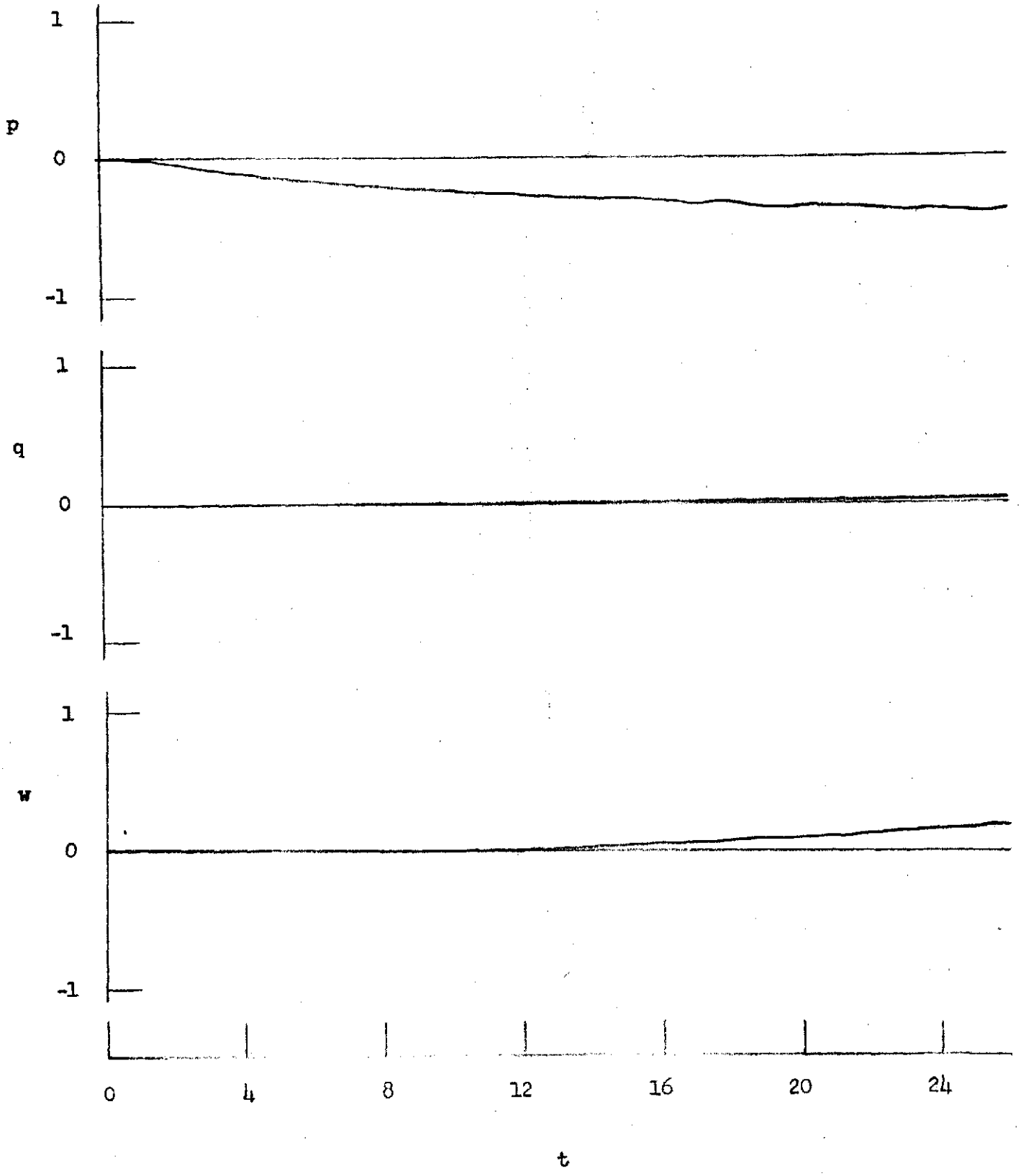
1
p
0
-1
1
q
0
-1
1
w
0
-1
0
4
8
12
16
20
24
t

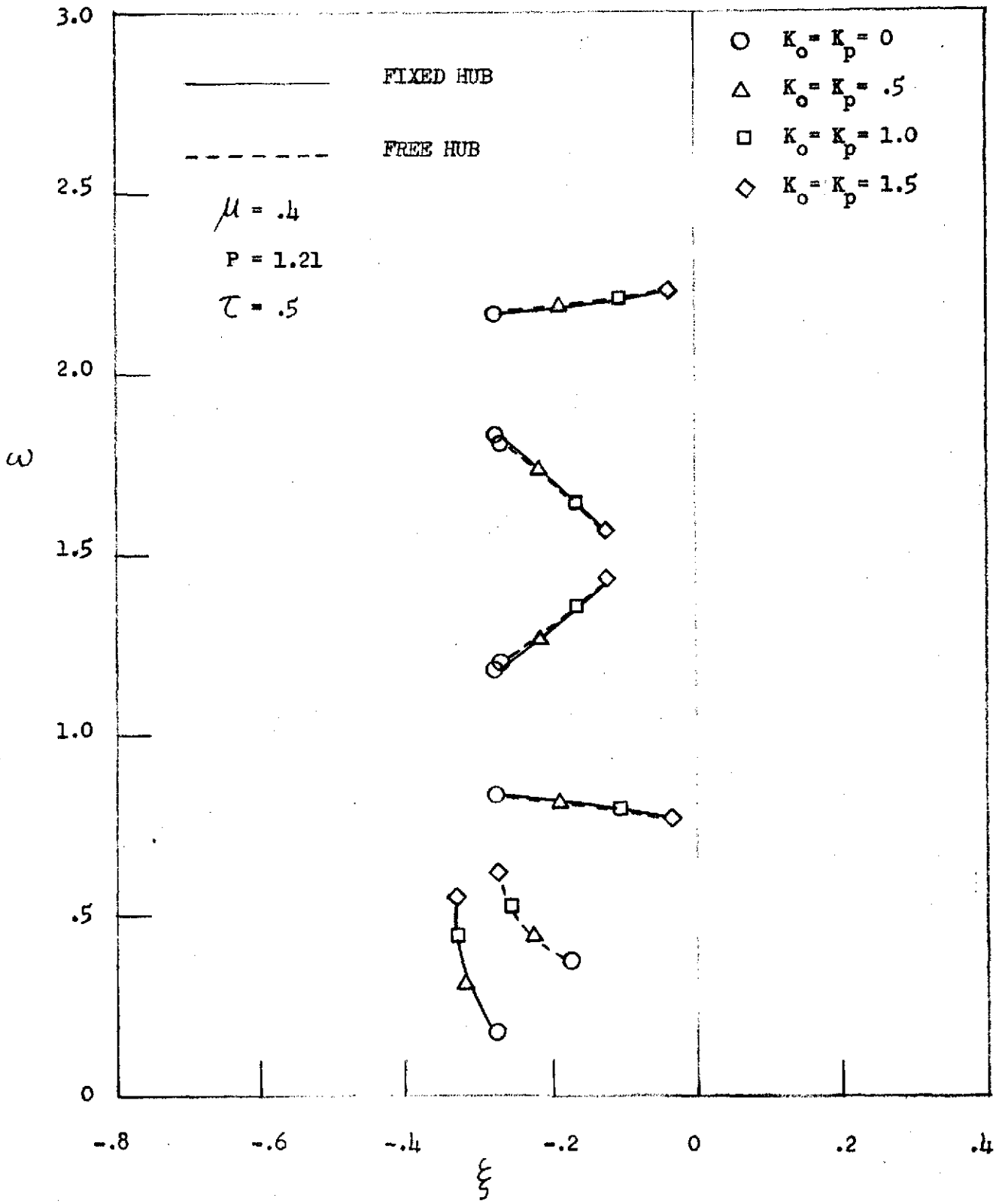
3.0
2.5
2.0
1.5
1.0
.5
0
ω
FIXED HUB
FREE HUB
μ = .4
P = 1.21
τ = .5
K_o = K_p = 0
K_o = K_p = .5
K_o = K_p = 1.0
K_o = K_p = 1.5
-.8
-.6
-.4
-.2
0
.2
.4
ξ

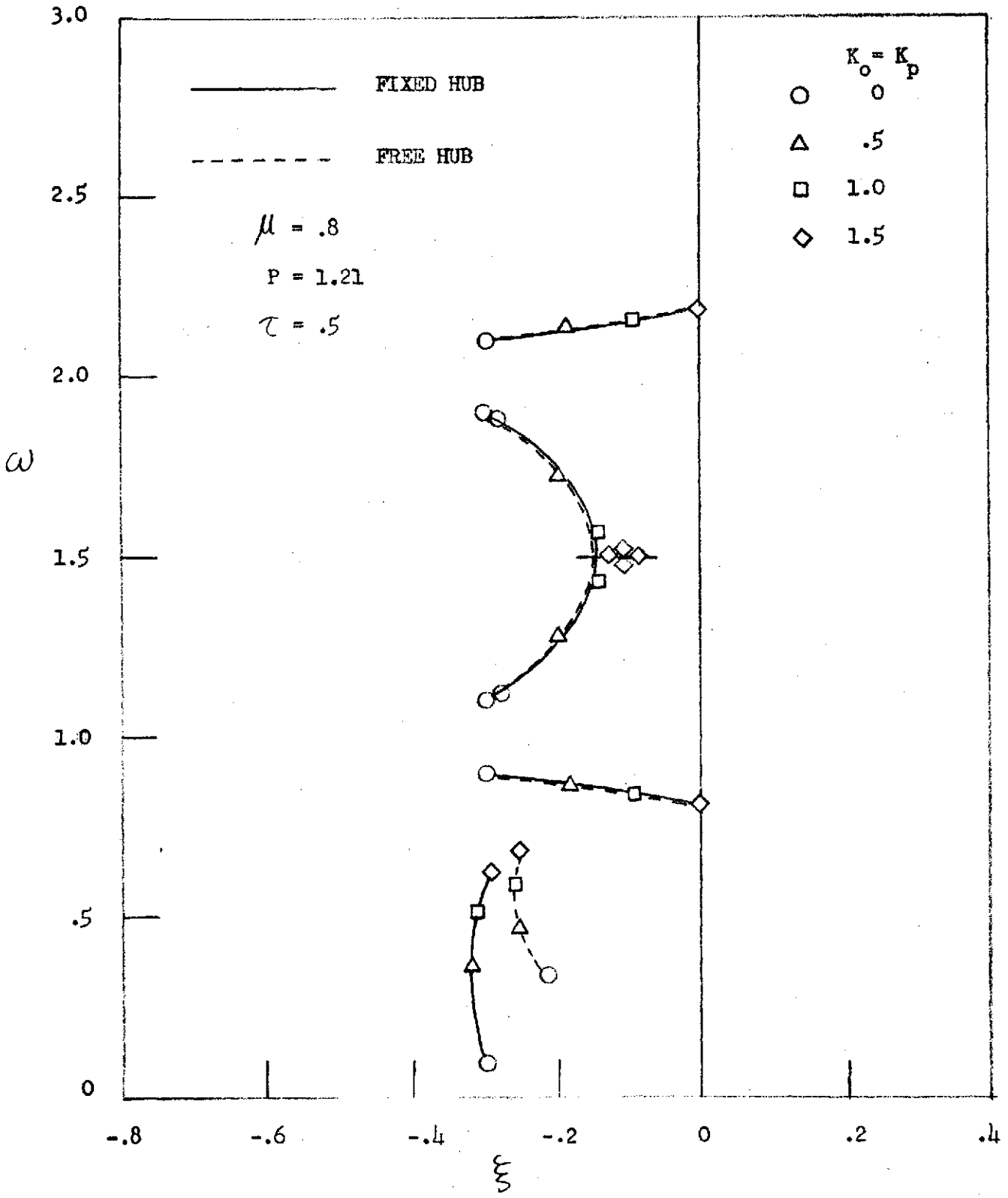
FIXED HUB
FREE HUB
μ = .8
P = 1.21
τ = .5
$K_o = K_p$
0
.5
1.0
1.5
3.0
2.5
2.0
1.5
1.0
.5
0
ω
-.8
-.6
-.4
-.2
0
.2
.4
ξ

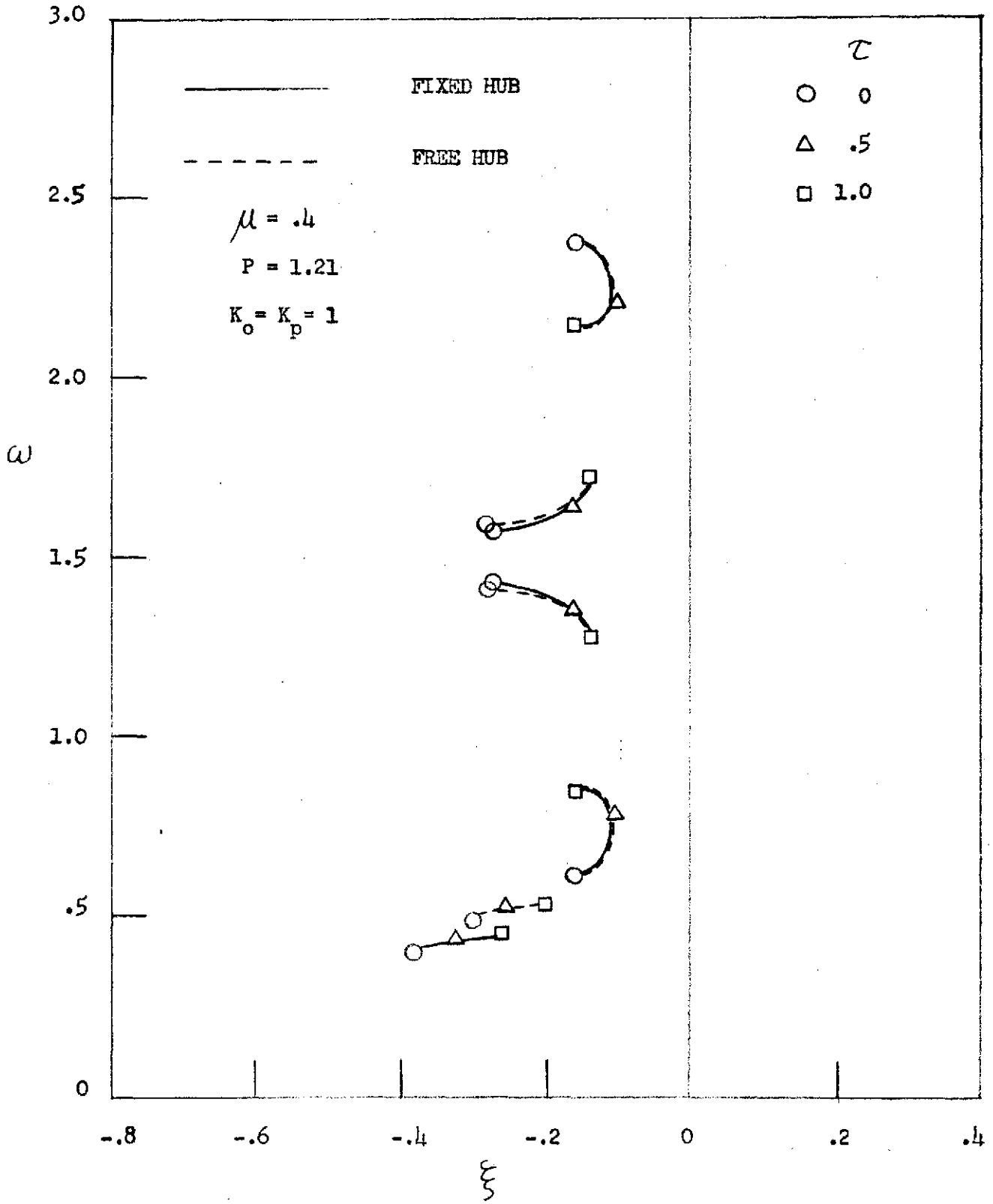
3.0
2.5
2.0
1.5
1.0
.5
0
ω
FIXED HUB
FREE HUB
μ = .4
P = 1.21
K_o = K_p = 1
τ
0
.5
1.0
-.8
-.6
-.4
-.2
0
.2
.4
ξ

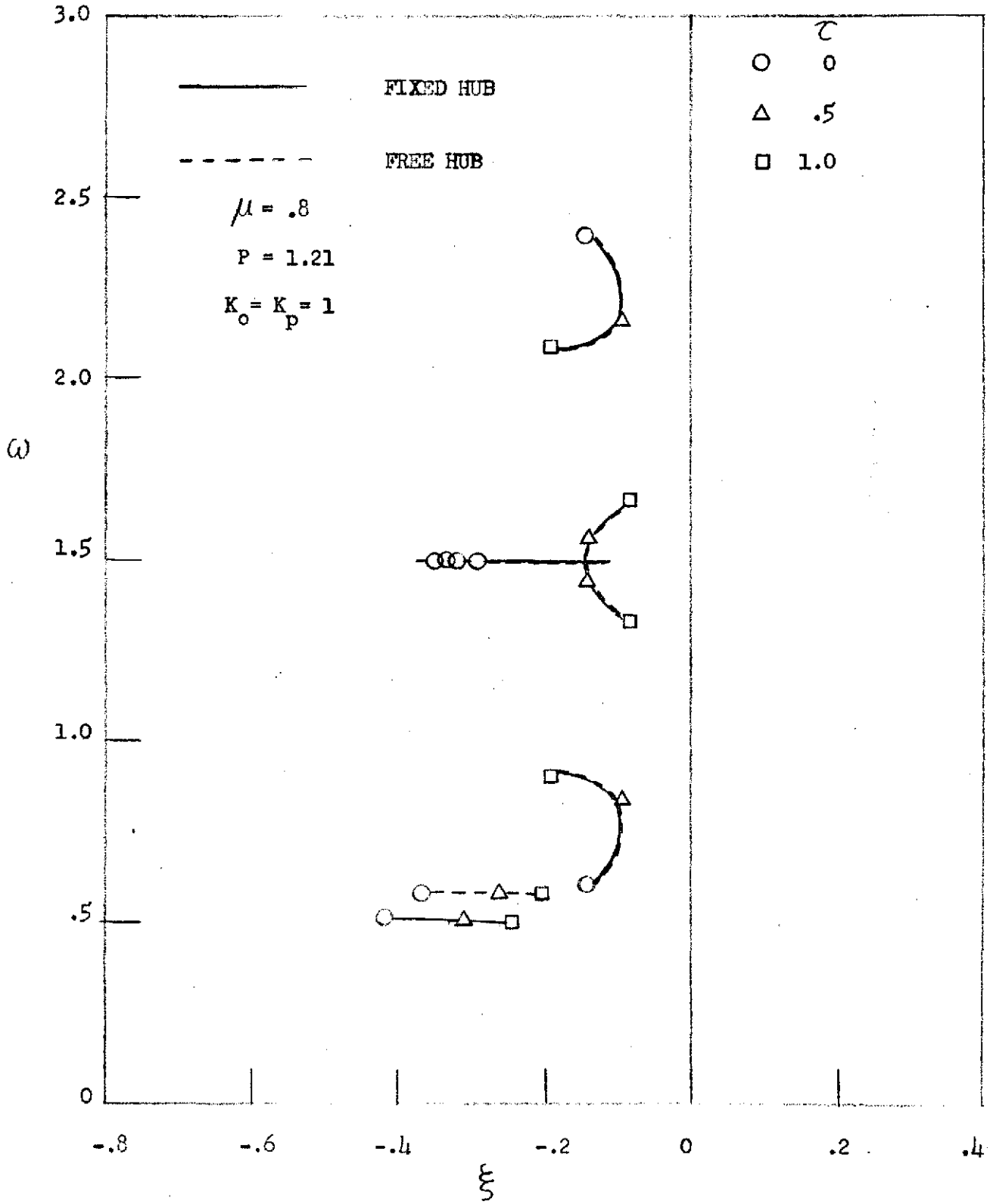
3.0
2.5
2.0
1.5
1.0
.5
0
ω
FIXED HUB
FREE HUB
μ = .8
P = 1.21
K_o = K_p = 1
τ
0
.5
1.0
-.8
-.6
-.4
-.2
0
.2
.4
ξ

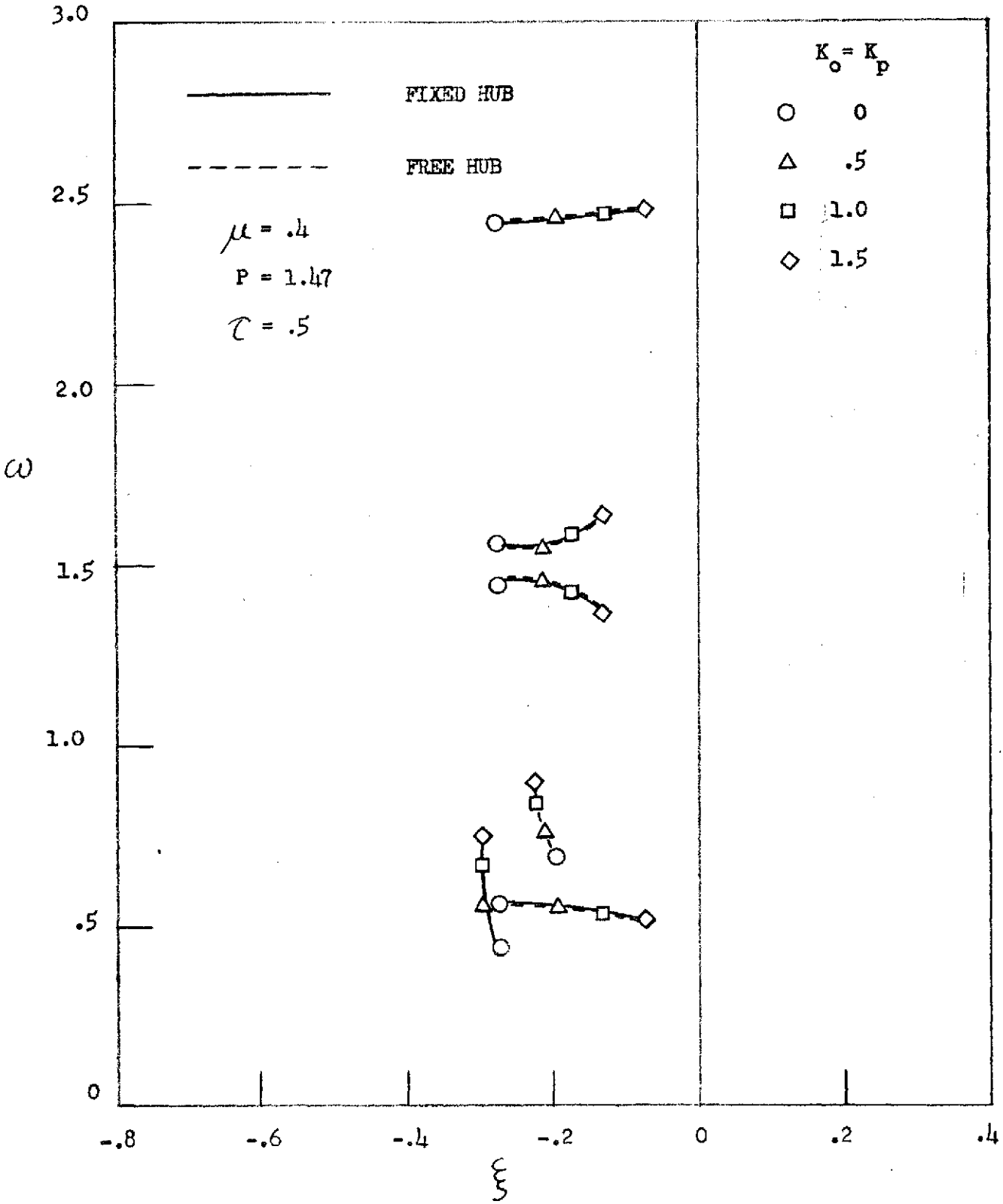
3.0
2.5
2.0
1.5
1.0
.5
0
ω
FIXED HUB
FREE HUB
μ = .4
P = 1.47
τ = .5
$K_o = K_p$
0
.5
1.0
1.5
-.8
-.6
-.4
-.2
0
.2
.4
ξ

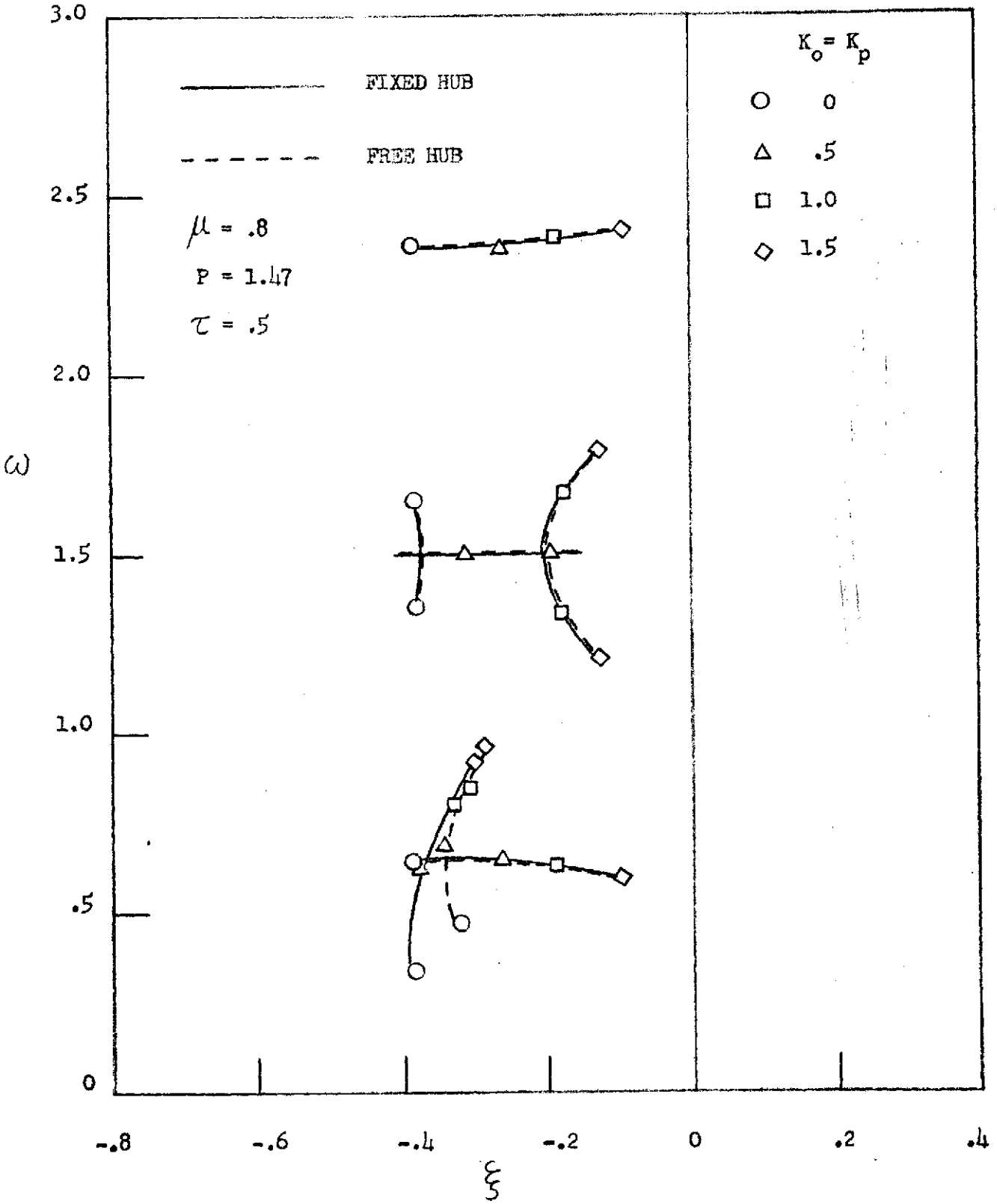
3.0
2.5
2.0
1.5
1.0
.5
0
ω
FIXED HUB
FREE HUB
μ = .8
P = 1.47
τ = .5
$K_o = K_p$
0
.5
1.0
1.5
-.8
-.6
-.4
-.2
0
.2
.4
ξ

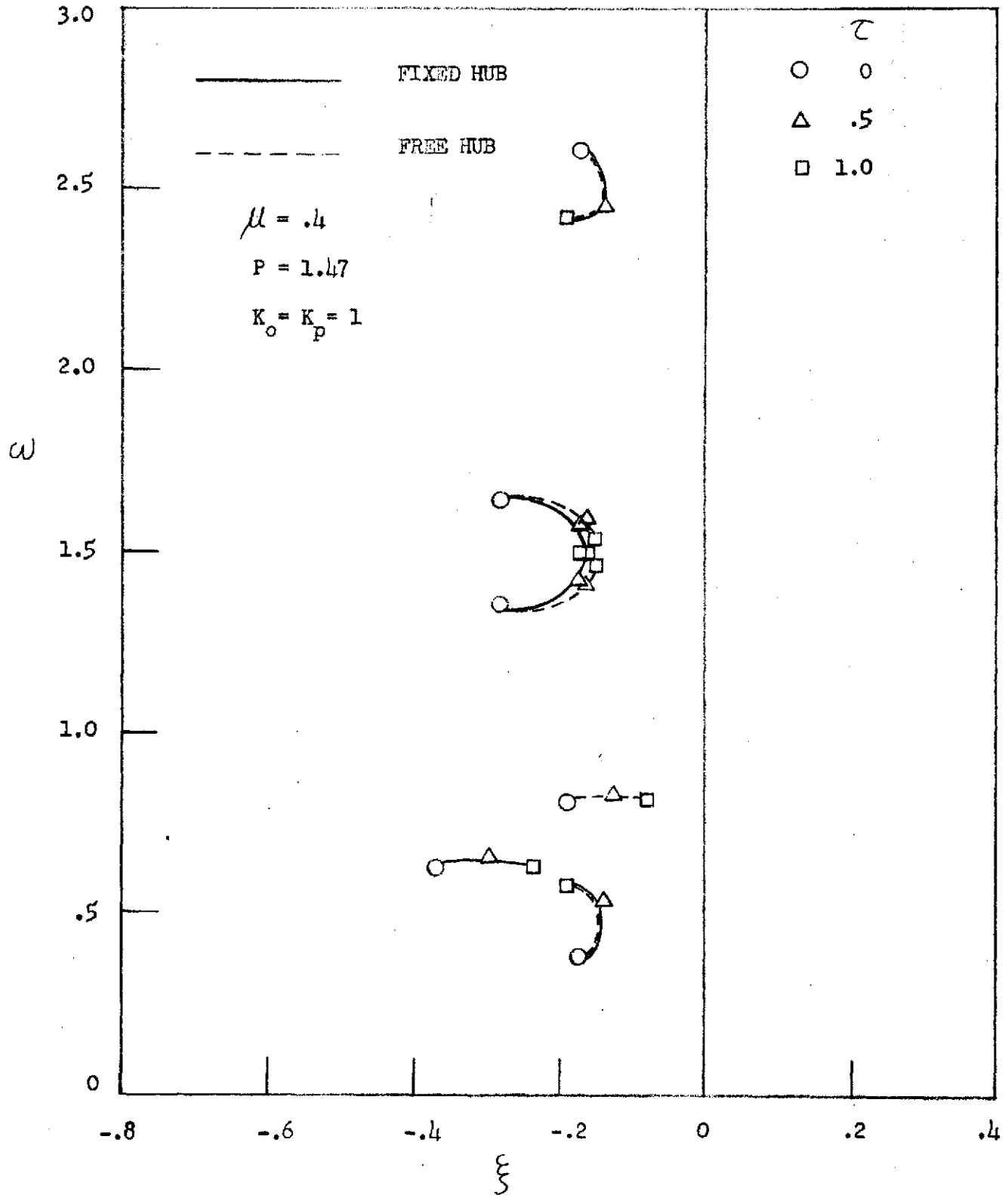
3.0
2.5
2.0
1.5
1.0
.5
0
ω
FIXED HUB
FREE HUB
μ = .4
P = 1.47
K_o = K_p = 1
τ
0
.5
1.0
-.8
-.6
-.4
-.2
0
.2
.4
ξ

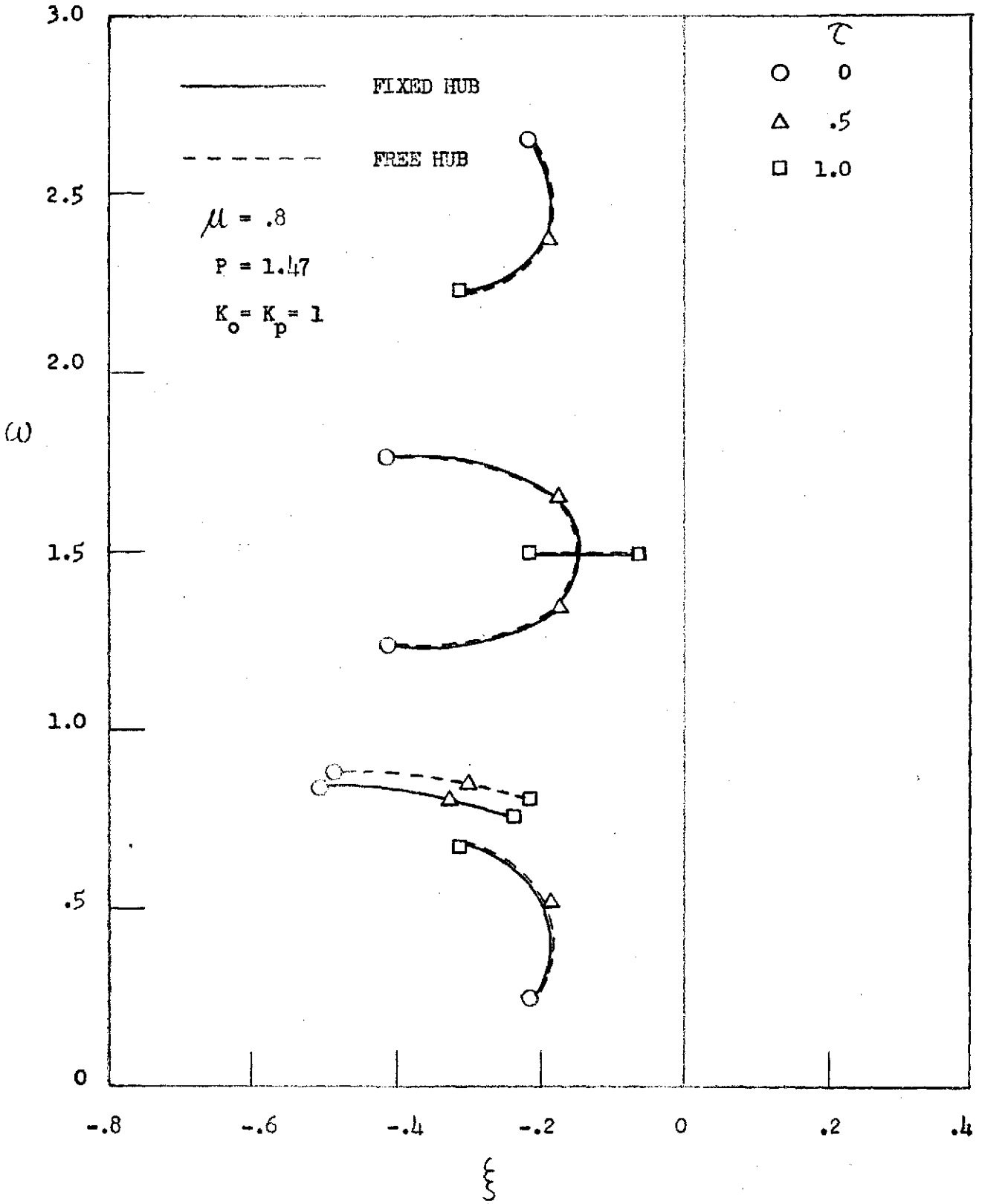
3.0
2.5
2.0
1.5
1.0
.5
0
ω
FIXED HUB
FREE HUB
μ = .8
P = 1.47
K_o = K_p = 1
τ
0
.5
1.0
-.8
-.6
-.4
-.2
0
.2
.4
ξ

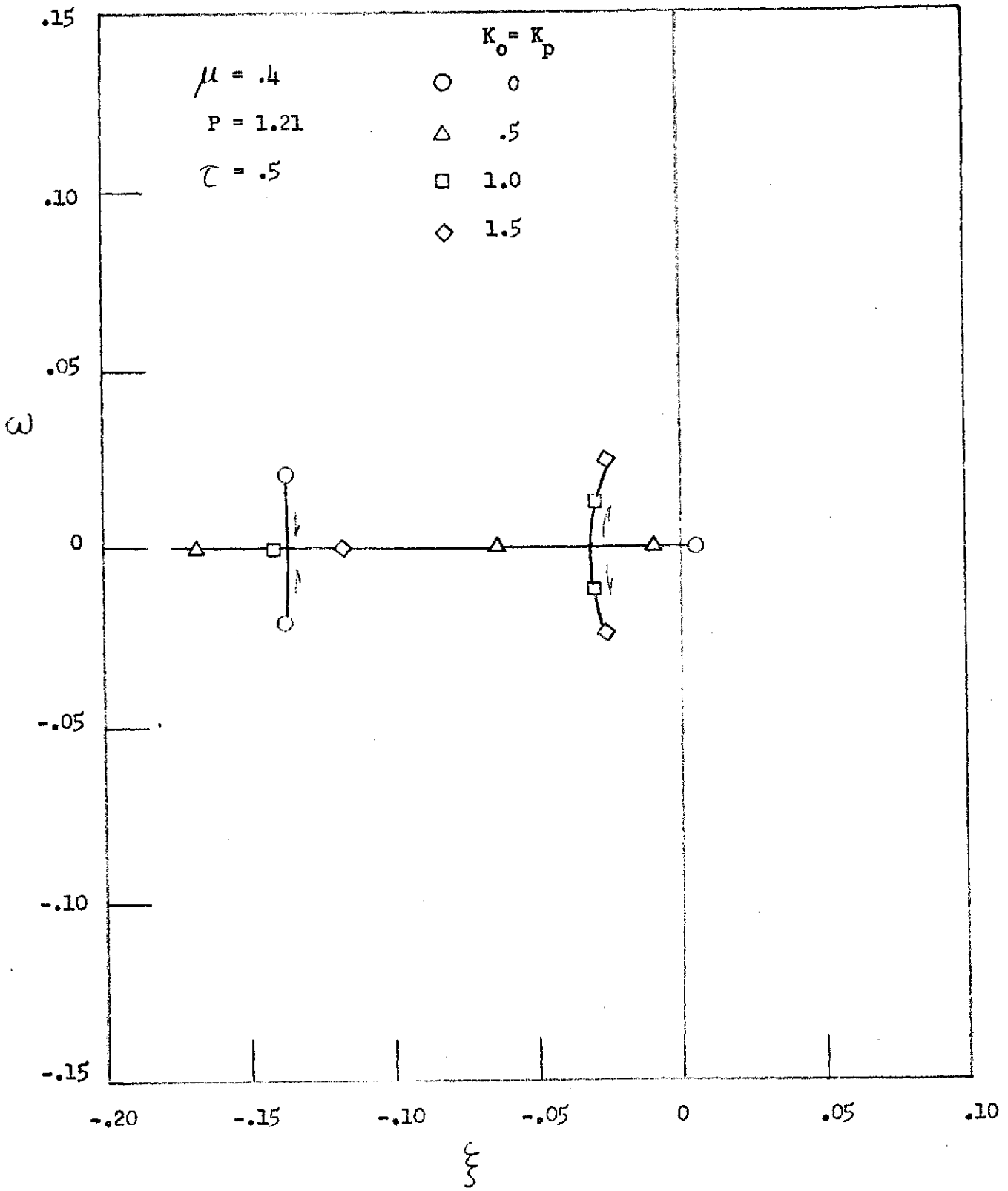
.15
.10
.05
0
-.05
-.10
-.15
ω
μ = .4
P = 1.21
τ = .5
$K_o = K_p$
0
.5
1.0
1.5
-.20
-.15
-.10
-.05
0
.05
.10
ξ

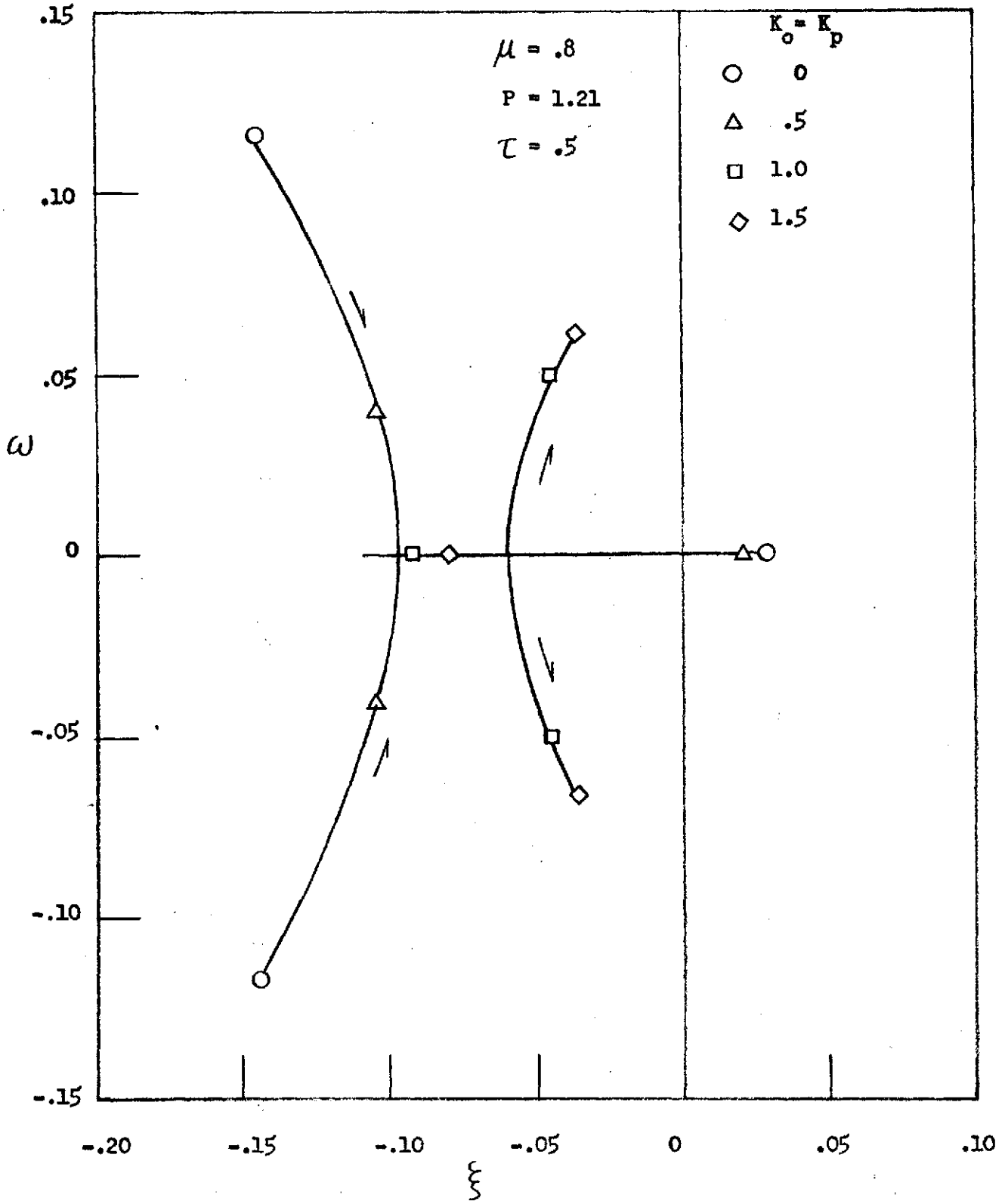
.15
.10
.05
0
-.05
-.10
-.15
ω
-.20
-.15
-.10
-.05
0
.05
.10
ξ
μ = .8
P = 1.21
τ = .5
K_o = K_p
0
.5
1.0
1.5

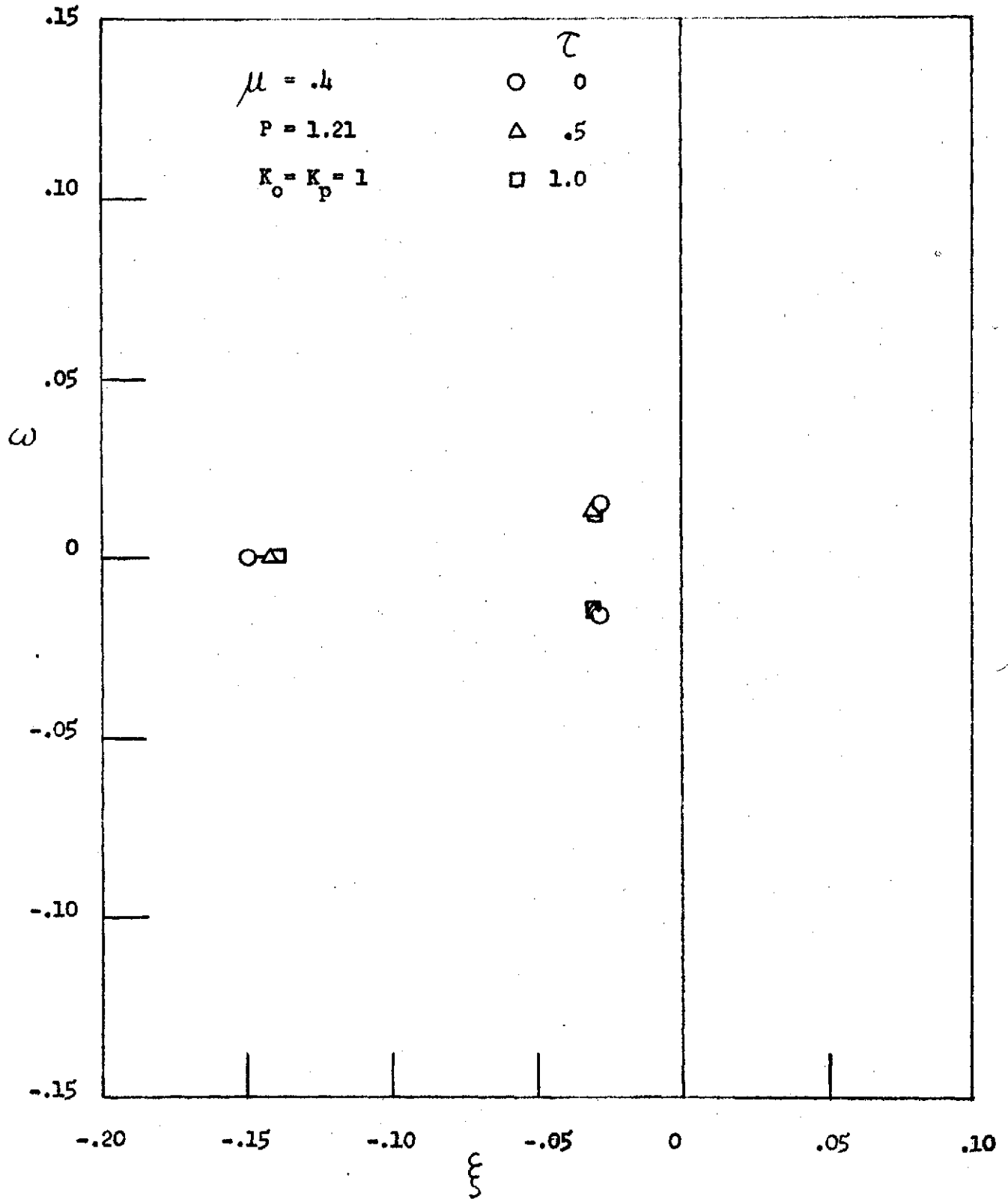
.15
.10
.05
0
-.05
-.10
-.15
ω
-.20
-.15
-.10
-.05
0
.05
.10
ξ
τ
μ = .4
P = 1.21
K_o = K_p = 1
0
.5
1.0

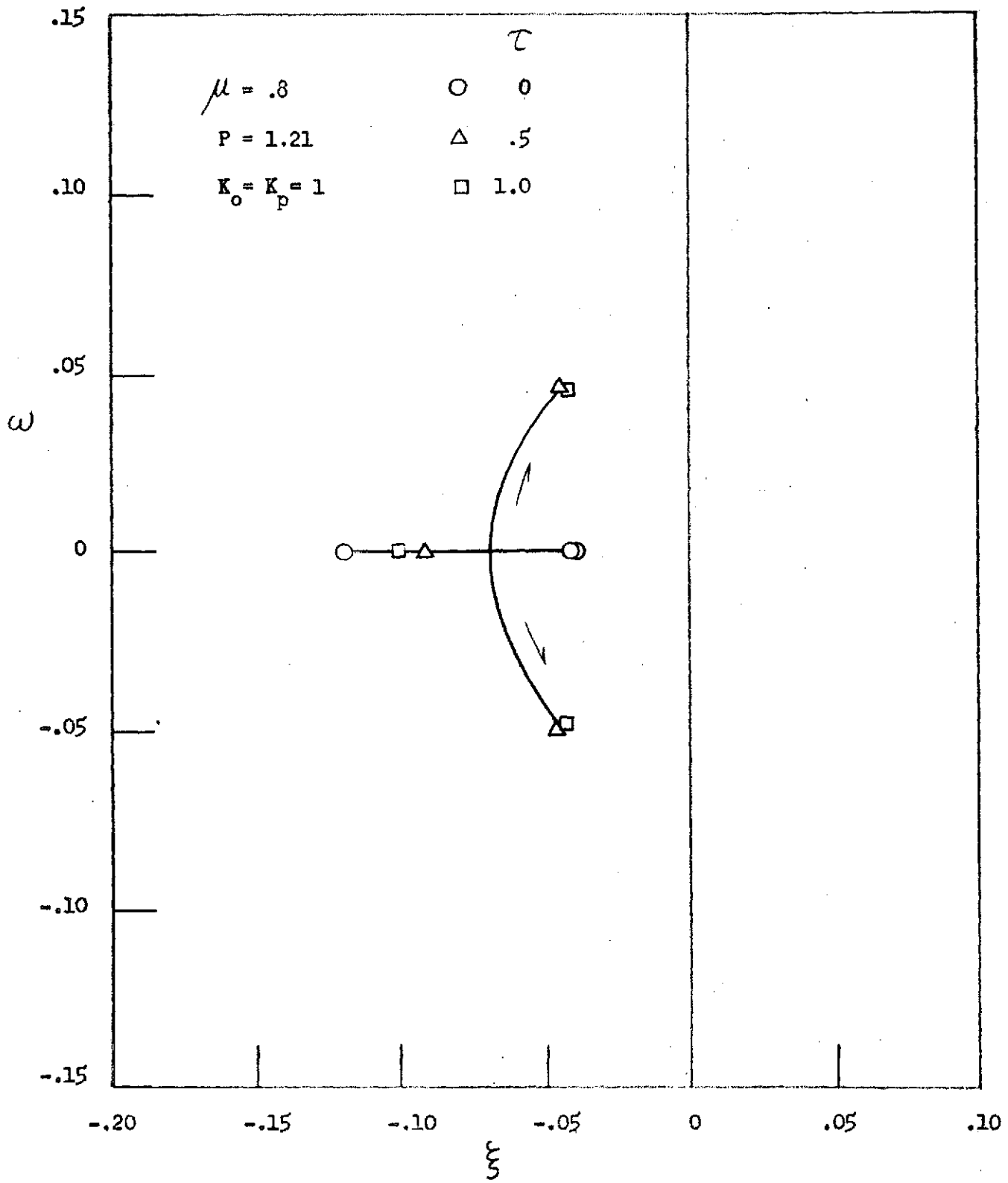
.15
.10
.05
0
-.05
-.10
-.15
ω
τ
μ = .8
P = 1.21
K_o = K_p = 1
0
.5
1.0
-.20
-.15
-.10
-.05
0
.05
.10
ξ

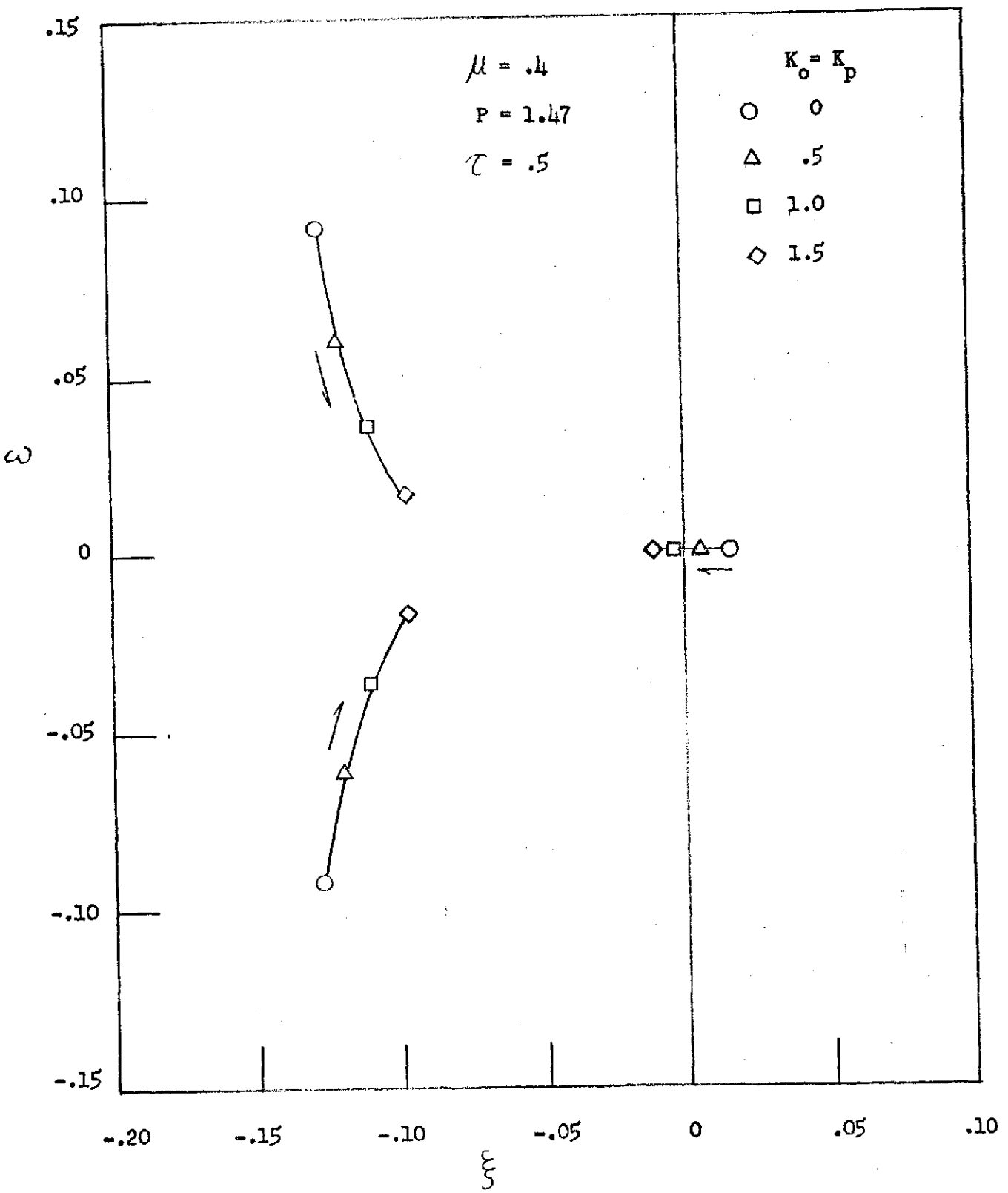
.15
.10
.05
0
-.05
-.10
-.15
ω
-.20
-.15
-.10
-.05
0
.05
.10
ξ
μ = .4
P = 1.47
τ = .5
K_o = K_p
0
.5
1.0
1.5

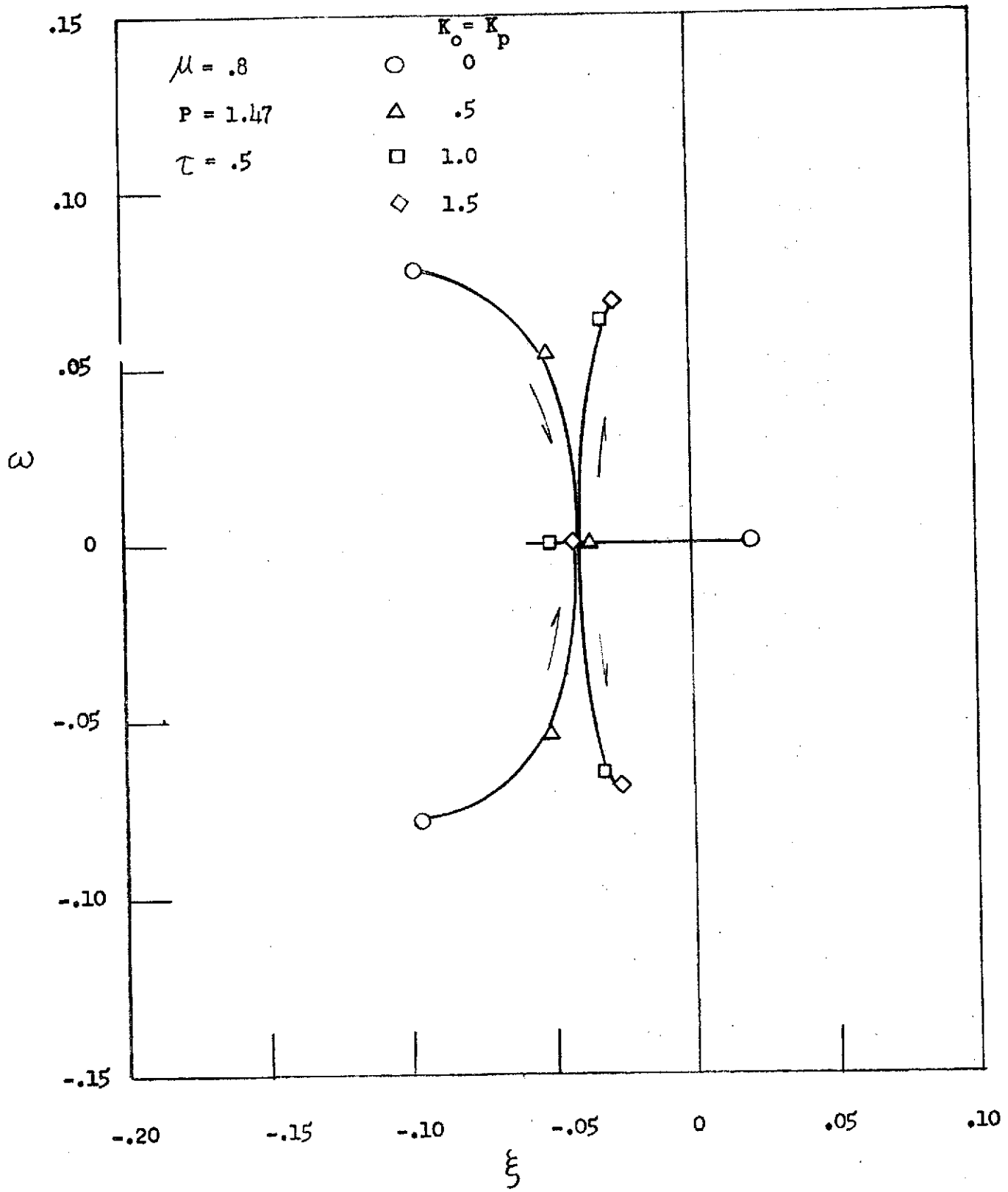
.15
.10
.05
0
-.05
-.10
-.15
ω
-.20
-.15
-.10
-.05
0
.05
.10
ξ
$K_o = K_p$
μ = .8
P = 1.47
τ = .5
0
.5
1.0
1.5

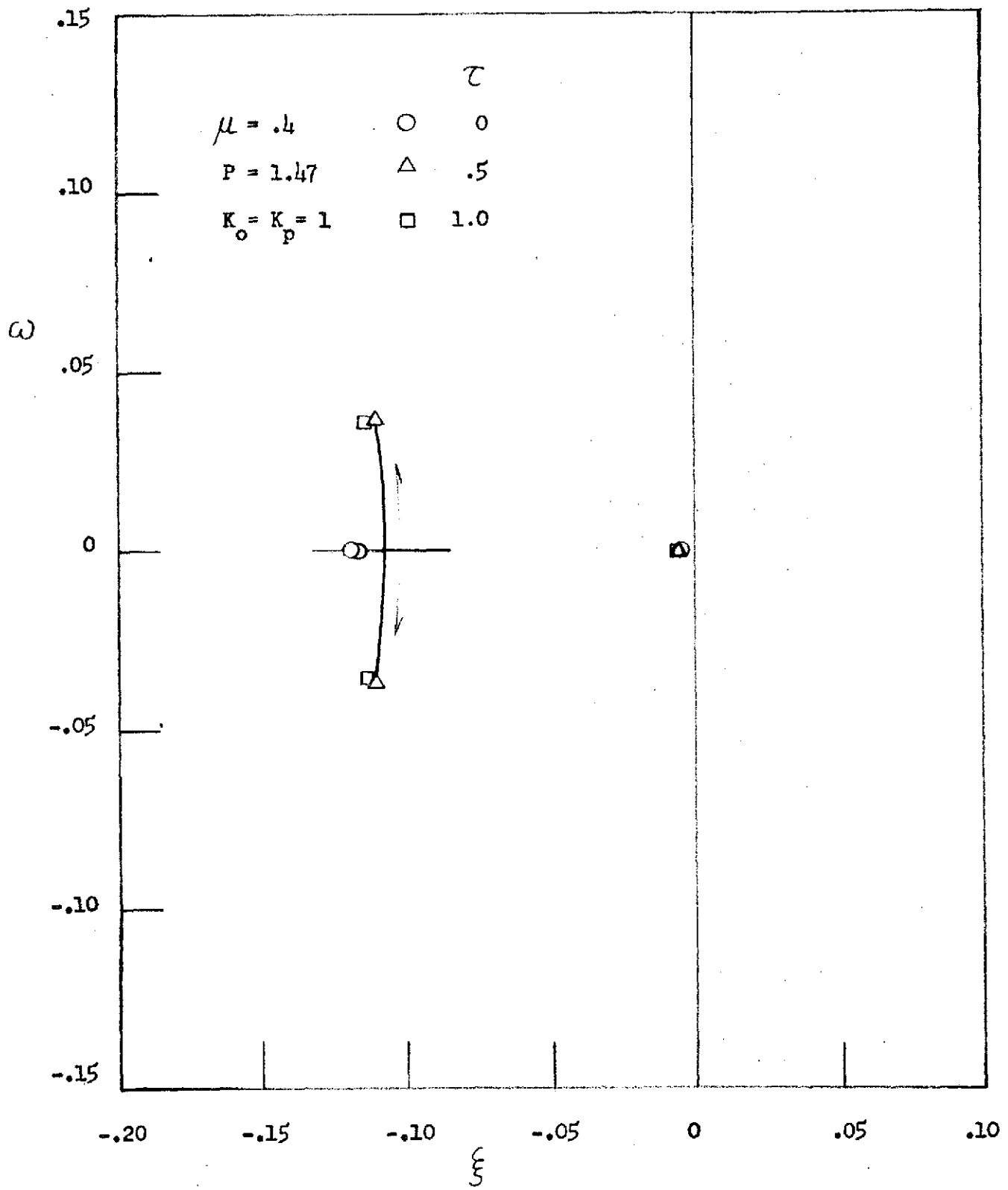
τ
μ = .4
P = 1.47
K_o = K_p = 1
0
.5
1.0
.15
.10
.05
0
-.05
-.10
-.15
ω
-.20
-.15
-.10
-.05
0
.05
.10
ξ

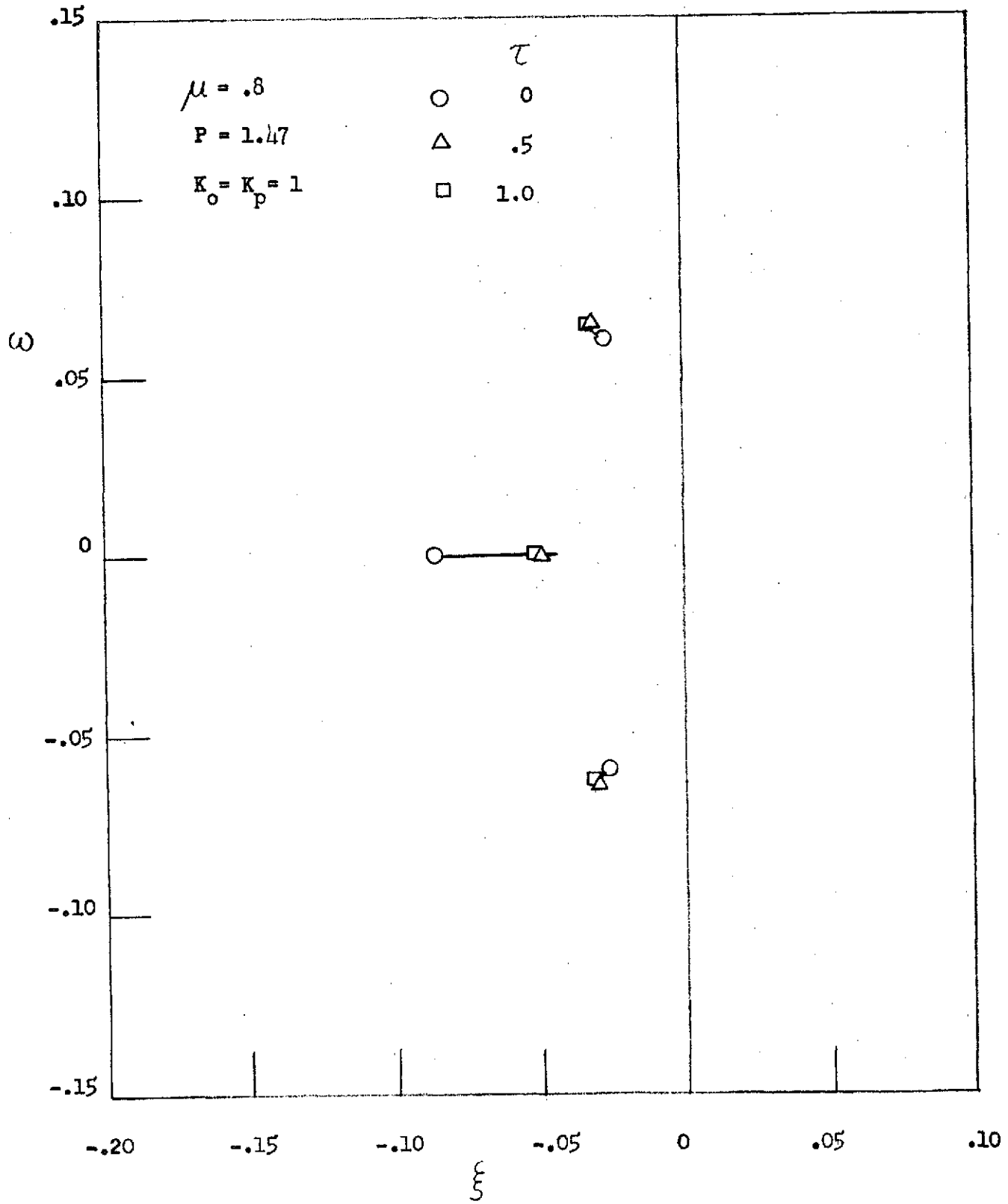
.15
.10
.05
0
-.05
-.10
-.15
ω
μ = .8
P = 1.47
K_o = K_p = 1
τ
0
.5
1.0
-.20
-.15
-.10
-.05
0
.05
.10
ξ

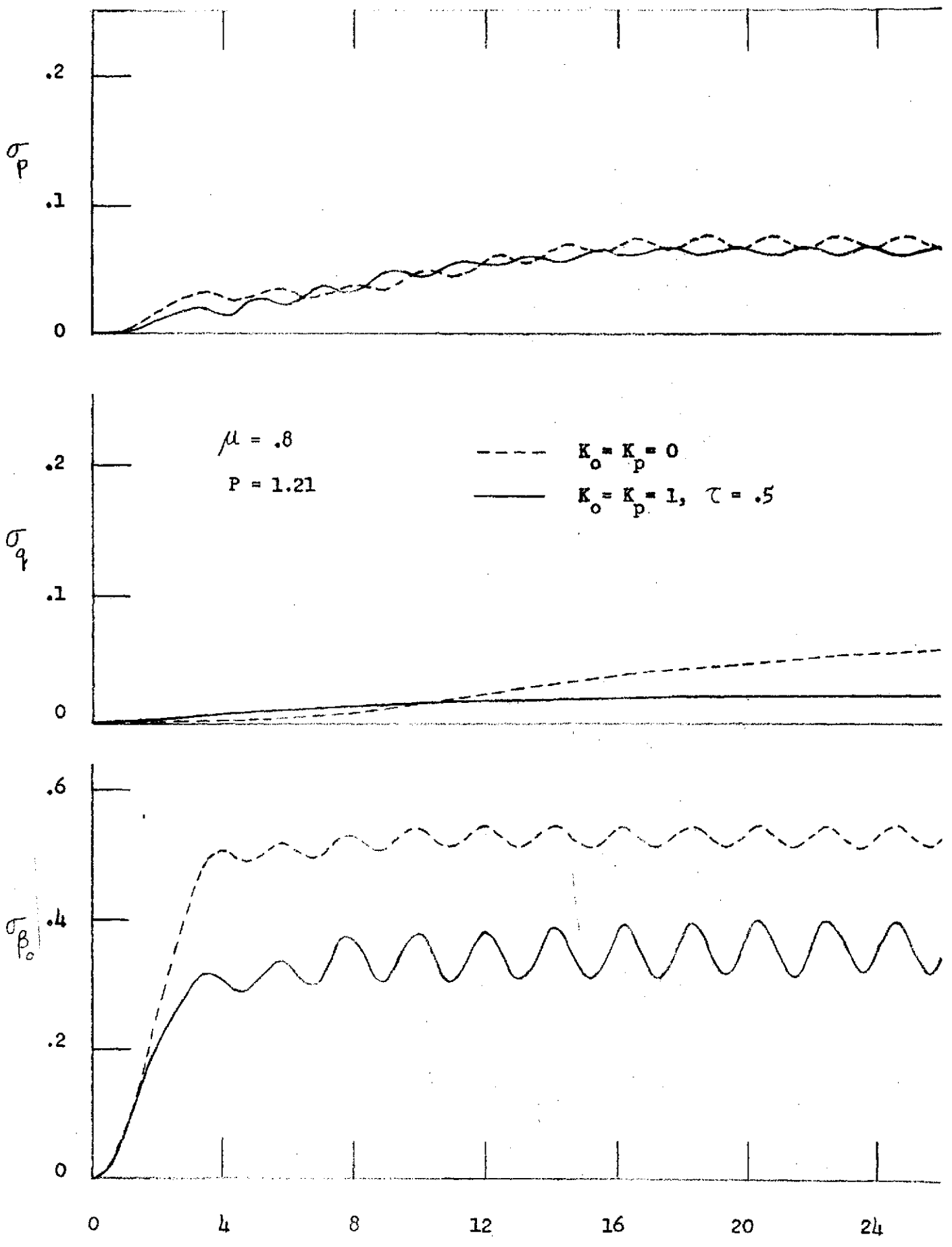
.2
.1
0
σ_p
μ = .8
P = 1.21
$K_o = K_p = 0$
$K_o = K_p = 1$, τ = .5
.2
.1
0
σ_q
.6
.4
.2
0
σ_{β_o}
0
4
8
12
16
20
24
t

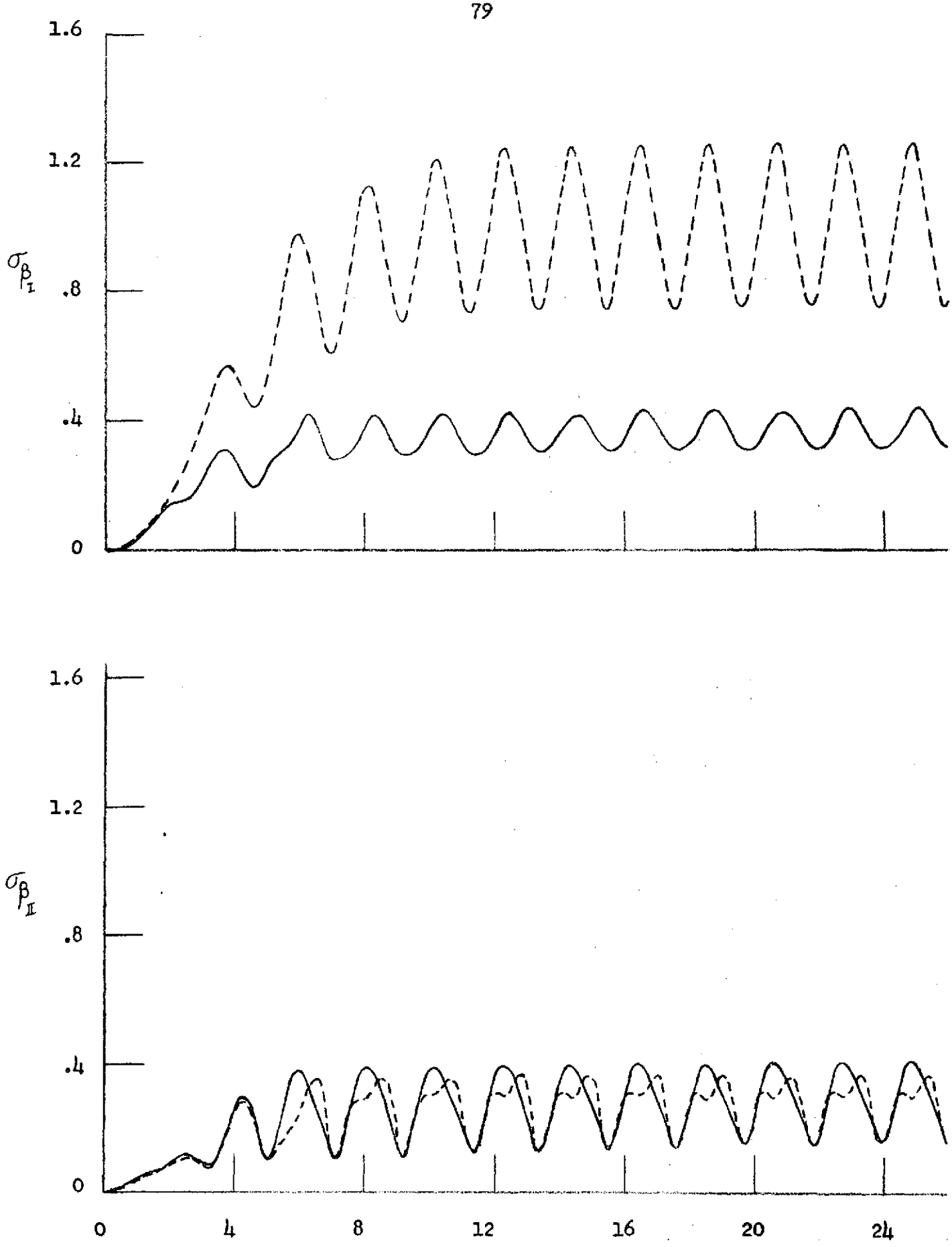
1.6
1.2
.8
.4
0
σ_{β_I}
1.6
1.2
.8
.4
0
$\sigma_{\beta_{II}}$
0
4
8
12
16
20
24
t

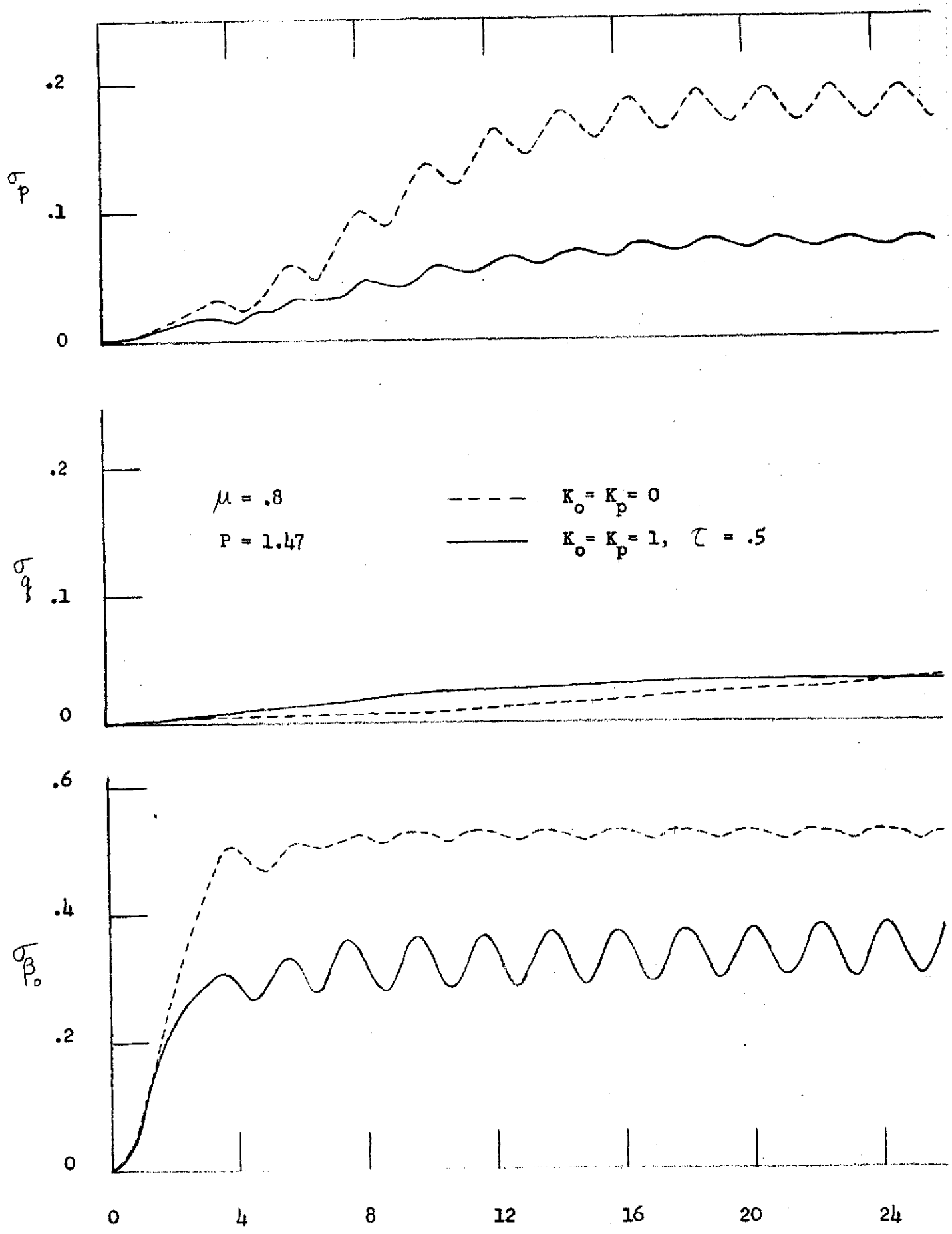
.2
.1
0
σ_p
.2
.1
0
σ_q
μ = .8
P = 1.47
$K_o = K_p = 0$
$K_o = K_p = 1$, τ = .5
.6
.4
.2
0
σ_{β_o}
0
4
8
12
16
20
24
t

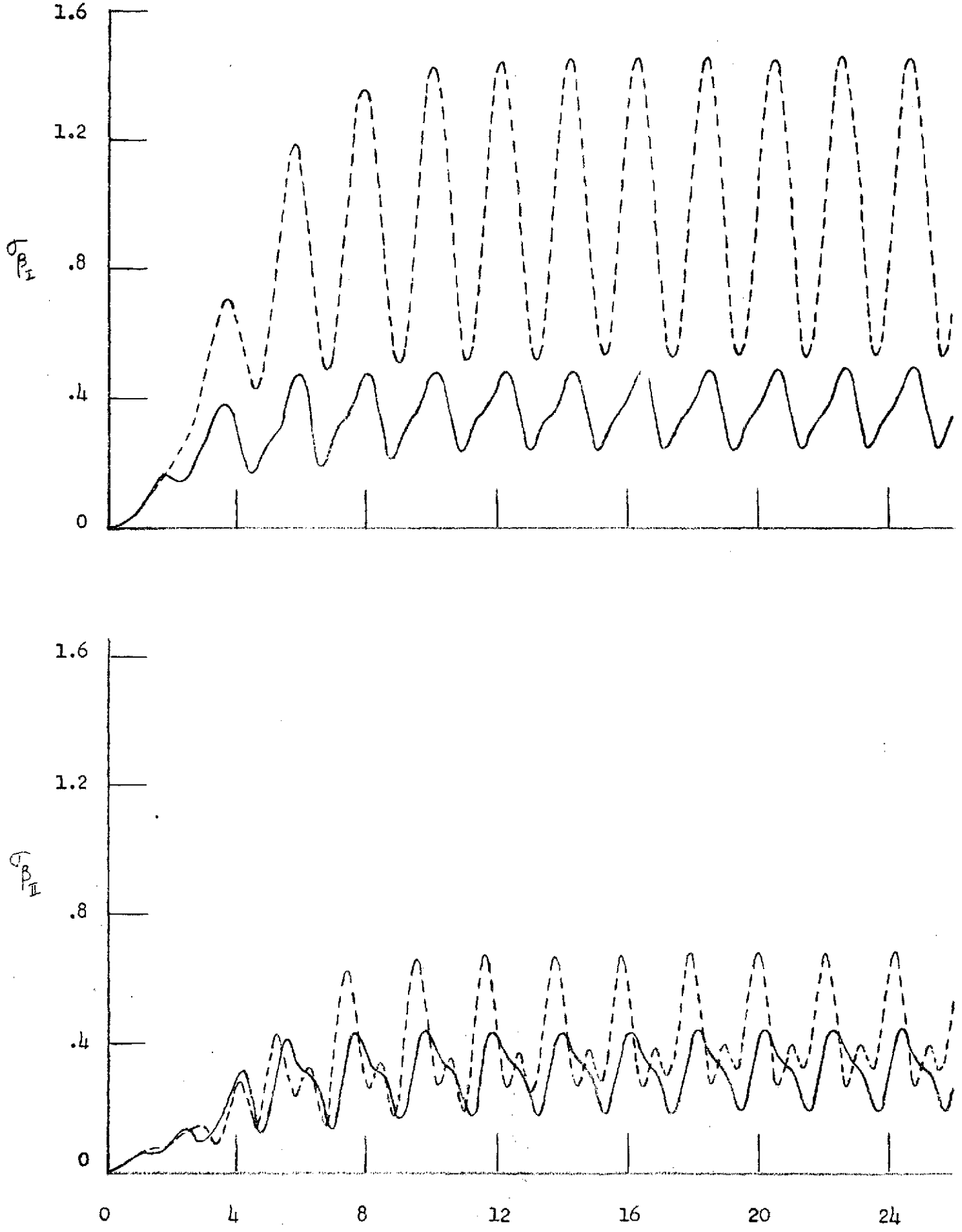
1.6
1.2
.8
.4
0
σ_{β_I}
1.6
1.2
.8
.4
0
$\sigma_{\beta_{II}}$
0
4
8
12
16
20
24
t